ADDENDUM

RAC 970
ARD 965-250
Revision A of
18 June 1963

# ABLATION RESISTANCE OF PHENOLIC ASBESTOS LAMINATE


Prepared by: Harry J. Doyle
Harry J. Doyle
Plastics Engineer

Approved by:
Robert Bastian, Chief
Chemistry Section

Approved by:
Harry A. Pearl, Chief
Materials - Research Div.



REPUBLIC AVIATION CORPORATION
Farmingdale, New York

INTRODUCTION

These tests were conducted as retests of ablation exposure determinations originally conducted under task no. 240-2040 of Project Fire and reported in RAC Report no. RAC 970 - ARD 965-250 of 22 October, 1962 and Revision A of 18 June, 1963. The retests were necessitated because of a malfunction of the calorimeter used in the original determination which caused a sizable error in the heat flux density calculation for the arc jet environment. A recalculation of the data indicates that the original tests were conducted at a relatively low heat flux and it was felt that substantiating data at a higher flux density were required to verify the design data. This report includes retest on heat of ablation of phenolic asbestos laminate of 100 pounds per cubic foot density at a heat flux of approximately 1400 BTU/ft$^2$-sec and an enthalpy of approximately 5000 BTU/lb.

DESCRIPTION

The material was similar to the Type II phenolic-asbestos described in the parent report. The density of each specimen was .0601 pounds per cubic foot; the similarity was achieved by machining the specimens from the same sheet. Processing was in accordance with the parent report. Since the higher heat flux which was achieved in these tests was accomplished for one thing by reducing the diameter of the arc nozzle, the dimension of the specimen had to be modified. Therefore, a button type specimen was used which had a .750 inch diameter to coincide with the flame dimension. Thickness was .395 inch for all specimens, and was mounted in a phenolic-asbestos holder so that approximately .100 inch was recessed and .295 protruded from the surface to limit the cavitation error. Procedural control was facilitated by the use of a chromel-alumel thermocouple placed on the rear surface of the button-coupon and subsequently imbedded in the phenolic-asbestos holder.

METHOD

The ablation environment was provided by the RAC Megawatt arc-jet operating at about 65-70% of capacity. The arc was sustained by nitrogen gas flowing at 4.50 pounds per minute through a .750-inch-diameter-water-cooled-copper-anode-nozzle. The cathode was blunt-nosed-water-cooled tungsten. Gas enthalpy was determined by a power balance analysis through direct measurement of the heat loss by water temperature rise and power input determinations. Heat flux determinations were made by a standard Arthur D. Little steady-state calorimeter which was developed especially for arc jet environmental determinations.

The specimens were exposed in the arc until the monitoring thermocouple on the back face reached approximately 500°F when the test was terminated. Since this temperature is the minimum at which the phenolic resin will char and decompose, it was arbitrarily assumed that this point represented the bottom of the char layer. For purposes of this analysis the entire char depth was considered to have been consumed. This is strictly a realistic approximation since the virgin material must be present for the formation of the char layer.

Specimen No. 1 was terminated after 11 seconds to assure the recovery of a substantial portion of the specimen so that correlation analysis could be made between the 500°F end-point and its interpolated position to represent the bottom of the char-layer. The other specimens were exposed for 16 to 18 seconds to achieve the 500°F back face temperature.

RESULTS

The average heat of ablation ($H_{eff}$) on medium density phenolic asbestos was 6500 BTU/lb at a heat flux ( $\dot{q}$ ) of 1400 BTU/Ft$^2$-sec and an enthalpy of 5000 BTU/lb. Data is tabulated in Table I. This $H_{eff}$ value compares favorably with the recalculated data of the original tests reported in revision A which were averaged at $H_{eff}$ = 4500 BTU/lb at an average ( $\dot{q}$ ) of 250-300 BTU/ft$^2$-sec at a similar density. This data proportionately verifies the normal trend of increased $H_{eff}$ with an increase in the ( $\dot{q}$ ) density. Therefore, these data are in agreement with the original data and show an increase in efficiency as the ( $\dot{q}$ ) flux is increased.

It is interesting to note that the specimen which gave a lower value of $H_{eff}$ also was the specimen which had the shortest test duration. To simplify the analytical procedure, the transient condition was considered nil and was not considered (for test of substantial duration transient effects are minimized); however, the erosion during the transient heat-up would be magnified for short duration test. Consequently, the specimen with the shortest duration gave the lowest $H_{eff}$.

CONCLUSIONS

Data presented in this report tend to verify the recalculated heat of ablation data ($H_{eff}$) reported in revision A of report No. RAC 970-ARD 965-250-A.

The $H_{eff}$ values generated in this investigation, 6500 BTU/lb. for 100 lb/cu. ft. material, can be considered minimum and conservative when used for environments with greater flux densities than 1400 BTU/ft$^2$-sec, where the enthalpy is 5000 to 6000 BTU/lb.

TABLE I

RESULTS OF RETESTS ON ABLATION RESISTANCE OF MEDIUM DENSITY PHENOLIC ASBESTOS LAMINATES

| | Density $lbs/ft^3$ | Thickness in. | Erosion Mils | Rate Mils/Sec. | Time Sec. | Heat Flux $BTU/ft^2$-sec | Enthalpy BTU/lb. | Effective Heat of Ablation BTU/lb |
|---|---|---|---|---|---|---|---|---|
| 1. | .0601 | .395 | .229 | 22.9 | 11 | 1490 | 4780 | 5760 |
| 2. | .0601 | .395 | .395 | 21.9 | 18 | 1356 | 4830 | 7110 |
| 3. | .0601 | .395 | .395 | 24.6 | 16 | 1400 | 5125 | 6570 |
| Avg. | | | | | | | | 6480 |

RAC 970-A
(ARD 965-250-A)
18 June 1963

# DEVELOPMENT OF DESIGN DATA FOR THE APPLICATION OF PHENOLIC ASBESTOS LAMINATES ON FIRE VEHICLE HEAT PROTECTIVE SYSTEMS

RAC 970-A

Harry J. Doyle
Harry J. Doyle
Plastics Engineer

Approved: Robert Bastian
Robert Bastian, Chief
Chemistry Section

Approved: Harry A. Pearl
Harry A. Pearl
Chief - Materials Research

REPUBLIC AVIATION CORPORATION
Farmingdale, L. I., N. Y.

## CONTENTS

## TABLES

ILLUSTRATIONS

ILLUSTRATIONS

ILLUSTRATIONS

## ILLUSTRATIONS

ILLUSTRATIONS

## ILLUSTRATIONS

## ABSTRACT

Development data are presented for material requirements to parametric analysis of certain heat protective systems for application to the FIRE vehicle.

Physical and thermodynamic properties are developed for several grades of phenolic asbestos laminates. Physical properties include tensile compression, flexure, and bearing up to 1000°F for short time soak conditions and tensile up to peak transient heating conditions of 2200°F and 30 - 35 seconds. Thermal properties include thermal conductivity to 1000°F, coefficient of thermal expansion to 1000°F and heat of ablation up to 5800 BTU/lb. enthalpy. Types of phenolic asbestos include three densities for the forward heat shield, 90, 100, and 110 pounds per cubic foot nominal density and one additional density type 85 pounds per cubic foot for afterbody optimization. The data include some critical design information and indicate the suitability of the phenolic asbestos laminates for application to the FIRE vehicle.

Revision A was added on 18 June 1963 to consider a discrepancy in the heat of ablation data which was caused by a faulty calorimeter. The data contained in this revision are corrected data and show an average heat of ablation ($H_{eff}$) of 4500 BTU/lb. at a nominal density of 100 pounds per cubic foot in a corrected heat flux ($\dot{q}$) of 250-300 BTU/ft$^2$-sec.

## INTRODUCTION

This study was conducted as part of the design support of Project Fire contract in NAS-1-1945 as required by approved Test Directive No.40-20-4 dated June 5, 1962. "Evaluation of Phenolic Asbestos Laminates for Application to Project "Fire" Heat Shield and Afterbody Insulation Facing".

The FIRE vehicle requires two separate and different heat protection systems to adequately protect the vehicle during its reentry flight; one a severe heating environment for the forward heat shield and one a low critical insulating system for the afterbody vehicle. The former of these is significantly different from conventional forward heat shields for the hypersonic vehicle in that it must also act as calorimetric insulator for this particular mission. This complicating feature will greatly limit the material selection and will also provide substantial structural requirements of the ablation material not normally expected for ablation nose cones.

### Afterbody Insulation System

The thermal environment experienced by the afterbody vehicle over-laps considerably into areas of state-of-the art know-how for reinforced plastic applications. Therefore ,available data were utilized heavily for afterbody insulation system. The phenolic asbestos laminate was utilized for this application in conjunction with an efficient insulation system, MIN-K-1300; and assembled with HT424 adhesive system good for 1000°F.

Because of the limited schedule time and funds available, it became necessary to select the most promising material based on a comprehensive study of available data. The phenolic asbestos material was considered to be the most promising of the feasible materials for the forward heat shield application and experimental work was limited to this material.

To improve the insulating capabilities of this material, the density was varied to produce three separate types of phenolic-asbestos laminates. The work presented herein covers the development of design data for these three materials plus one low density grade for afterbody optimization.

## OBJECT

All efforts of the program were directed toward providing a concise design data package as possible within the limited time span available. These data include the structural characteristics of the materials up to the maximum expected temperature in conjunction with density sensitive heat of ablation and supplementary thermodynamic properties. Accordingly, tensile, flexural and bearing strength determinations were selected for temperatures up to 1000°F soak conditions and RT compression determinations, an ablation test, thermal conductivity, thermal expansion, and a transient heating environmental determination.

Object-contd

A fourth optimizing-density phenolic asbestos was added to the afterbody tests where the ablation environment is either non-existent or neglible and where the low conductivity and non-critical strength material is indicated for possible optimization.

## DESCRIPTION

Materials used in this investigation were purchased from Raybestos-Manhattan, Inc., Manheim, Pennsylvania, on June 12, 1962. Four grades of the 41RPD Phenolic-Asbestos felt, supplied in the preimpregnated form ready for laminating, were purchased; three density grades for possible usage on the forward-heat shield and a fourth material tailored for possible afterbody usage. All materials were kept under refrigeration at 32°F when not in use and were allowed to warm to room temperature for 24 hours prior to use. The purpose of the various grades of the material was to produce a broad range of densities so that the proposed design requirements may be fulfilled. The mechanics of the density reduction (from the normal 120 lb/cu.ft. density) were an increase in the lower density phenolic-resin component of the material and the reduction of the fabricating pressure to produce less compaction. Consequently, the following material compositions were used:

| Type | 1A | 1B | II | III |
|---|---|---|---|---|
| Resin Content, % | 49.0 | 40.6 | 42.1 | 34.1 |
| Flow, % | 22.5 | 14.7 | 18.5 | 11.3 |
| Volatile Content, % | 6.39 | 6.13 | 6.80 | 6.70 |

## MANUFACTURE OF LAMINATES

Test panels were laminated in the 125 ton Pasadena hydraulic press. The materials were grouped in four classes and the curing cycle was according to the following schedule.

| Type | Pressure, Psi | Temperature °F | Time (1/8 In) Min. | Target Density Lbs/cu ft |
|---|---|---|---|---|
| 1A | 15 | 300F | 30 | 80 |
| 1B | 30 | 300F | 30 | 90 |
| II | 75 | 300F | 30 | 100 |
| III | 150 | 300F | 30 | 110 |

Subsequent to the press cure all panels were post cured for 24 hours at 300F, 24 hours at 350; 24 hours at 400, and 8 hours at 450°F.

### Strength Orientation Panels

To establish the effect of fiber orientation on the strength of the material, panels were laid up in several different orientation composition so that the specimens were tested in the longitudinal direction, the transverse direction and various compositions in between these two directions. The panels were then cured as before.

Ablation specimens were molded to the shape of the desired test configuration which was selected to reproduce the fiber orientation and directionality of the design item. This was accomplished by the use of compress-

Strength Orientation Panels-contd

ion molds which are shown in an exploded view in Figure 4. The moldings were otherwise cured and post-cured with the same procedure as the flat panels, trimmed off at the edges, and mounted with a chrome-alumel thermocouple at the center of the inside surface.

## METHOD

Three density grades of phenolic-asbestos for the forward-heat shield and one additional afterbody grade were tested for tensile, flexural, and bearing properties from room temperatures to 1000°F under short time soaks, and compression properties at room temperature.

### Thermal Properties

Thermal properties which were generated include effective heat of ablation, coefficient of thermal expansion, and thermal conductivity.

### Transient Environmental Determination

To simulate the afterbody environment for the determination of transient structural characteristics, tensile coupons were exposed to the radiant heating output of a quartz-lamp facility and residual strength determinations were made. When the expected thermal conditioning for the more severe flight profile as shown in Figure 50 had been accomplished, the test coupon was rapidly pulled.

## Physical Properties

### Tensile

Tensile properties were determined in accordance with Method 1011 of Federal Specification L-P-406 except that the rate of head travel was increased to .7 inches per minute so that the ultimate stress was attained within 4 to 6 seconds. The purpose of the increase in speed of head travel was to minimize the degradation in the material due to the high testing temperature, since this degradation would be extensive at 1000°F.

Blank coupons for each of the testing temperatures 300F, 500F, 700F, 800F and 1000F were instrumented with chromel-alumel thermocouples placed on either surface and at the center of the thickness. These blank coupons were then exposed in the radiant facility to determine the approximate time required to obtain uniform temperature. All subsequent test coupons were soaked for an additional 120 seconds after the attainment of the uniform testing temperature. (It was found that for .125 inch thick coupons heated from both sides, the center of the specimen did not lag more than 30 seconds from the surface temperatures for all temperatures including the 1000F temperature). The tensile apparatus is shown in Figure 7.

### Flexure

Flexural determinations were made in accordance with Method 1031 of Specification L-P-406 with the exception that the quarter-

Flexure-contd

point loading technique was used to facilitate the radiative heating method.

To attain the rapid rate required for the short time soak it was required to use radiant lamps and the center point loading ram would have shaded out the area of maximum stress. The quarter point technique allows the attainment of uniform stress over the central 50% of the specimen area between the (lower) supports.

The rate of cross head speed was again increased to 1.5 inches per minute so that failure would occur in 4 to 6 seconds after the 120 seconds temperature soaking time. Span-depth ratio was 16 to 1. The flexural apparatus is shown in Figure 3 with a close up in Figure 4.

Compression

Compression strength determination were made in accordance with Method 1021.1 of L-P-406 using the support tool described therein.

Bearing Strength

The method used for the bearing determinations were based on the Method 1051 of L-P-406, however, substantial modifications were required to cope with the heating requirements.

All steel jig masses which could act as a heat sink were eliminated from the specimen. The bearing hole was increased to .250 inches since this was the dimension of the intended design. Edge distance ratio was 2D and the specimen was changed to a double lap shear so that the

Bearing Strength-contd

heating rate would be facilitated as much as possible. The bearing pin was changed to a .250 inch monel rivet which would be the sole limiting factor of the rate of heating used. A Chromel-Alumel thermocouple was positioned into a cored hole in the rivet and was used as the monitoring temperature source. It was necessary to coat the rivet with a suitable emissivity coating for adequate response.

Transient Thermal Exposure

In addition to the soak tests, tensile coupons were prepared and were exposed to a transient heating environment which approximated the time-temperature conditioning shown in Figure 50. This heating curve represents the thermal input of the afterbody vehicle for a .125 inch phenolic asbestos at a density of 100 $lbs/ft^3$. To expedite the test program, and for purposes of simplicity, it was assumed that a standardized radiant flux, programmed to a power-input, that would reproduce a surface temperature shown in Figure 50 for the .125 inch thickness would yield a corresponding surface temperature expected on the afterbody flight vehicle when the thickness and the density of the material are changed. With the use of a high emissivity coating a large percentage of the radiant energy was made available to the surface. The coating used for this purpose had an emissivity of .93.

To satisfactorily measure surface temperature of the test specimen, it was found necessary to use a platinum 5% rhodium vs. platinum 20% rhodium with a gage of .0025 inch to achieve a satisfactory response without thermocouple failure. The Chromel-Alumel limitation and failure point is dramatically illustrated in Figure 50 . Because of the still experimental nature (and early stage of development) of this thermocouple system the temperature calibration curve is given in Figure 51 . The thermocouple read out was made on a Sanborn 150 recorder. The testing facility is shown in Figure 7 & 8. Correlation of the actual surface temperatures experienced by the specimens and the programmed surface temperatures are shown in Figure 50 . This programmed surface temperature was calculated from an analytical heat pulse for a -15° reentry referenced to a point 2.4 feet aft of the stagnation point.

## Ablation

Ablation simulation determinations were made on a Plasma-dyne one mega-watt arc-jet performing at about 32-35% capacity. A water-cooled copper-jacketed shutter shown in Figure 10 was used during the arc-jet run-up to protect the specimen during this period. The arc-jet consisted of a 12 inch long, water-cooled copper anode with a 1.25 inch inside diameter and a blunt-nosed water-cooled tungsten cathode. The nitrogen arc fed the gas at a rate of 1.87 pounds per minute as measured by a

Ablation-contd

Baily flowmeter with the standard orifice.

Gas enthalpy was measured from a power input determination by a amperage and voltage measurement less the heat loss through the water-cooled anode and cathode. Heat-flux impingement was measured by use of a cold-wall copper calorimeter of a similar shape to the specimen and located at the same position.

The flat disc shaped specimen as described in the material section was mounted on a water cooled sting support and protected during the run-up period of about five seconds by the shutter. At the attainment of peak power buildup the shutter was mechanically removed and the specimen was exposed for thirty seconds. Back face temperature was monitored to protect against burn-through. The transient ablation period was estimated to be approximately 2 to 3 seconds and was considered to be negligible in the determinations.

Thermal Conductivity

A modified 7" diameter ASTM-C177-45 apparatus was used for the thermal conductivity measurements. The 7" diameter rig, except for its smaller size, is identical in operating procedure to the 14" x 14" ASTM-C177-45 apparatus which is described in the appendix. The calibration of the 7" diameter is also shown in the appendix along with the calibration of the 14" x 14" apparatus.

## Thermal Expansion

Thermal expansion determinations were made in accordance with Method 2031 of L-P-406. The apparatus is shown in Figure 11 and a close-up of the quartz-tube dilatometer is shown in Figure 12. Expansion coefficients were made up to 1000°F. The top and bottom of a 3.4 unit specimen were temperature monitored. The temperature was held ± 3°F up to 600°F and from 600°F to 1000°F temperature was held to ± 8°F.

The heating unit was approximately 30 inches long; the quartz tube was put into the furnace a distance of 11-1/2 inches. The specimens with an average length of 3.4 inch were placed in the bottom of the tube. Two thermocouples were mounted on the specimen, approximately 2 inches apart, one toward the top and one toward the bottom.

A thermocouple used by the control panel was mounted on the outside of the quartz tube approximately 10 inches into the furnace centered in line with the specimen. The dial gauge was mounted on the quartz tube which rested on the top of the specimen. A pre-load was put on the indicator before the start of the run to zero on the gauge. The thermocouples were read by a normal potentiometer.

# RESULTS

## Physical Properties

Tension and Flexural values are given in Table I and II respectively for the Ultimate Strength and Modulus of Elasticity at six temperatures up to 1000°F. Plots of strength and modulus of elasticity vs. temperature are given in Figures 29 to 44 for four grades of phenolic asbestos. The higher density material, 109 lb/cu ft (type III) has a tensile ultimate of 45,000 psi and an E of 4.58 x$10^6$ psi at room temperature and along the axis of its maximum strength (longitudinal).

## Effect of Temperature

The same material at 1000°F after two minutes at 1000°F (measured after attainment of uniform, soak condition equilibrium) shows a longitudinal tensile strength of 11,500 psi and an E of 3.18 x$10^6$ psi.

## Strength Directionality

Data in Tables I and II give values along the axis of maximum strength (Longitudinal direction) and minimal strength (transverse direction) longitudinal and transverse directions are 90° to each other. It was noted that the tensile strength differential between these two directions was significantly greater than had hither-to been reported. This differential ratio is approximately 2 to 1 whereas other data reported by Forest Products Laboratory, Wright Air Development Division, and the manufacturer, Strength Directionality-contd

Raybestos-Manhattan show a ratio of approximately 3 to 2. Actual strength change vs. fiber orientation is plotted in Figures 29 to 48 for tensile, compression, bearing and flexure.

Density Effect

The data indicate that strength is density sensitive as would be expected. Average (bidirectional) tensile strength at RT. changes from 28,700 psi for a density of 109 lbs/cu ft to 24,300 psi for a density of 84.5 lbs/cu ft; at 1000°F (after 2 minutes) average (bidirectional) tensile strength changes from 14,400 psi to 109 lbs/cu ft to 10,200 psi at 84.5 lbs/cu ft.

Tensile values in general agree with published data of reference (FPL), (WADD), and (R.M.). However, flexural values of Table II run about 30% lower than other published data. Since this discrepancy could be due to the quarter-point loading technique which results in a continuous stress across 50% of the entire span, and which is considerably longer than the local stress resulting from the mid-span technique, re-tests were run using the mid-span loading for comparative purposes. These data are plotted in the temperature curves as a dotted line and show only a modest improvement in the strength level for most cases. Flexural values, therefore, are substantially below values reported by other investigators and established in the applicable military specifications.

## Compression and Bearing

Compression strength and stiffness values shown in Table III are less sensitive to density change with the exception of the lowest density. The orientation data show a more modest ratio of about 3 to 2 from longitudinal to transverse directions.

## Bearing

The bearing strength values given in Table IV do not show the usual strength orientation with fiber directionality of the other tests. The transverse strength is almost equal to the longitudinal values in all cases. Density effects are not severe; the 300°F bearing strength average is 29,900 psi for Type 1B density, 34,200 psi for Type II density and 33,900 psi for Type III density.

## Stress - Strain Relationship

Typical stress-strain curves are shown in Figures 63 to 74 for room temperature and 1000°F only.

## Ablation

Results tabulated in Table V show a minimum cold wall effective heat of ablation ($H_{eff}$), range from value of 3,440 BTU/lb to a maximum cold wall heat of ablation value of 5,630 BTU/lb as measured to the base of the virgin material. (It was assumed that the total char layer was consummed for conservative determinations). Heff values plotted against density in

Ablation-contd

Figure 49 show approximately a straight line function which indicates that a lower density can be safely used in a predictable manner if it is desirous to take advantage of other improved properties; in particular, a lower thermal conductivity is available in a lower density material. Although enthalpy variable on heat of ablation properties was beyond the scope of the authorizing test Directive, a later attempt to uncover the effect of this parameter was unsuccessful primarily due to the limited number of test specimens.

Thermal Conductivity

Thermal conductivity values shown in Table VII indicate that the higher density mentioned has about 2 times the conductivity as the lowest density, 1.91 vs. .98 BTU/in/ft$^2$/$^{\circ}$F/in. at room temperature. Although the trend of the conductivity value for those materials is to merge at the higher temperatures (approaching 1000$^{\circ}$F) a substantial variation is maintained for a significantly long temperature span as shown in Figure 52. Conductivity vs. density plots shown in Figure 53 transgress from a straight line function and show a greater reduction as density approaches its lower value. This transgression possibly can be due to the increased porosity produced in the lowest grade material relative to a change in the resin content experienced at the higher end of the density variable.

Thermal Expansion

Raw data thermal expansion data are shown in Figures 54 to 61. The summary curve, Figure 62, shows substantially equivalent coefficients of thermal expansion, about $2.3 \times 10^{-6}$ °F; however, the material does show a reversal at higher temperatures. This temperature of reversal is density sensitive. Transition points, typical of phenolic resin systems are also shown in the raw data, figures 54 to 61. For analysis purposes the average lines have been drawn and are summarized in Figure 62.

Transient Thermal Exposure

Data shown in Table V indicate that the lowest density investigated (84.5 lbs/ft$^3$) has maintained satisfactory structural continuity under the thermal environment described by Figure 50 except possibly at the lightest gage tested (.060 inch). For this gage the residual strength approaches a possibly critical level of 810 psi residual tensile strength.

Although all specimens exposed in this environment experienced a load-carrying capability, it was noted that reproducibility was highly unattainable and a larger number of specimens should be considered for realistic strength of materials determinations for this type of environment. This condition is also reflected in the lack of a well defined structural relationship which was in evidence in the soak tests. However, a trend to a higher stress attainment for higher density and thicker gages is indicated. The maximum strength level attained under this transient heating environment was 6500 psi for the 109 lbs/cu ft material at .125 thickness.

# CONCLUSIONS

The phenolic asbestos material can be utilized for structural application up to 1000°F in short time soak conditions and up to 2200°F in transient heating conditions of 30 seconds duration and is a satisfactory material for usage on structural components of the Project FIRE vehicle.

The phenolic asbestos material must be used as a rotated lay-up to produce an "isotropic" material. This can be accomplished by rotating 50% of the plies 90° to the longitudinal direction.

The tensile strength values of Table I are representative data for the various densities indicated.

The flexural strength allowables should be reduced as is indicated by Table II until the data descrepancies can be resolved and firm values established. The strength of materials developed in this investigation can be considered conservative as evidenced by the low flexural values obtained.

The heat of ablation properties for the various densities of phenolic asbestos laminates can be traded off in a predictable manner to achieve a significant improvement in thermal conductivity properties for design optimization. The average heat of ablation at a flux density of 250-300 BTU/ft$^2$-sec. is 4500 BTU/lb. for a nominal density of 100 pounds per cubic foot.

## ACKNOWLEDGMENT

The Author wishes to express his appreciation for the assistance of Dr. Robert Perry and his associates of the Reentry Simulation Laboratory in particular for the performance of the arc jet erosion testing and calorimetric analysis.

## TABLE I

TENSILE PROPERTIES OF FOUR PHENOLIC ASBESTOS LAMINATES SHOWING TEMPERATURE AND DIRECTIONALITY VARIABLES[3]

| Type | | 1A | | 1B | | II | | III | |
|---|---|---|---|---|---|---|---|---|---|
| Density[2] lbs/cu ft | | 84.5 | | 91.9 | | 101.7 | | 109.0 | |
| F° | | Ult. Psi | E'[1] Psix10-6 | Ult. Psi | E' Psix10-6 | Ult. Psi | E' Psix10-6 | Ult. Psi | E' Psix10-6 |
| RT | Longitudinal | 26,000 | 2.81 | 37,800 | 3.82 | 39,800 | 3.20 | 45,100 | 4.58 |
| | Bidirectional | 20,300 | 2.24 | 26,400 | 2.86 | 31,500 | 2.58 | 33,800 | 3.35 |
| | Transverse | 14,800 | 1.70 | 15,800 | 1.92 | 23,100 | 1.82 | 22,500 | 2.13 |
| 300 | Longitudinal | 23,100 | 2.47 | 32,050 | 3.48 | 32,000 | 3.28 | 36,200 | 3.92 |
| | Bidirectional | 16,200 | 1.97 | 23,100 | 2.56 | 25,600 | 2.78 | 27,500 | 2.82 |
| | Transverse | 9,400 | 1.41 | 14,100 | 1.67 | 19,400 | 1.75 | 19,000 | 1.75 |
| 500 | Longitudinal | 19,700 | 2.15 | 23,900 | 3.07 | 25,200 | 3.16 | 25,700 | 3.55 |
| | Bidirectional | 13,100 | 1.57 | 17,400 | 2.24 | 20,600 | 2.28 | 20,400 | 2.55 |
| | Transverse | 6,600 | 1.01 | 12,000 | 1.41 | 15,700 | 1.40 | 15,000 | 1.57 |
| 700 | Longitudinal | 15,600 | 1.91 | 18,100 | 2.55 | 18,500 | 2.81 | 24,000 | 3.40 |
| | Bidirectional | 10,400 | 1.30 | 13,000 | 1.72 | 13,100 | 1.87 | 17,000 | 2.42 |
| | Transverse | 5,700 | 0.72 | 8,000 | 0.90 | 7,800 | 0.95 | 10,100 | 1.43 |
| 800 | Longitudinal | 13,000 | 1.77 | 16,100 | 2.27 | 15,300 | 2.45 | 21,200 | 3.30 |
| | Bidirectional | 8,500 | 1.15 | 11,900 | 1.42 | 11,100 | 1.61 | 15,200 | 2.28 |
| | Transverse | 4,100 | 0.55 | 7,500 | 0.62 | 7,000 | 0.79 | 9,450 | 1.27 |
| 1000 | Longitudinal | 3,500 | 1.68 | 4,000 | 2.18 | 7,300 | 2.38 | 11,500 | 3.18 |
| | Bidirectional | 2,100 | 1.02 | 3,100 | 1.35 | 6,100 | 1.54 | 9,900 | 2.17 |
| | Transverse | 1,000 | 0.40 | 2,000 | 0.54 | 5,000 | 0.71 | 8,300 | 1.19 |

1. Modulus of Elasticity in Tension.

2. Based on experimental average value of all test coupons used in this study.

3. Data given in this table are extrapolations of the strength curves shown in figures 29 to 36.

# TABLE II

## FLEXURAL STRENGTH OF FOUR PHENOLIC ASBESTOS LAMINATES SHOWING TEMPERATURE AND DIRECTIONALITY VARIABLES[3]

| Type | | | 1A | | 1B | | II | | III | |
|---|---|---|---|---|---|---|---|---|---|---|
| Density Lbs/Ft cu. | | | 84.5 | | 91.9 | | 101.7 | | 109.0 | |
| | | | Ult. Psi | E* x$10^{-6}$ PSI | Ult. | E* x$10^{-6}$ Psi | | E* x$10^{-6}$ Psi | | |
| Center-Span-Loaded (long.) | | | 30,250 | | 36,800 | | 38,000 | | 36,100 | |
| Quarter-Point Loading | | | | | | | | | | |
| .250 Thickness | | | | | 33,300 | 3.85 | 32,800 | 3.62 | 37,200 | 4.52 |
| .125 Thickness | | | | | | | | | | |
| °F | Longitudinal | Psi | 27,000 | 3.09 | 33,100 | 3.88 | 31,700 | 4.18 | 35,000 | 4.74 |
| RT | Bidirectional | Psi | 24,300 | 2.38 | 27,500 | 2.90 | 26,600 | 2.96 | 28,700 | 3.53 |
| | Transverse | Psi | 21,700 | 1.66 | 22,000 | 1.91 | 22,500 | 1.30 | 22,500 | 2.33 |
| | Longitudinal | Psi | 25,000 | 2.80 | 28,100 | 3.08 | 27,000 | 3.16 | 29,000 | 4.23 |
| 300 | Bidirectional | Psi | 22,600 | 2.20 | 23,000 | 2.33 | 23,300 | 2.35 | 24,000 | 3.15 |
| | Transverse | Psi | 20,200 | 1.58 | 18,000 | 1.57 | 20,000 | 1.53 | 19,000 | 2.05 |
| | Longitudinal | Psi | 15,000 | 2.33 | 23,700 | 2.76 | 23,800 | 2.65 | 24,800 | 3.93 |
| 500 | Bidirectional | Psi | 13,500 | 1.85 | 19,300 | 2.09 | 21,200 | 2.07 | 20,700 | 2.91 |
| | Transverse | Psi | 12,000 | 1.37 | 15,000 | 1.42 | 18,800 | 1.48 | 16,700 | 1.87 |
| | Longitudinal | Psi | 13,000 | 1.78 | 19,000 | 2.61 | 18,800 | 2.37 | 23,000 | 3.63 |
| 700 | Bidirectional | Psi | 12,000 | 1.40 | 14,450 | 1.92 | 16,100 | 1.92 | 19,200 | 2.62 |
| | Transverse | Psi | 10,500 | 1.02 | 10,000 | 1.21 | 13,600 | 1.45 | 15,500 | 1.55 |
| | Longitudinal | Psi | 12,500 | 1.56 | 17,700 | 2.47 | 16,500 | 2.26 | 21,500 | 3.44 |
| 800 | Bidirectional | Psi | 11,500 | 1.25 | 13,400 | 1.73 | 14,500 | 1.78 | 18,200 | 2.42 |
| | Transverse | Psi | 9,700 | 0.92 | 9,100 | 0.99 | 12,500 | 1.31 | 14,800 | 1.42 |
| | Longitudinal | Psi | 11,500 | 1.42 | 15,700 | 2.32 | 11,000 | 2.19 | 17,600 | 3.25 |
| 1000 | Bidirectional | Psi | 10,200 | 1.15 | 12,100 | 1.60 | 10,200 | 1.71 | 14,400 | 2.28 |
| | Transverse | Psi | 9,300 | 0.87 | 9,000 | 0.89 | 9,400 | 1.22 | 11,000 | 1.31 |

1. "E* Modulus of Elasticity in Flexure."

2. Based on experimental average values of all test coupons used.

3. Data given in this table are extrapolations of the strength curves shown in figures 37 to 44.

## TABLE III

### COMPRESSION PROPERTIES OF FOUR PHENOLIC ASBESTOS LAMINATES VS FIBER ORIENTATION[1]

| Type Mat'l | Density Lbs/CuFt | Longitudinal Ultimate PSI | Longitudinal Modulus of Elasticity PSI X $10^{-6}$ | Bidirectional Ultimate PSI | Bidirectional Modulus of Elasticity PSI X $10^{-6}$ | Transverse Ultimate PSI | Transverse Modulus of Elasticity PSI X $10^{-6}$ |
|---|---|---|---|---|---|---|---|
| IA | 84.5 | 16, 500 | 2.96 | 13, 200 | 2.17 | 10, 000 | 1.39 |
| IB | 91.9 | 23, 000 | 3.23 | 19, 000 | 2.35 | 15, 000 | 1.46 |
| II | 101.7 | 23, 500 | 3.61 | 19, 500 | 2.73 | 15, 500 | 1.83 |
| III | 109.0 | 24, 000 | 3.96 | 20, 000 | 3.12 | 16, 000 | 2.28 |

1. Data given in this table are extrapolations of the strength curves shown in figure 45.

## TABLE IV

BEARING STRENGTH OF THREE PHENOLIC ASBESTOS LAMINATES VS FIBER ORIENTATION[1]

| Type<br>Density Lb/Cu. Ft.<br>°F | | IB<br>91.9<br>PSI | II<br>101.7<br>PSI | III<br>109<br>PSI |
|---|---|---|---|---|
| RT | Longitudinal | 31 000 | 39, 500 | 43, 700 |
| | BiDirectional | 29, 900 | 37, 200 | 42, 000 |
| | Transverse | 28, 500 | 35, 000 | 40, 500 |
| 300 | Longitudinal | 29, 900 | 34, 200 | 33, 900 |
| | BiDirectional | 28, 200 | 32, 700 | 31, 900 |
| | Transverse | 26, 500 | 31, 300 | 30, 000 |
| 500 | Longitudinal | 25, 000 | 29, 600 | 34, 000 |
| | BiDirectional | 22, 800 | 28, 000 | 31, 900 |
| | Transverse | 20, 500 | 26, 300 | 27, 100 |
| 700 | Longitudinal | 22, 200 | 26, 100 | 26, 500 |
| | BiDirectional | 20, 300 | 25, 400 | 24, 700 |
| | Transverse | 18, 400 | 24, 600 | 23, 000 |
| 800 | Longitudinal | 21, 000 | 22, 500 | 21, 500 |
| | BiDirectional | 19, 000 | 21, 800 | 20, 300 |
| | Transverse | 17, 000 | 21, 000 | 19, 100 |
| 1000 | Longitudinal | 12, 000 | 11, 500 | 17, 000 |
| | BiDirectional | 11, 500 | 10, 700 | 16, 200 |
| | Transverse | 11, 000 | 10, 000 | 15, 400 |

1. Data given in this table are extrapolations of the strength curves shown in figures 45 to 48.

## TABLE V

## RESIDUAL TENSILE STRENGTH OF PHENOLIC ASBESTOS LAMINATES AFTER TRANSIENT HEATING EXPOSURE UP TO 2200°F FOR 30 SECONDS

| Thickness (Longitudinal) Inches | Type IA 84.5 Ultimate Strength PSI | Type IB 91.9 Ultimate Strength PSI | Type II 101.7 Ultimate Strength PSI | Type III 109.0 Ultimate Strength PSI |
|---|---|---|---|---|
| .125 | 3000 | 3000 | 3600 | 6500 |
| .090 | 1200 | 2300 | 3300 | - |
| .060 | 810 | 1700 | 1420 | - |

1 - See Figure No. 56 for thermal environment reproduced.

## TABLE VI - REVISION A [1]

## RESULTS OF ARC-JET ABLATION TEST ON ASBESTOS REINFORCED PHENOLIC LAMINATES

| Specimen No. | Type | Thickness Inches | Density Lbs/in$^3$ | Erosion Inches | Rate of Eros. mil/sec | Heat Flux BTU/ft$^2$-sec | Enthalpy BTU/Lb | Effective Heat of Ablation BTU/Lb |
|---|---|---|---|---|---|---|---|---|
| 9 | I | .466 | .0508 | .377 | 12.57 | 320 | 5950 | 3440 |
| 7 | II | .477 | .05405 | .168 | 5.6 | 180 | 2990 | 4130 |
| 6 | II | .456 | .0524 | .291 | 9.7 | 285 | 5800 | 3900 |
| 16 | I | .462 | .0530 | .243 | 8.1 | 245 | 4575 | 4170 |
| 13 | II | .466 | .0557 | .296 | 9.87 | 327 | 6100 | 4110 |
| 11 | II | .479 | .0589 | .199 | 6.63 | 315 | 5870 | 5570 |
| 19 | II | .470 | .05625 | .210 | 7.0 | 258 | 5870 | 4530 |
| 20 | II | .469 | .0573 | .189 | 6.3 | 238 | 4460 | 4600 |
| 4 | III | .476 | .0628 | .171 | 5.7 | 295 | 5550 | 5700 |
| 10 | III | .475 | .0603 | .230 | 7.66 | 315 | 5880 | 4710 |
| 14 | III | .482 | .0607 | .161 | 5.37 | 245 | 4580 | 5120 |
| 15 | III | .479 | .0617 | .180 | 6.0 | 283 | 5750 | 5280 |
| 17 | III | .481 | .06445 | .147 | 4.9 | 242 | 4520 | 5310 |
| 18 | III | .482 | .0642 | .173 | 5.77 | 300 | 5640 | 5630 |

[1] — The data have been corrected from originally published data to account for a faulty calorimeter in the original.

# TABLE VII

## THERMAL CONDUCTIVITY OF THREE PHENOLIC ASBESTOS LAMINATES

| Mat'l Type | Density Lbs/Ft³ | Average Mean Temp. °F | Average $\Delta$ T °F | Total Heat Input Watts | K BTU/hr/ft²/°F/in |
|---|---|---|---|---|---|
| IA | 84.5 | 111.5 | 5.7 | 2.3 | .98 |
| | | 403.3 | 57.3 | 31.28 | 1.32 |
| | | 716.1 | 98.7 | 66.37 | 1.63 |
| | | 1035.4 | 111.3 | 119.60 | 2.60 |
| II | 91.9 | 136.5 | 10.3 | 6.44 | 1.60 |
| | | 438.8 | 54.0 | 40.22 | 1.80 |
| | | 694.2 | 84.9 | 67.92 | 1.94 |
| | | 1041.3 | 102.7 | 115.88 | 2.73 |
| III | 109.0 | 116.9 | 4.6 | 3.59 | 1.91 |
| | | 420.5 | 43.2 | 36.66 | 2.06 |
| | | 705.2 | 78.1 | 73.70 | 2.29 |
| | | 731.5 | 76.4 | 73.17 | 2.32 |
| | | 978.9 | 100.4 | 118.16 | 2.84 |
| | | 988.9 | 114.6 | 130.64 | 2.76 |

1 - Area of Central Heater = 12.57 in.$^2$

2 - Panel 7" diameter x .1239 thick

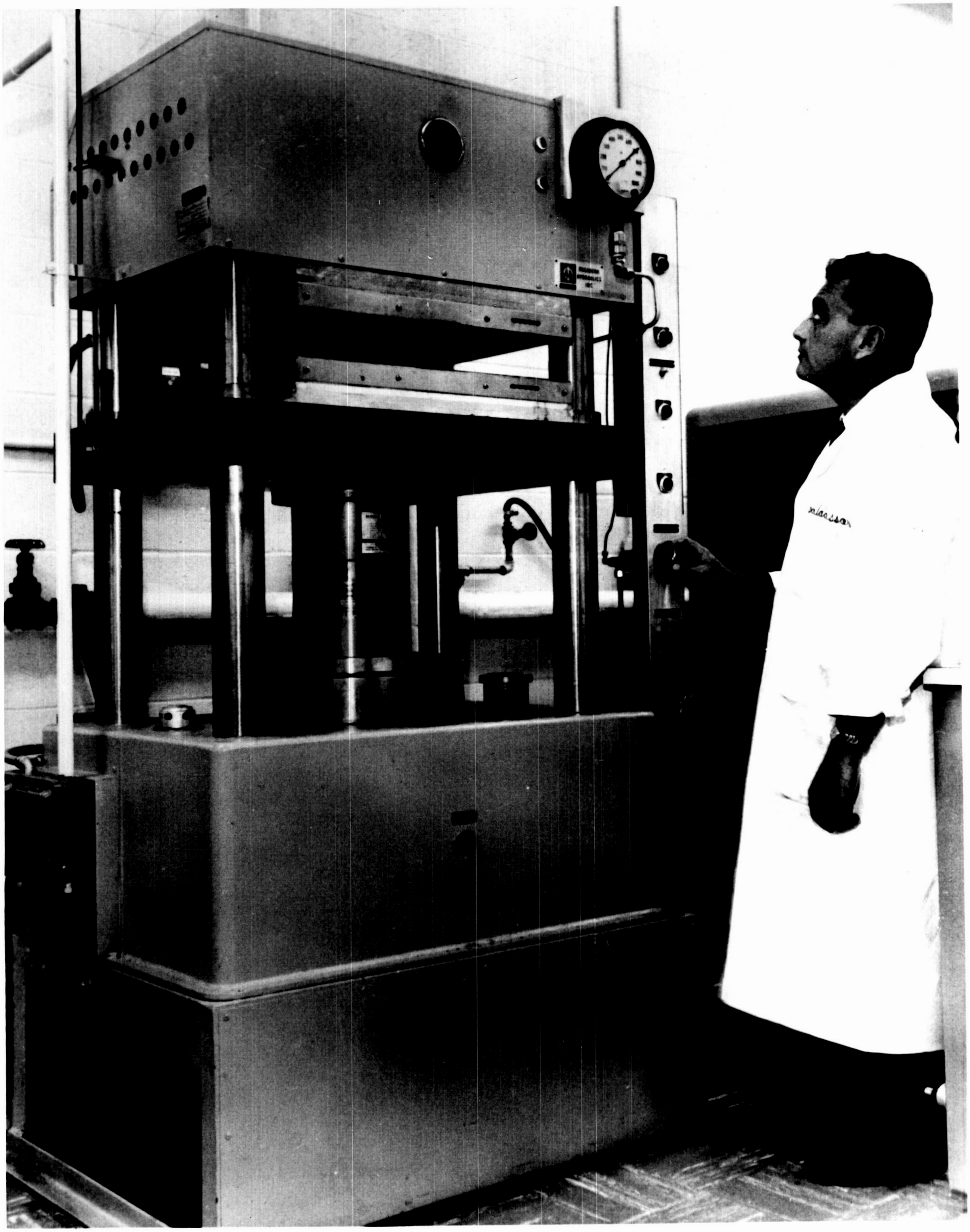

**Figure 1 — Molding of ablation specimen on 150 ton hydraulic press**

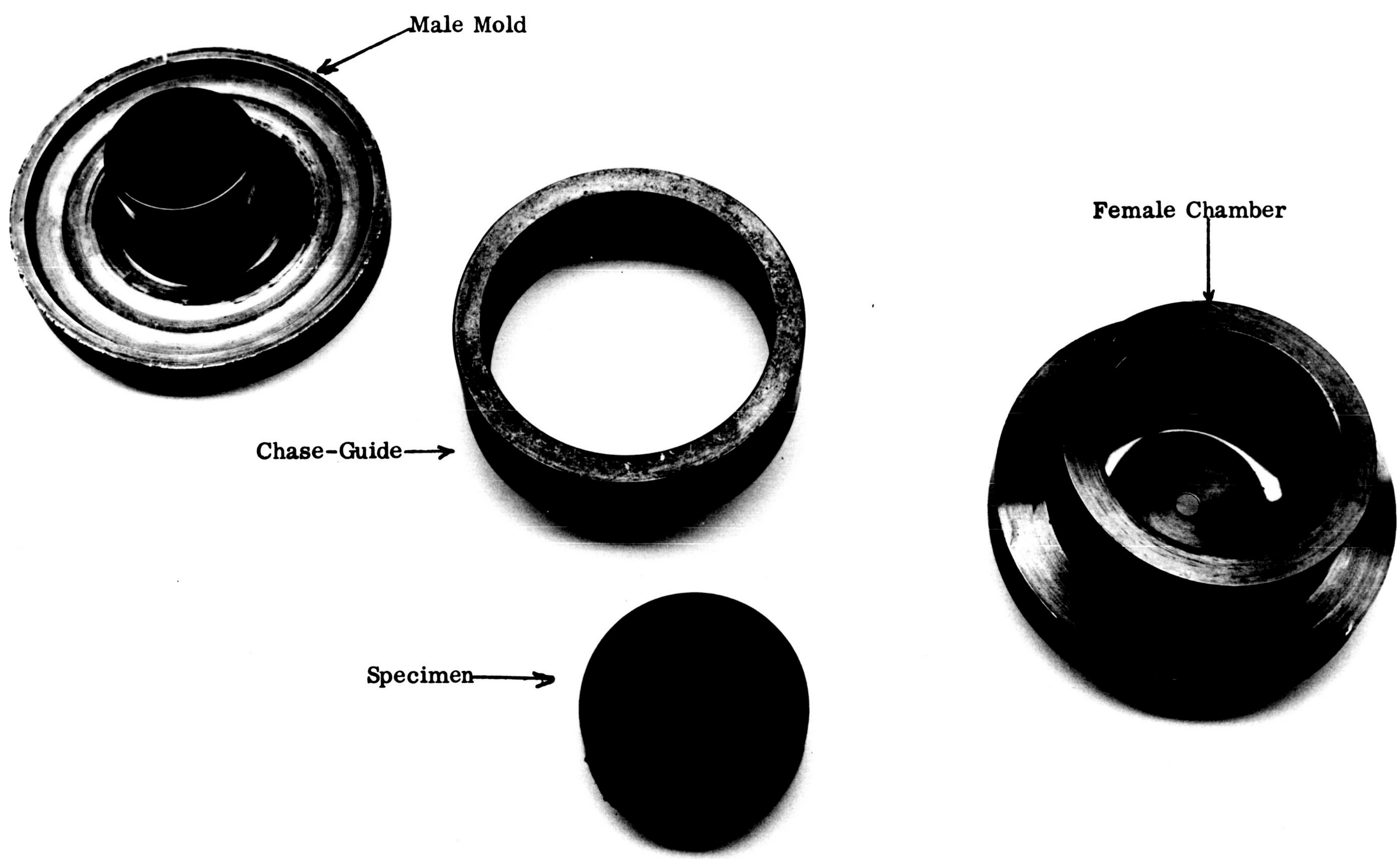


Figure 2 — Exploded view of compression molding tool for ablation specimen

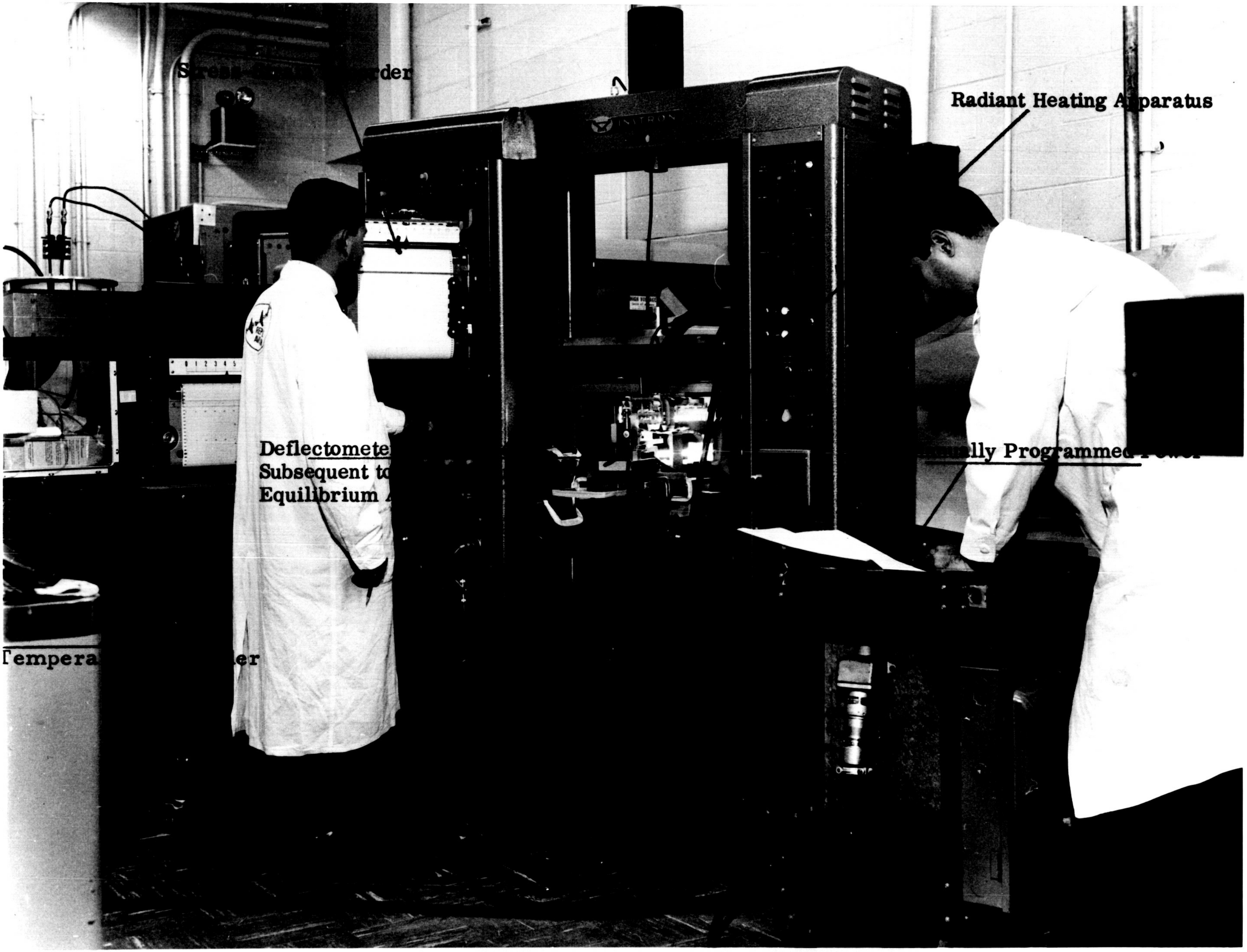


Figure 3 —Test set-up for rapid soak-condition heating for flexural test at 1000°F

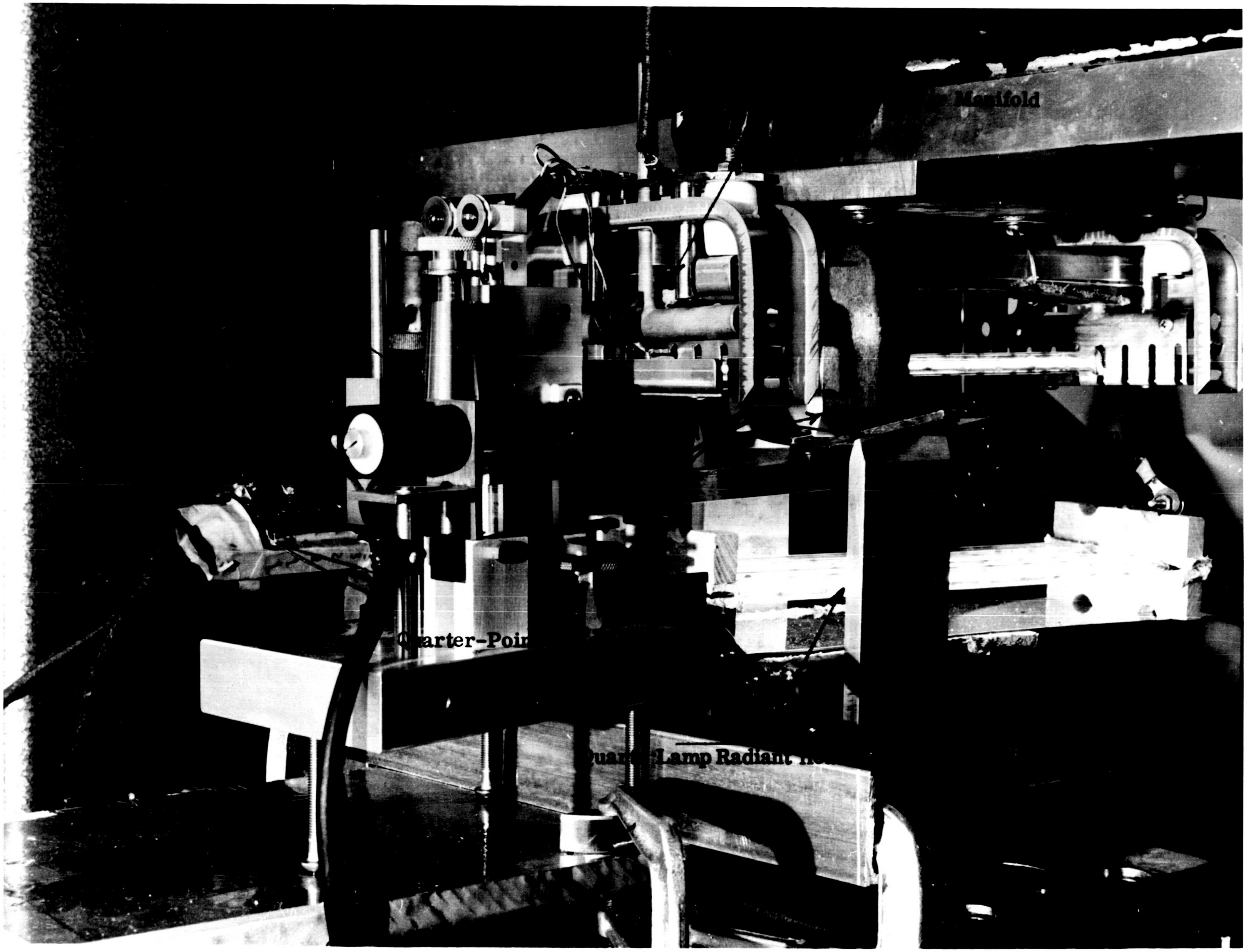


Figure 4 –Close-up of rapid soak heating assembly for flexural testing at 1000°F

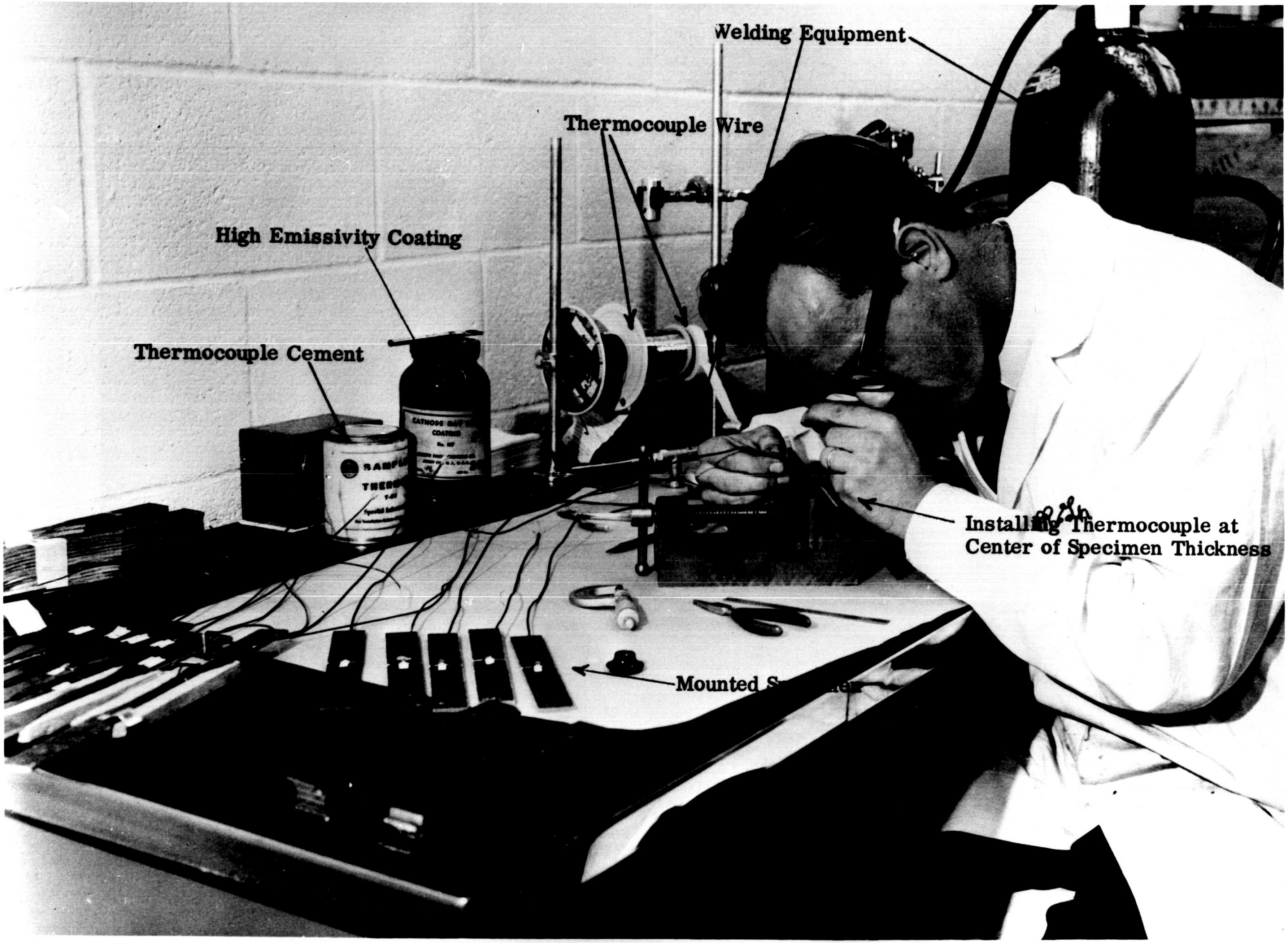


Figure 5 — Installing chromel-alumel and platinum rhodium thermocouples

Figure 6 – Measuring of ablation specimens before exposure

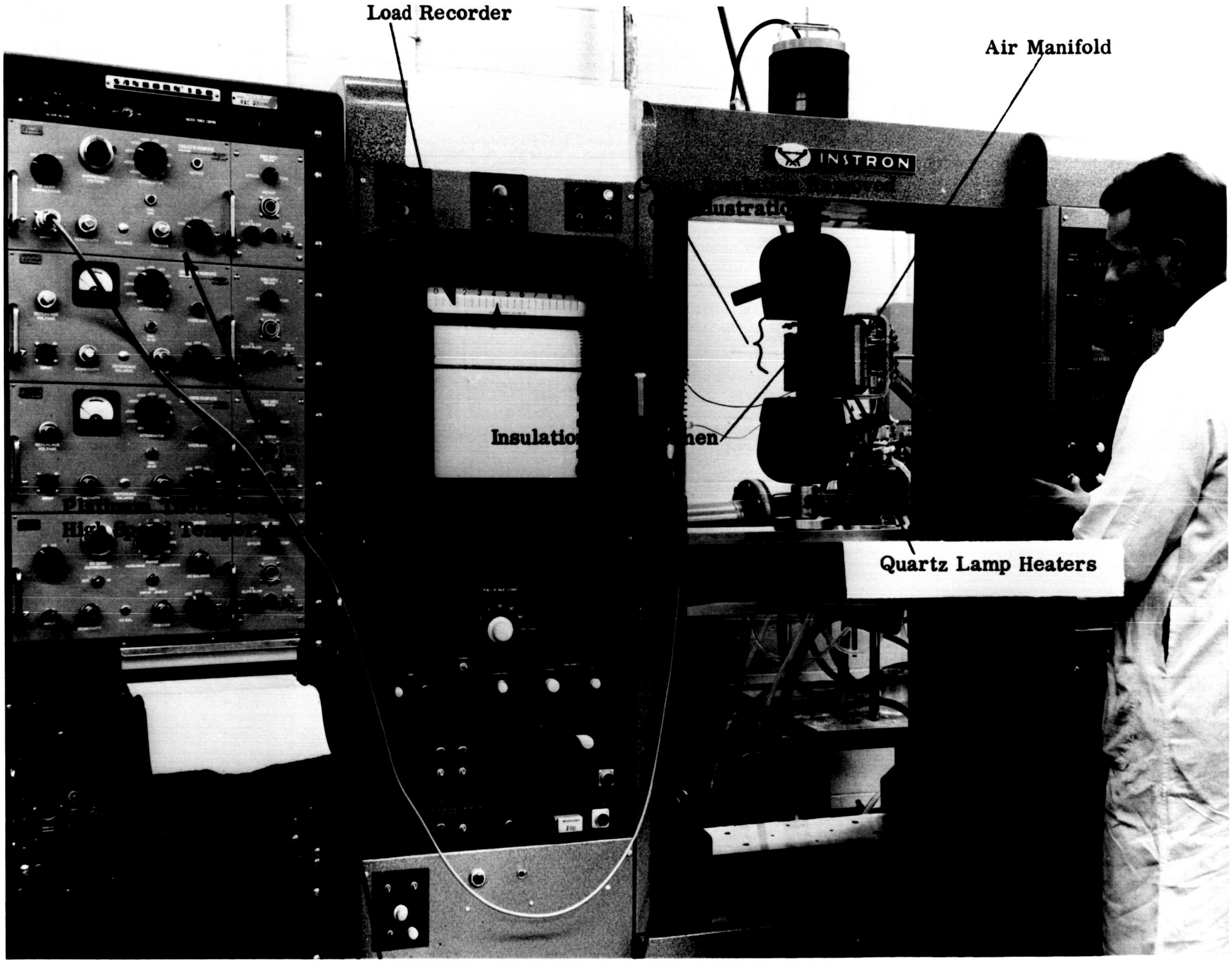


Figure 7 — Transient heating testing apparatus

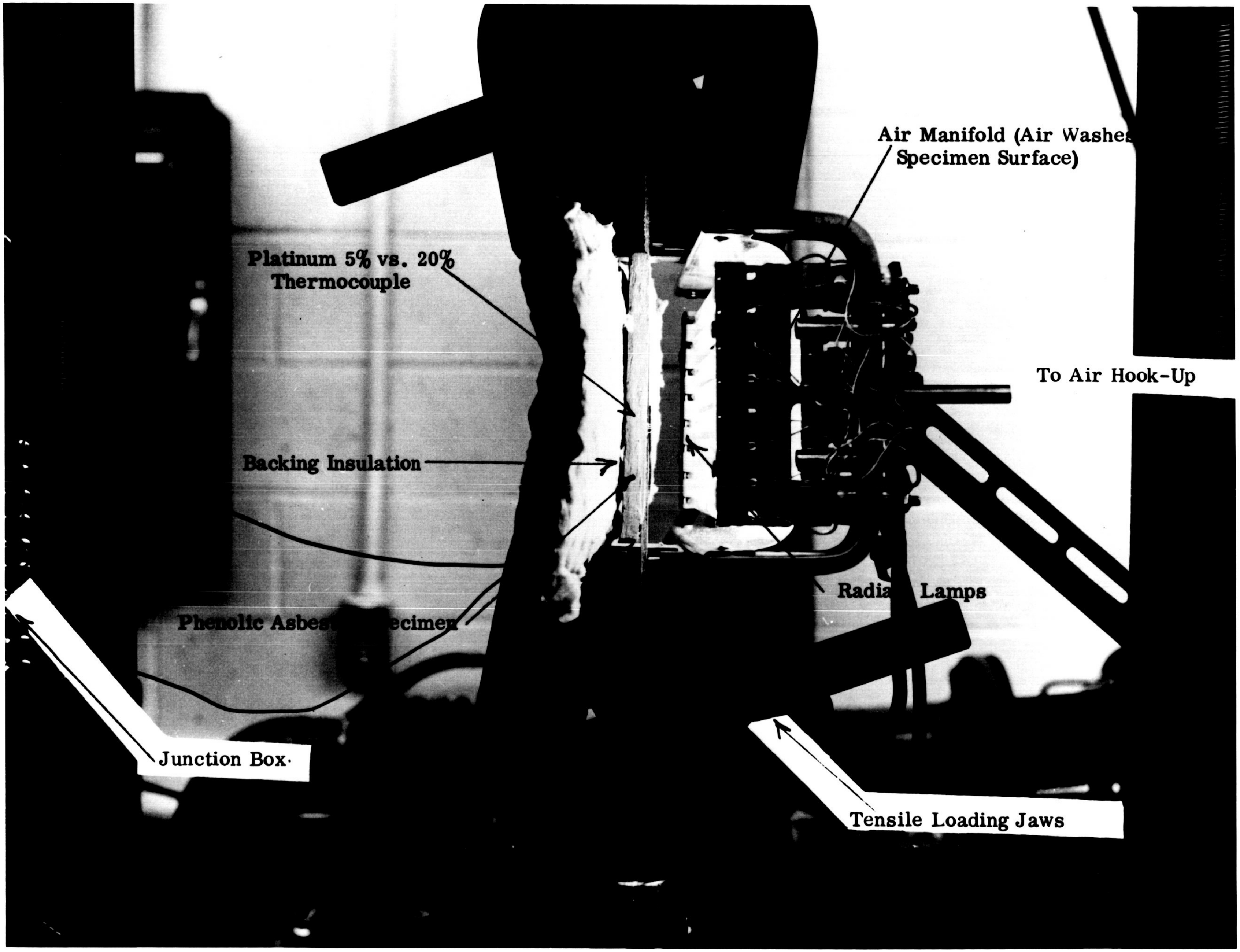


Figure 8 — Close-up of transient heating facility

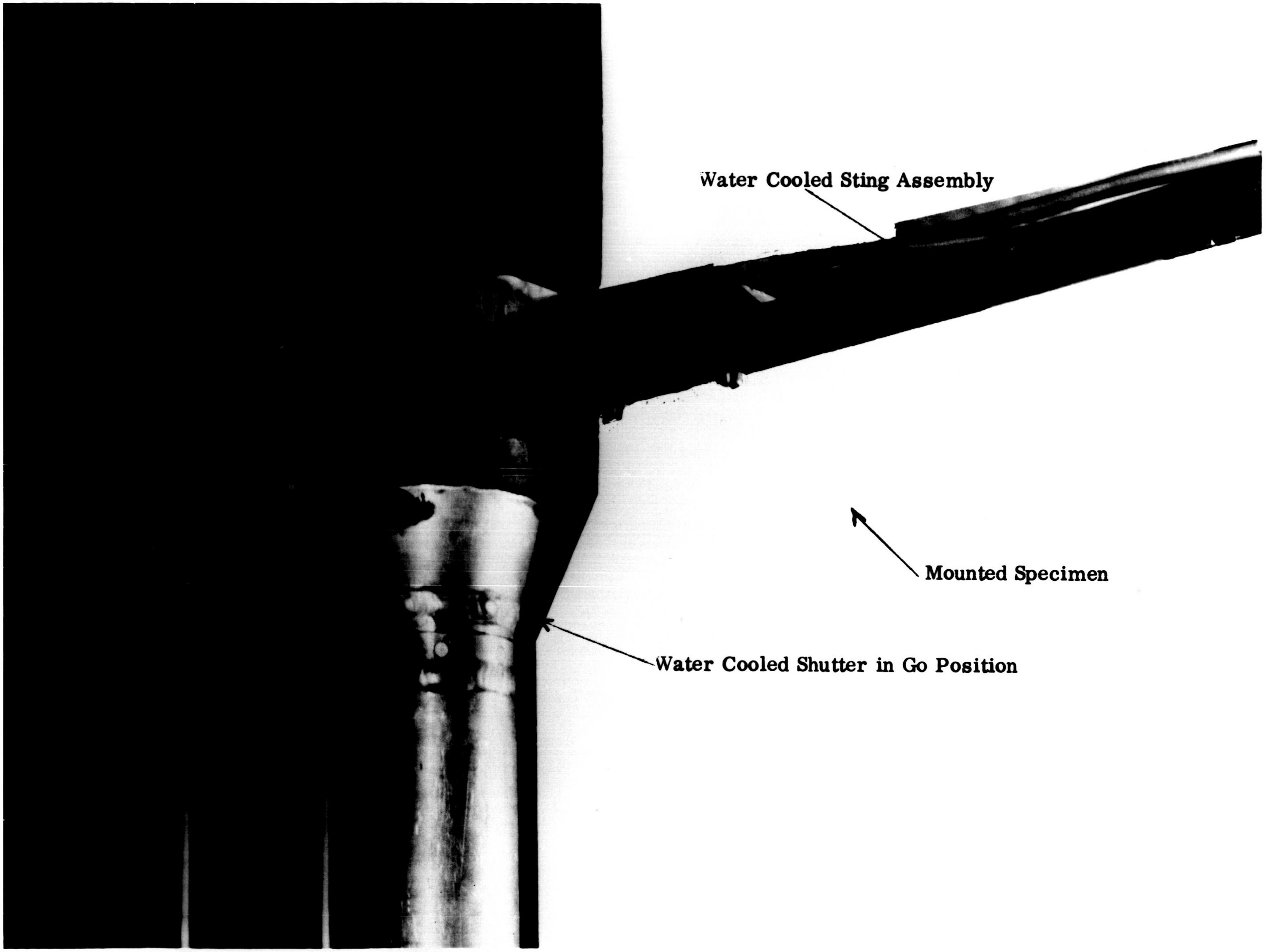


Figure 9 — Arc Jet Specimen

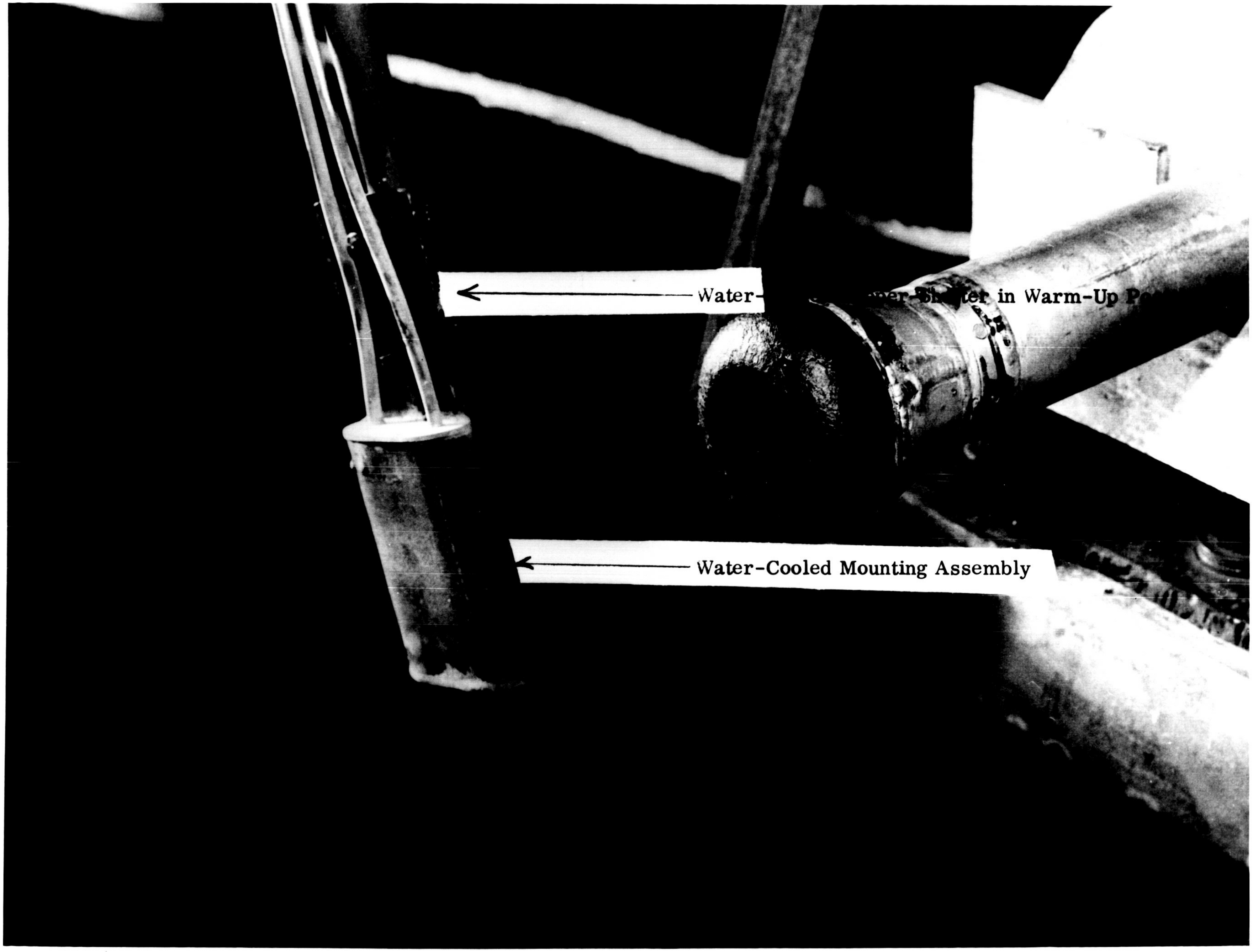


Figure 10 — Arc jet specimen with shutter in warm-up position

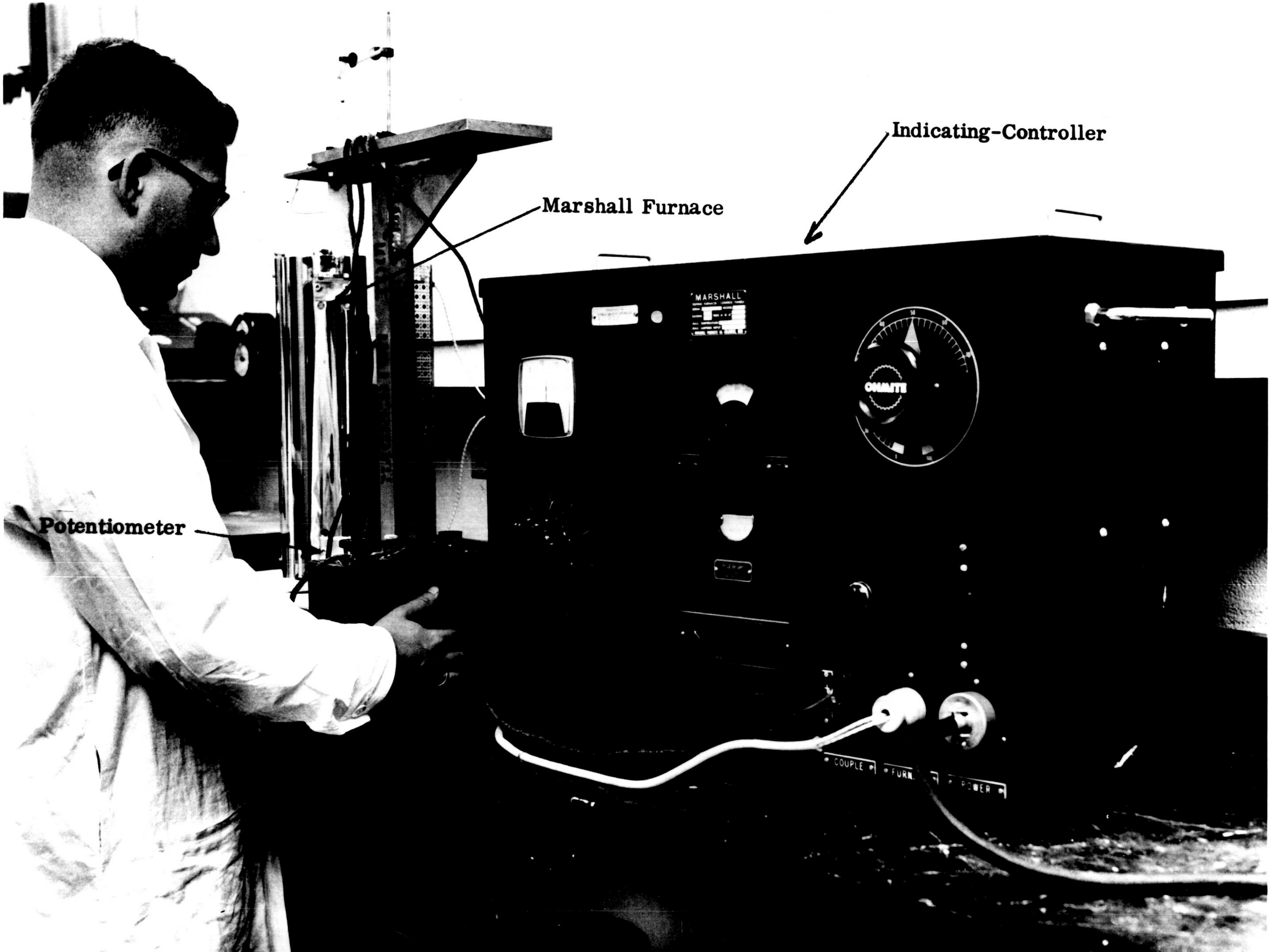


Figure 11 - Thermal Expansion Conductivity Test Set-up

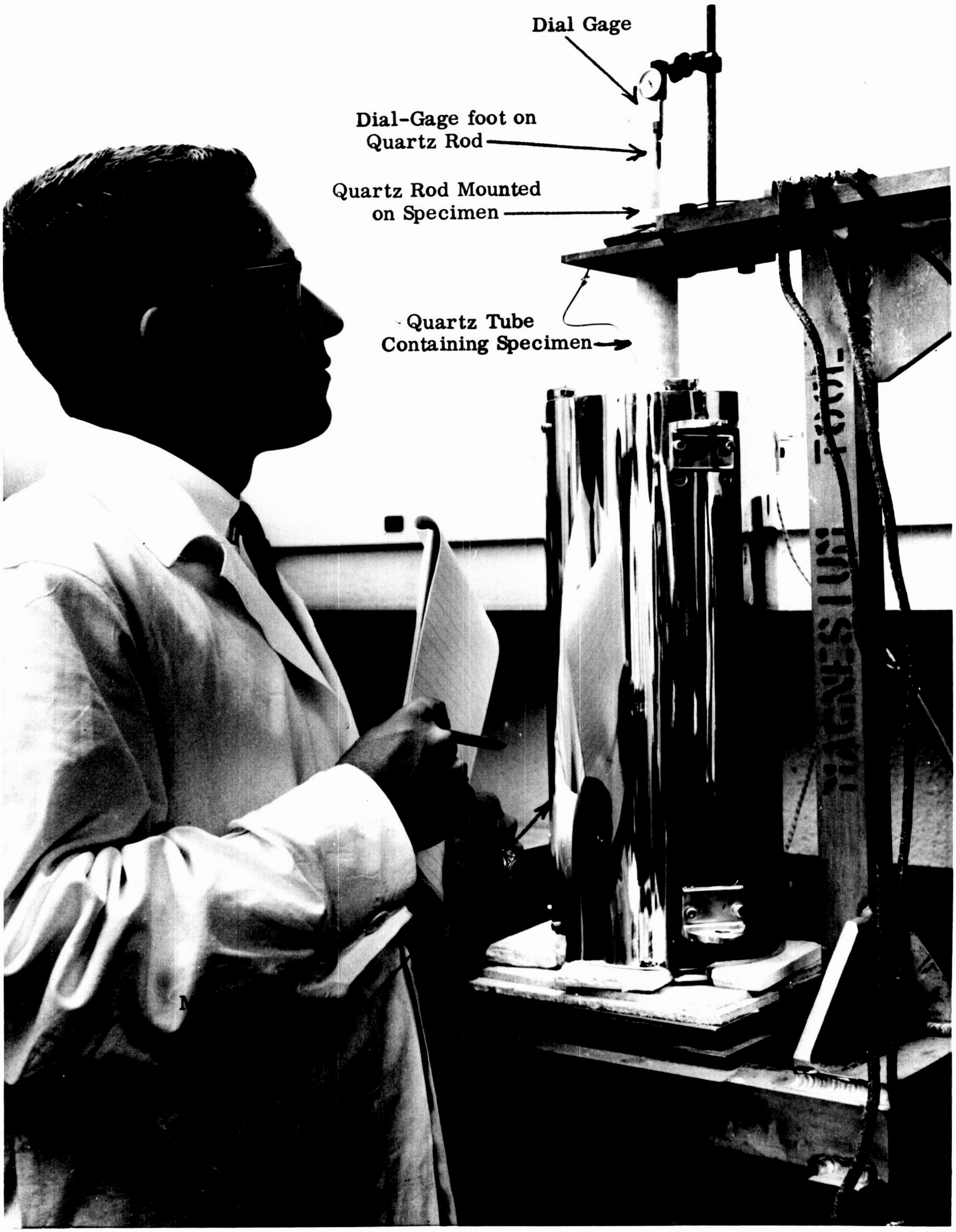


Figure 12 - Closeup of Thermal Expansion Test Set-up

Group II Specimen Numbers

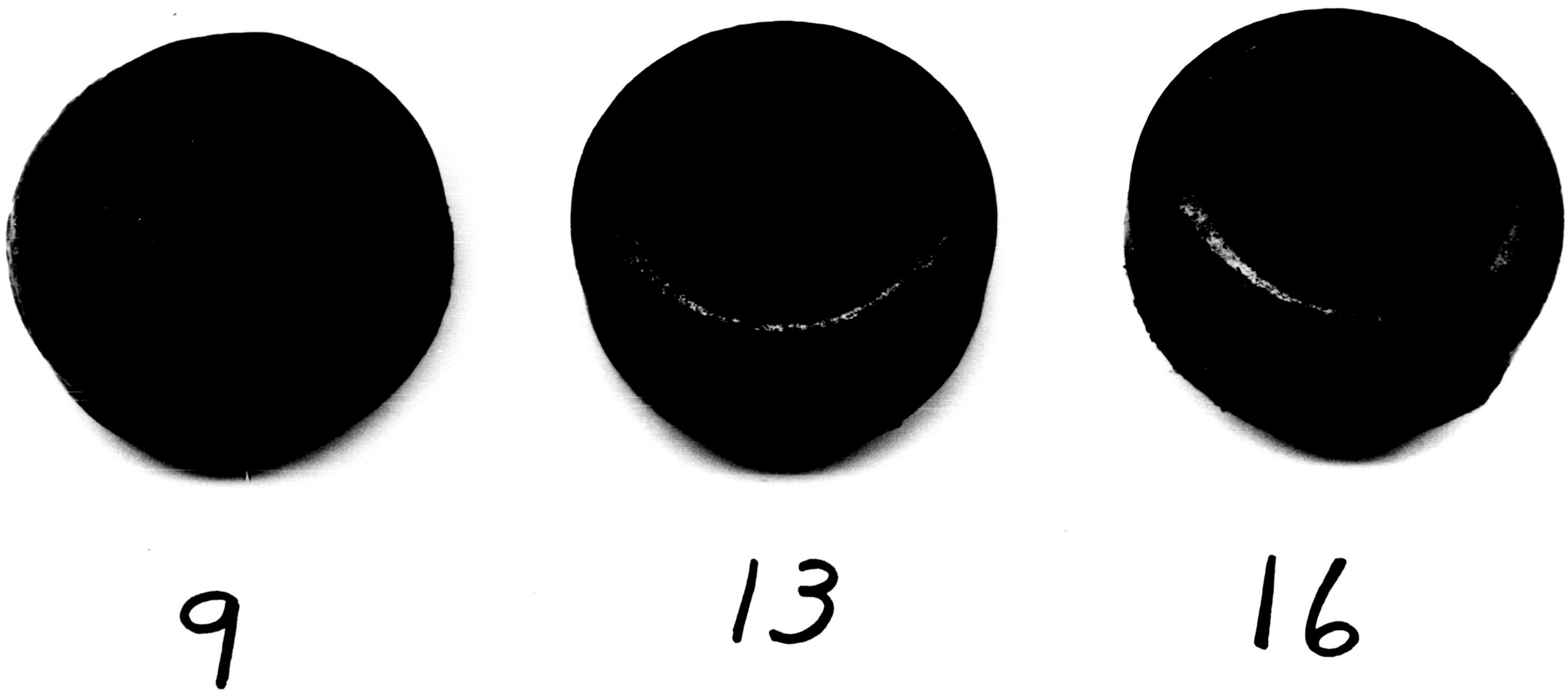


Figure 13 – Surface characteristics of group II ablation specimens before "exposure".

Group III Specimen Numbers

9586

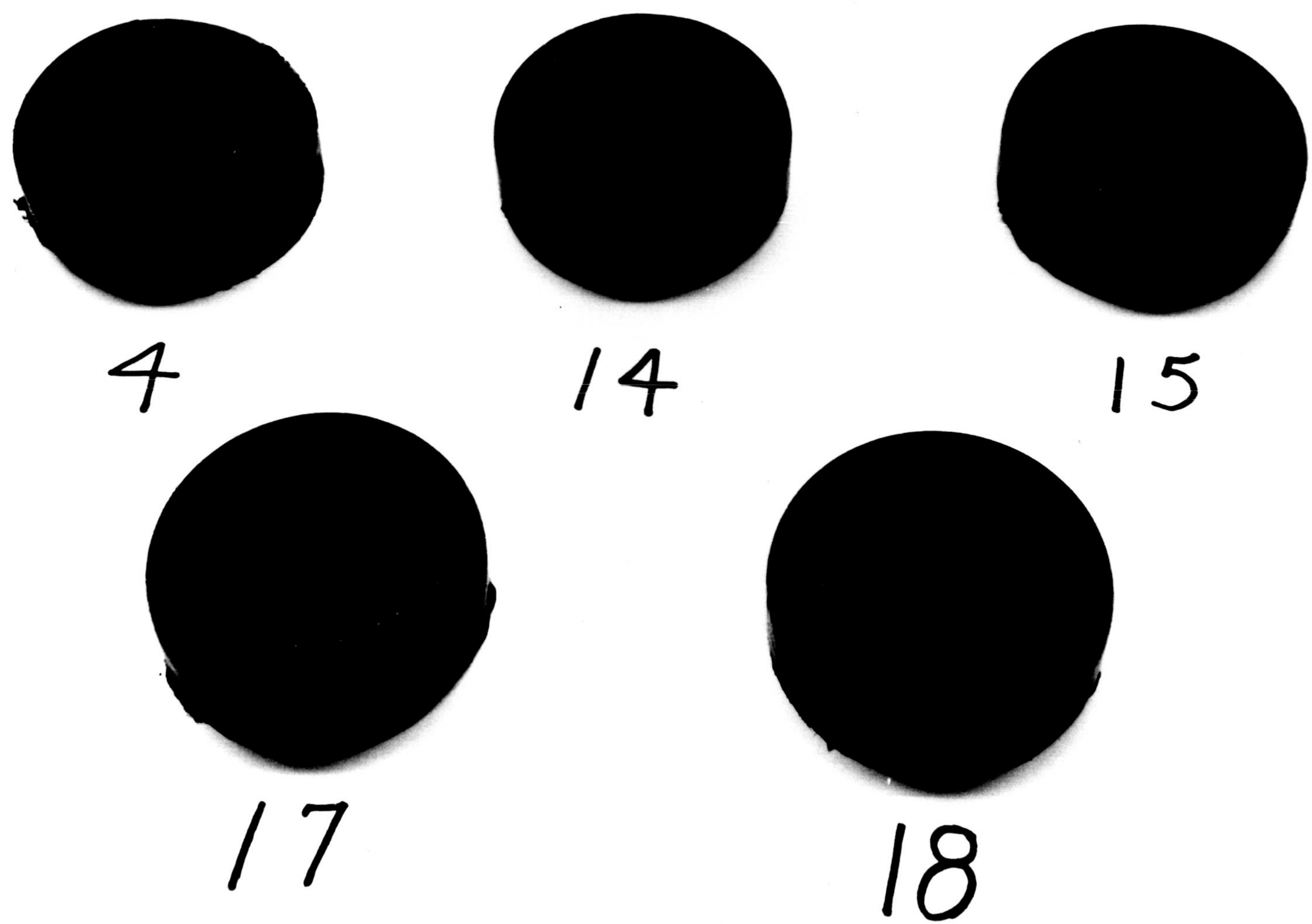


**Figure 14 – Surface characteristics of Group III ablation specimens before exposure**

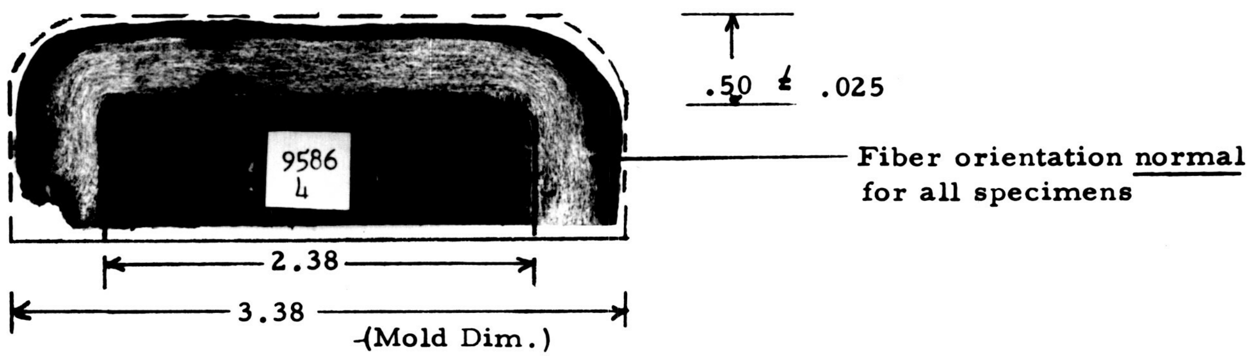


Density = .0628 lb/in$^3$

Figure 15 - Cross-Section of Phenolic-Asbestos Specimen No. 4 After 30 seconds Arc-jet Exposure at 294 BTU/ft$^2$ - second

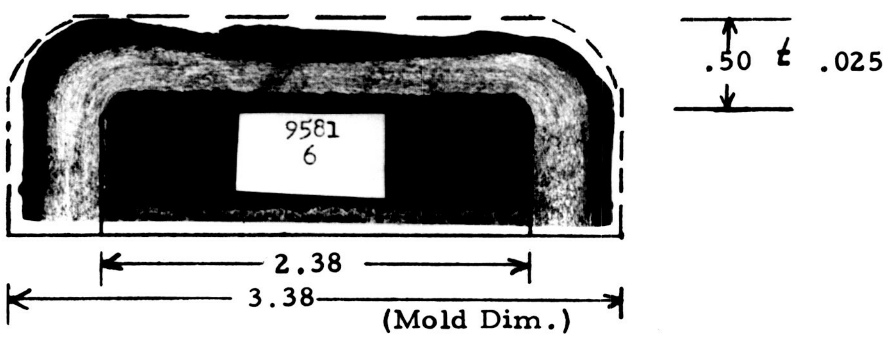


Density = .0524 lb/in$^3$

Figure 16 - Cross-Section of Phenolic-Asbestos No. 6 After 30 seconds Arc-jet Exposure At 285 BTU/ft$^2$ - second

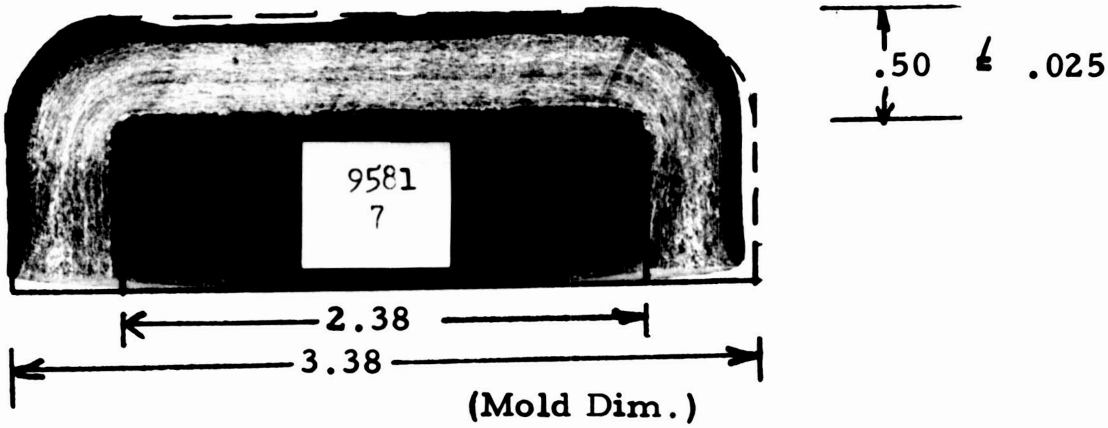


Density = .05405 lb/in$^3$

Figure 17 - Cross-Section of Phenolic-Asbestos
Specimen No. 7 After 30 seconds Arc-jet Exposure
at 180 BTU/ft$^2$- second

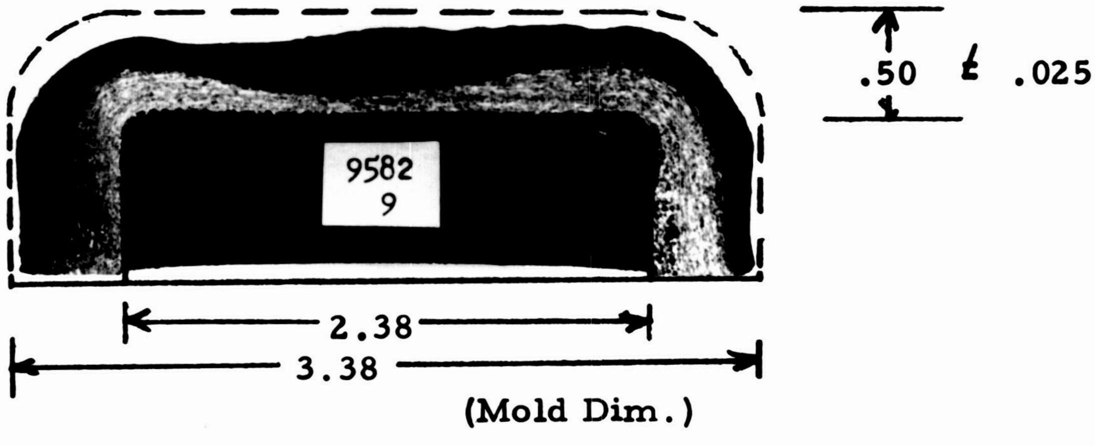


Density = .0508 lb/in$^3$

Figure 18 - Cross-Section of Phenolic-Asbestos
Specimen No. 9 After 30 seconds Arc-jet Exposure
at 320 BTU/ft$^2$- second

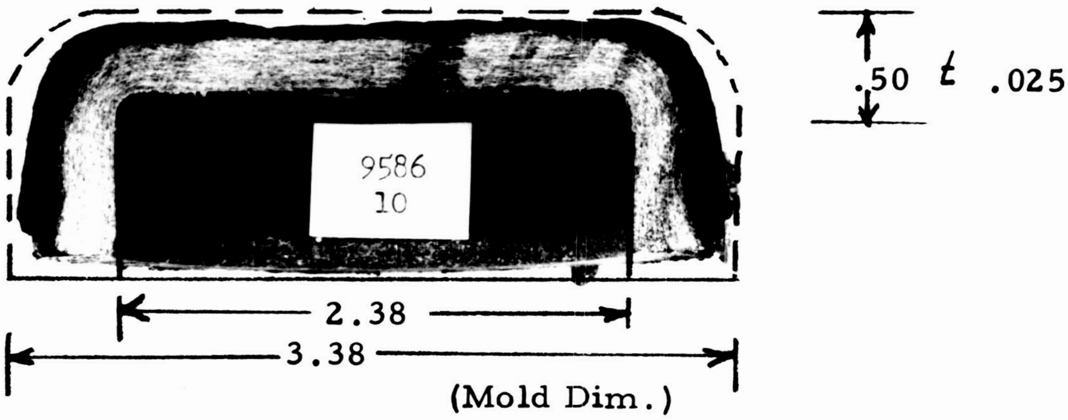


Density = .0603 lb/in$^3$

Figure 19 - Cross-Section of Phenolic-Asbestos Specimen No. 10 After 30 seconds Arc-jet Exposure at 315 BTU/ft$^2$ - second

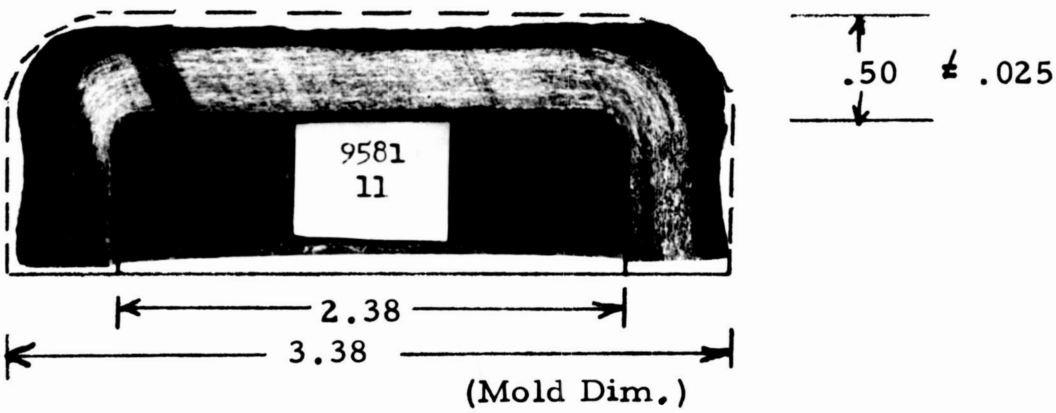


Density = .0589 lb/in$^3$

Figure 20 - Cross-Section of Phenolic-Asbestos Specimen No. 11 After 30 seconds Arc-jet Exposure at 315 BTU/ft$^2$ - second

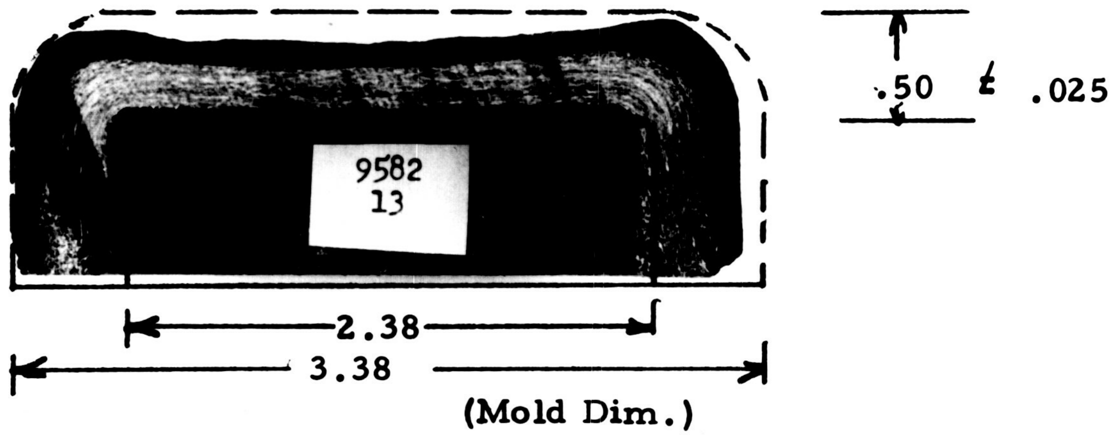


Density = .0557 lb/in$^3$

Figure 21 - Cross-Section of Phenolic-Asbestos Specimen No. 13 After 30 seconds Arc-jet Exposure at 327 BTU/ft$^2$ - second

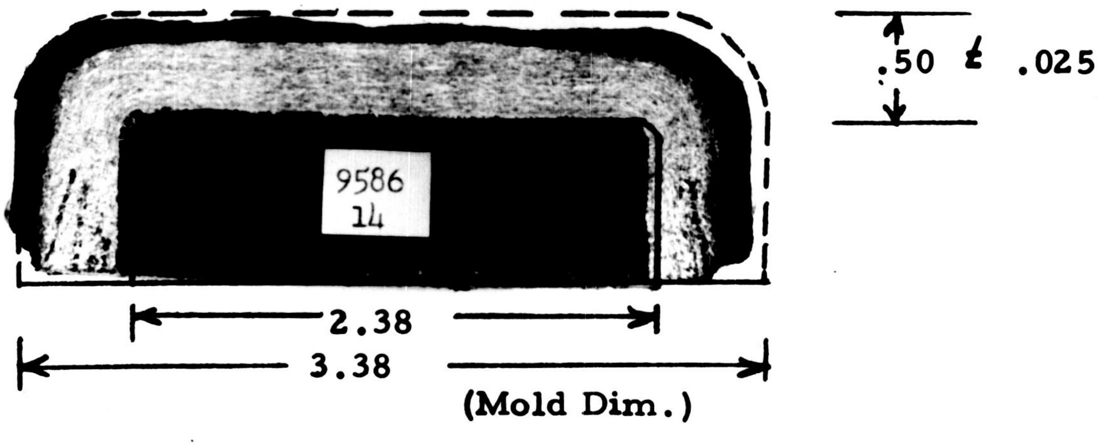


Density = .0607 lb/in$^3$

Figure 22 - Cross-Section of Phenolic-Asbestos Specimen No. 14 After 30 seconds Arc-jet Exposure at 245 BTU/ft$^2$ - second

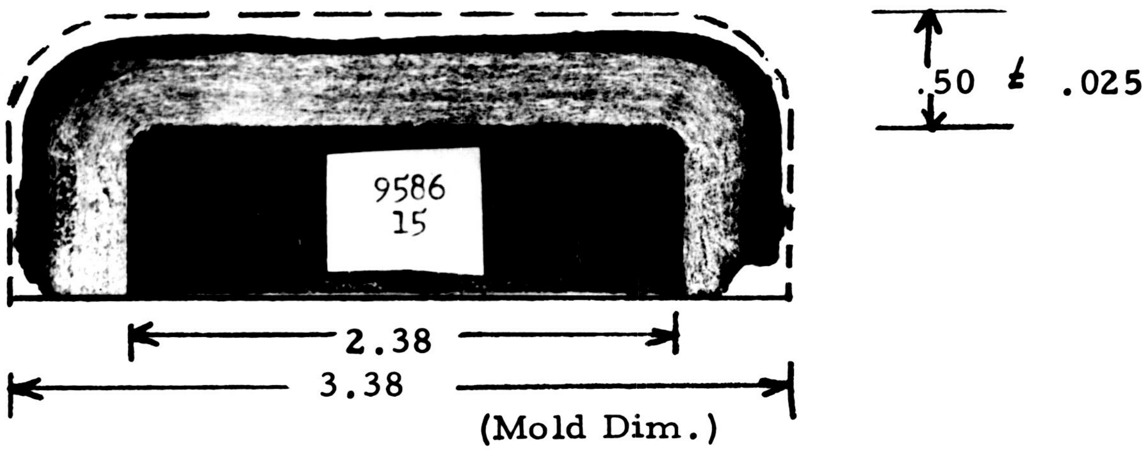


Density = .0617 lb/in$^3$

Figure 23 --Cross-Section of Phenolic-Asbestos Specimen No. 15 After 30 seconds Arc-jet Exposure at 283 BTU/ft$^2$- second

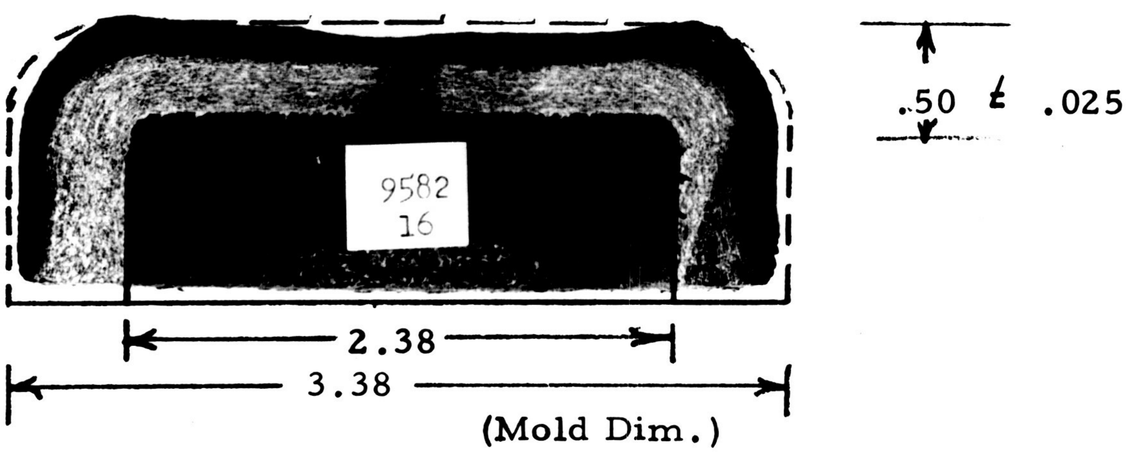


Density = .0530 lb/in$^3$

Figure 24 - Cross-Section of Phenolic-Asbestos Specimen No. 16 After 30 seconds Arc-jet Exposure at 245 BTU/ft$^2$- second

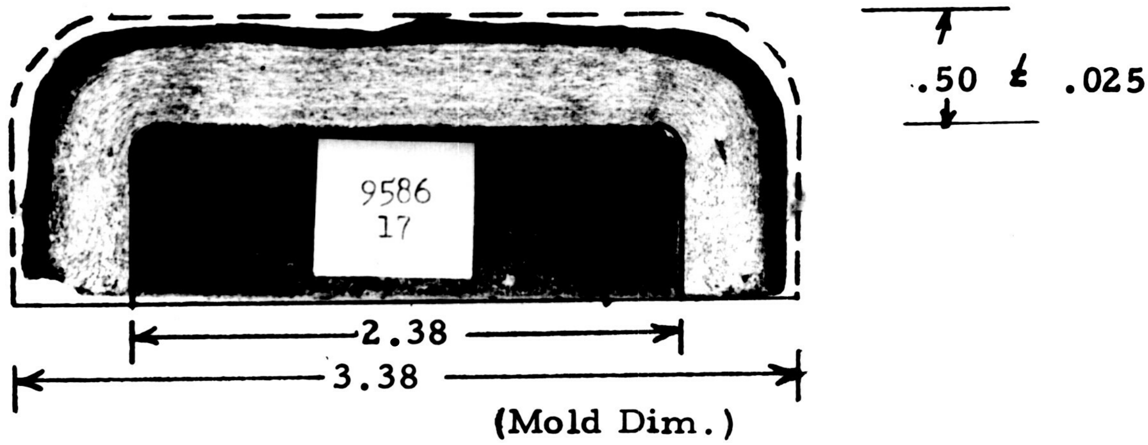


Density = .06445 lb/in$^3$

Figure 25 - Cross-Section of Phenolic-Asbestos Specimen No. 17 After 30 seconds Arc-jet Exposure at 242 BTU/ft$^2$ - second

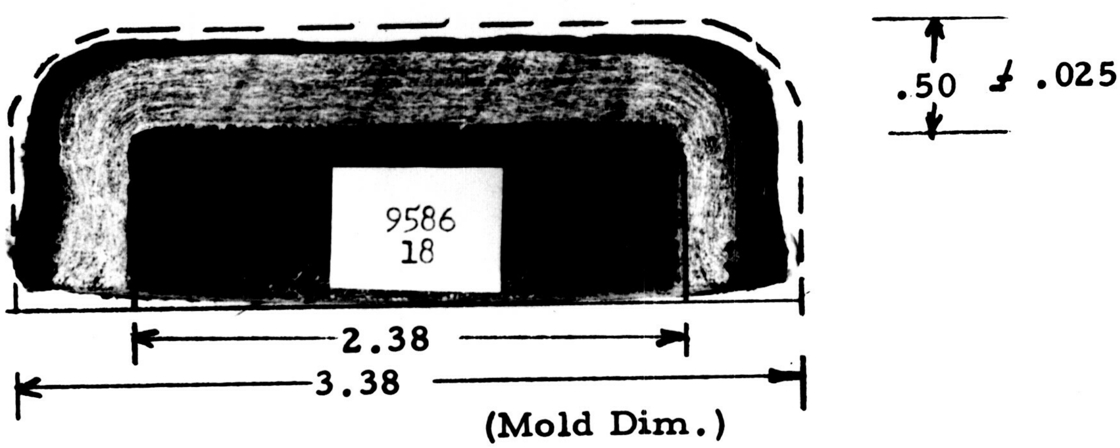


Density = .0642 lb/in$^3$

Figure 26 - Cross-Section of Phenolic-Asbestos Specimen No. 18 After 30 Seconds Arc-Jet Exposure at 300 BTU/ft$^2$ second

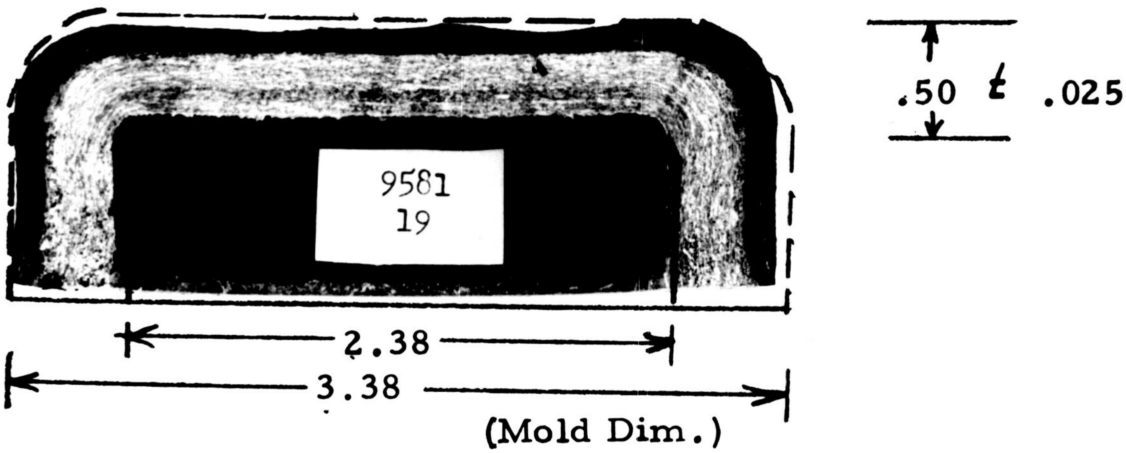


Density = .05625 lb/in$^3$

Figure 27 - Cross-Section of Phenolic-Asbestos Specimen No. 19 After 30 seconds Arc-jet Exposure at 258 BTU/ft$^2$- second

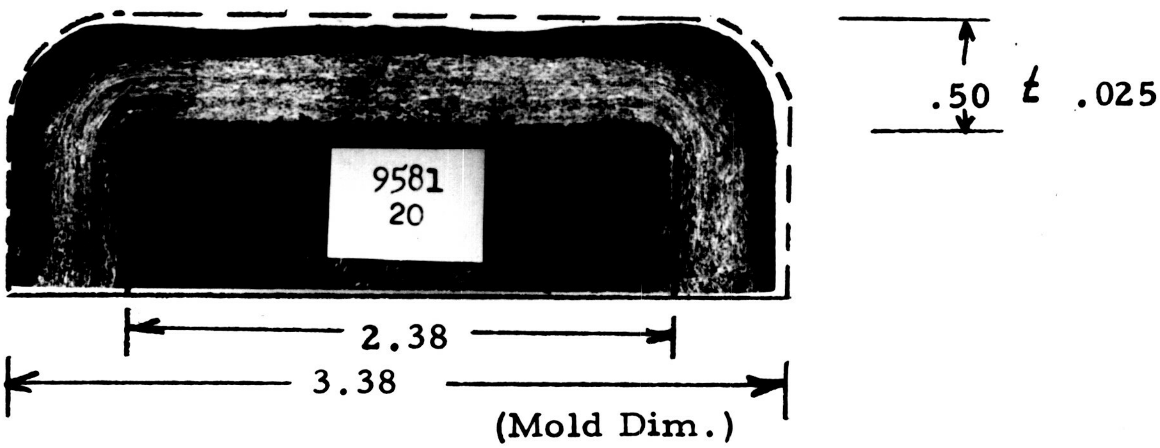


Density = .0573 lb/in$^3$

Figure 28 - Cross-Section of Phenolic-Asbestos Specimen No. 20 After 30 seconds Arc-jet Exposure at 238 BTU/ft$^2$- second

RD - 1616-1

RD-1615-1

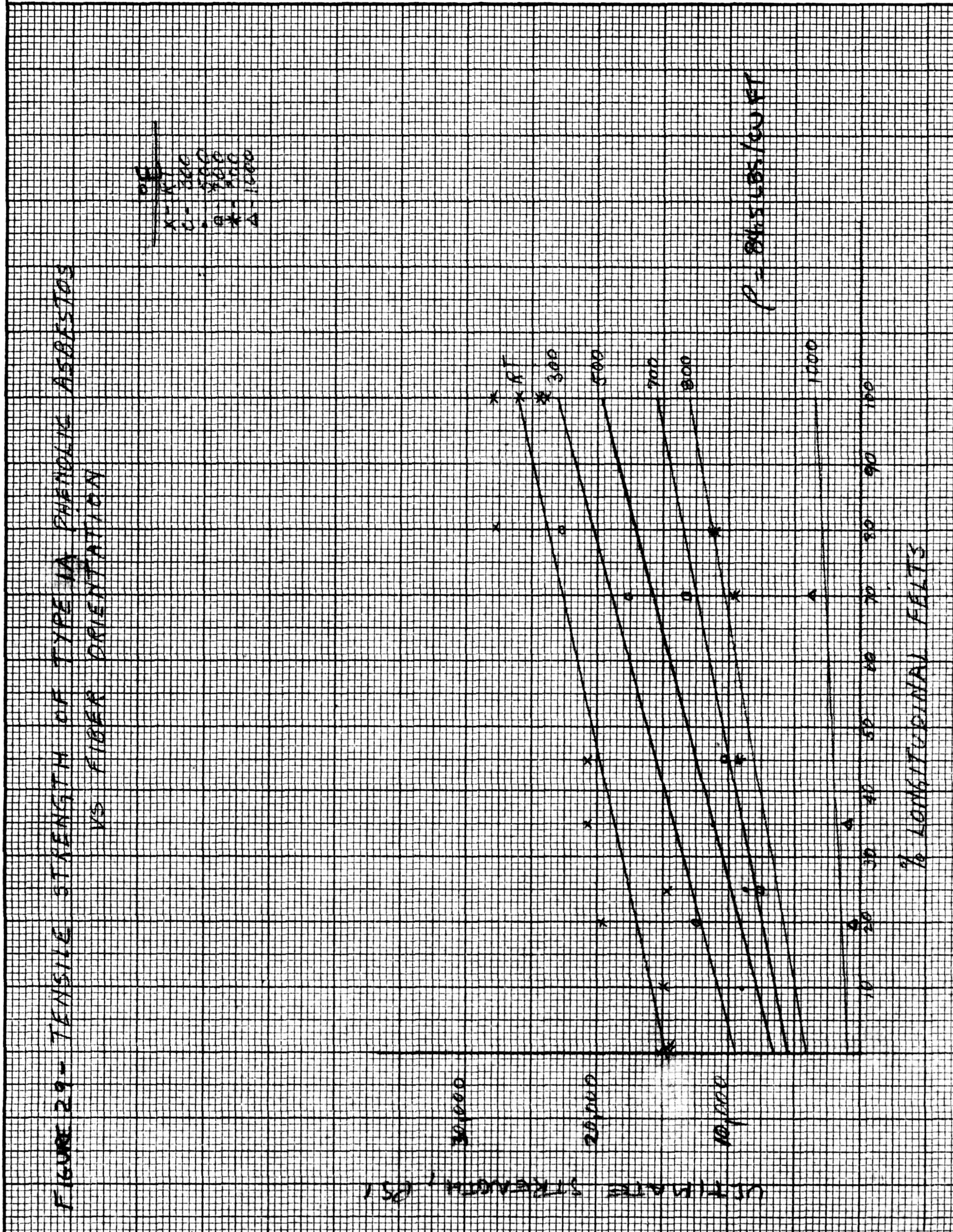


FIGURE 29 - TENSILE STRENGTH OF TYPE 1A PHENOLIC ASBESTOS VS FIBER ORIENTATION

PREPARED
CHECKED
REVISED

REPUBLIC AVIATION

PAGE
REPORT NO.
MODEL

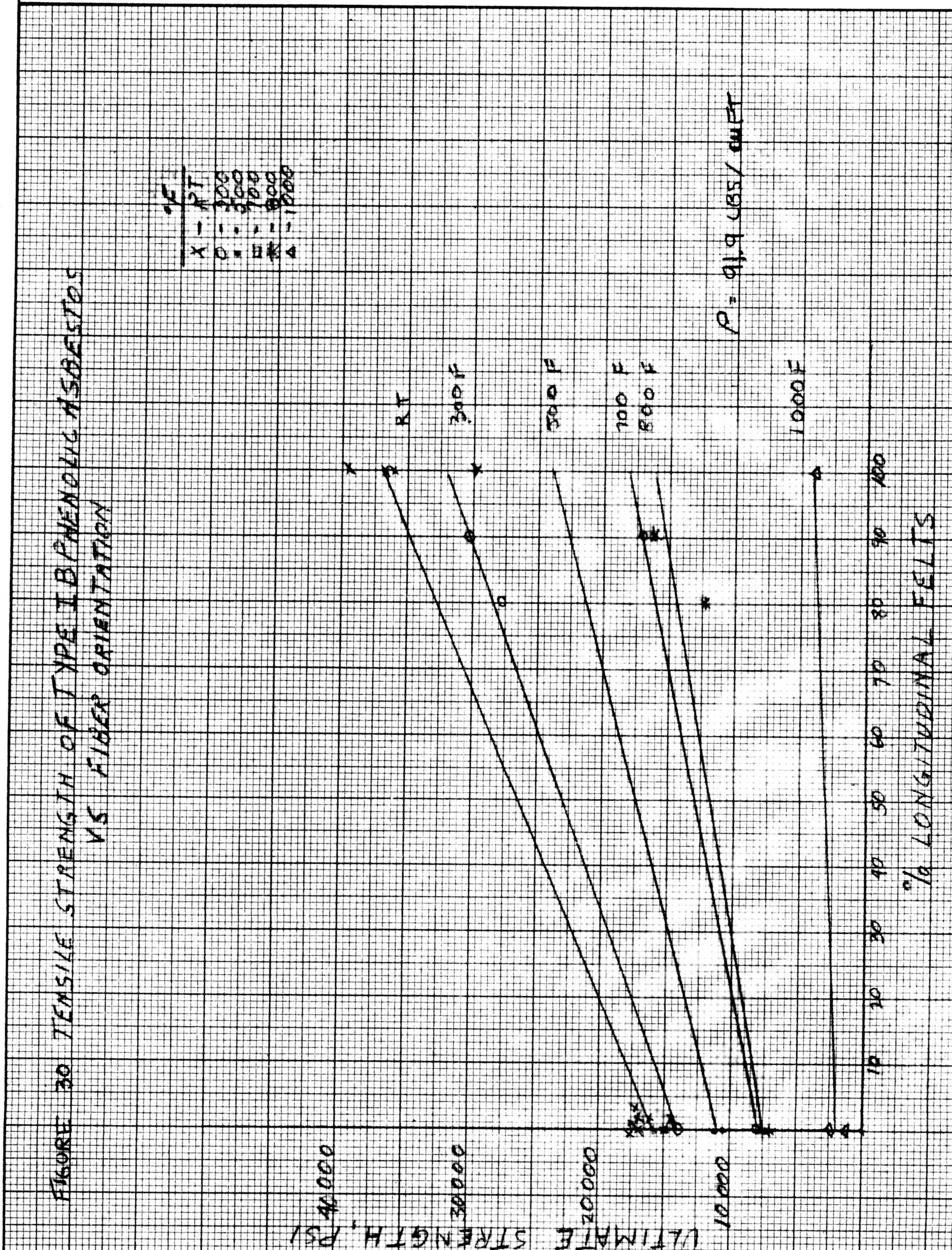


FIGURE 30 TENSILE STRENGTH OF TYPE I B PHENOLIC ASBESTOS VS FIBER ORIENTATION

E-1-10A
REV. 2/49

PREPARED ______ ______

CHECKED ______ ______

REVISED ______ ______

PAGE ______

REPORT NO. ______

MODEL ______

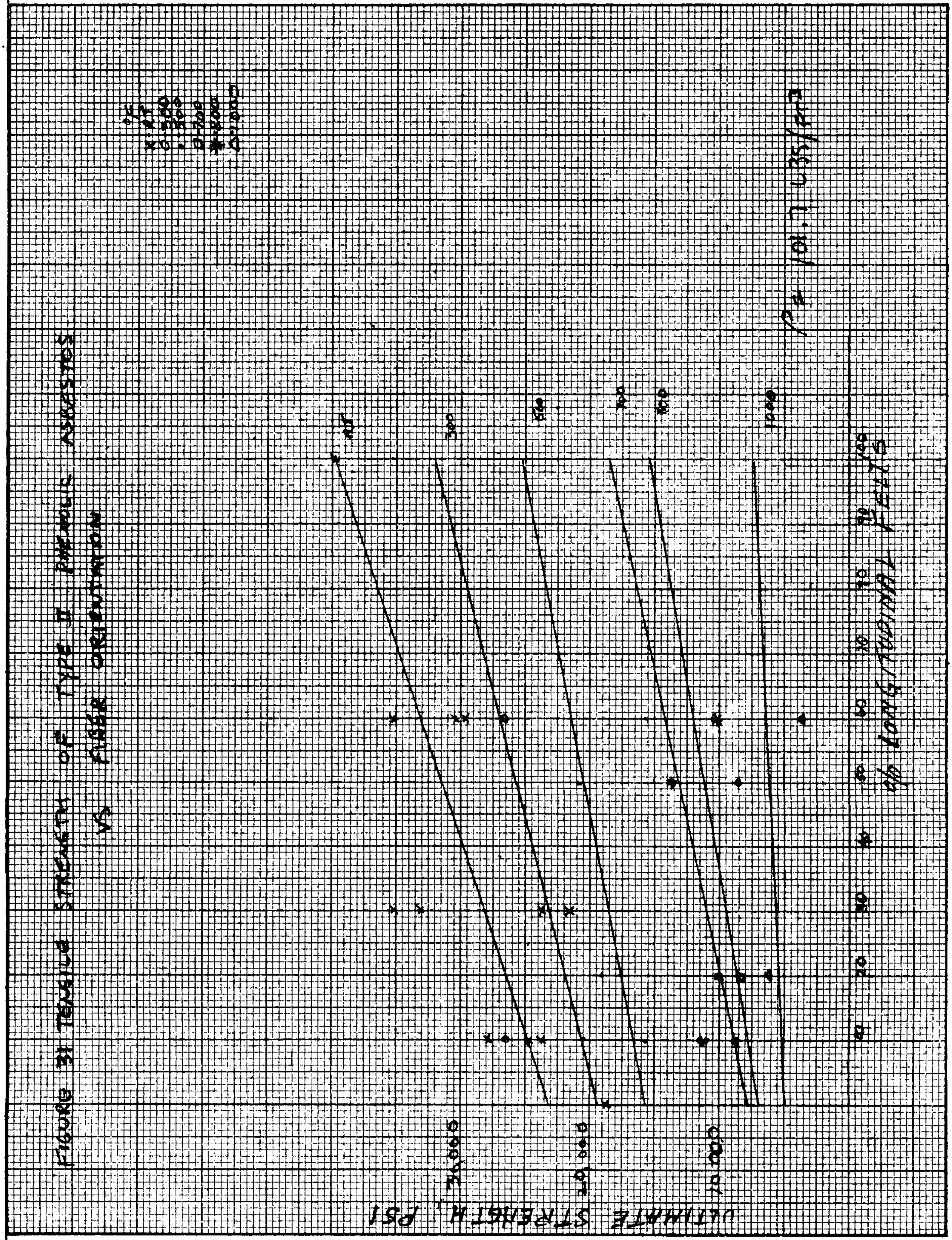


E-1-10A
REV. 2/49

PREPARED

CHECKED

REVISED

REPUBLIC AVIATION

PAGE

REPORT NO.

MODEL

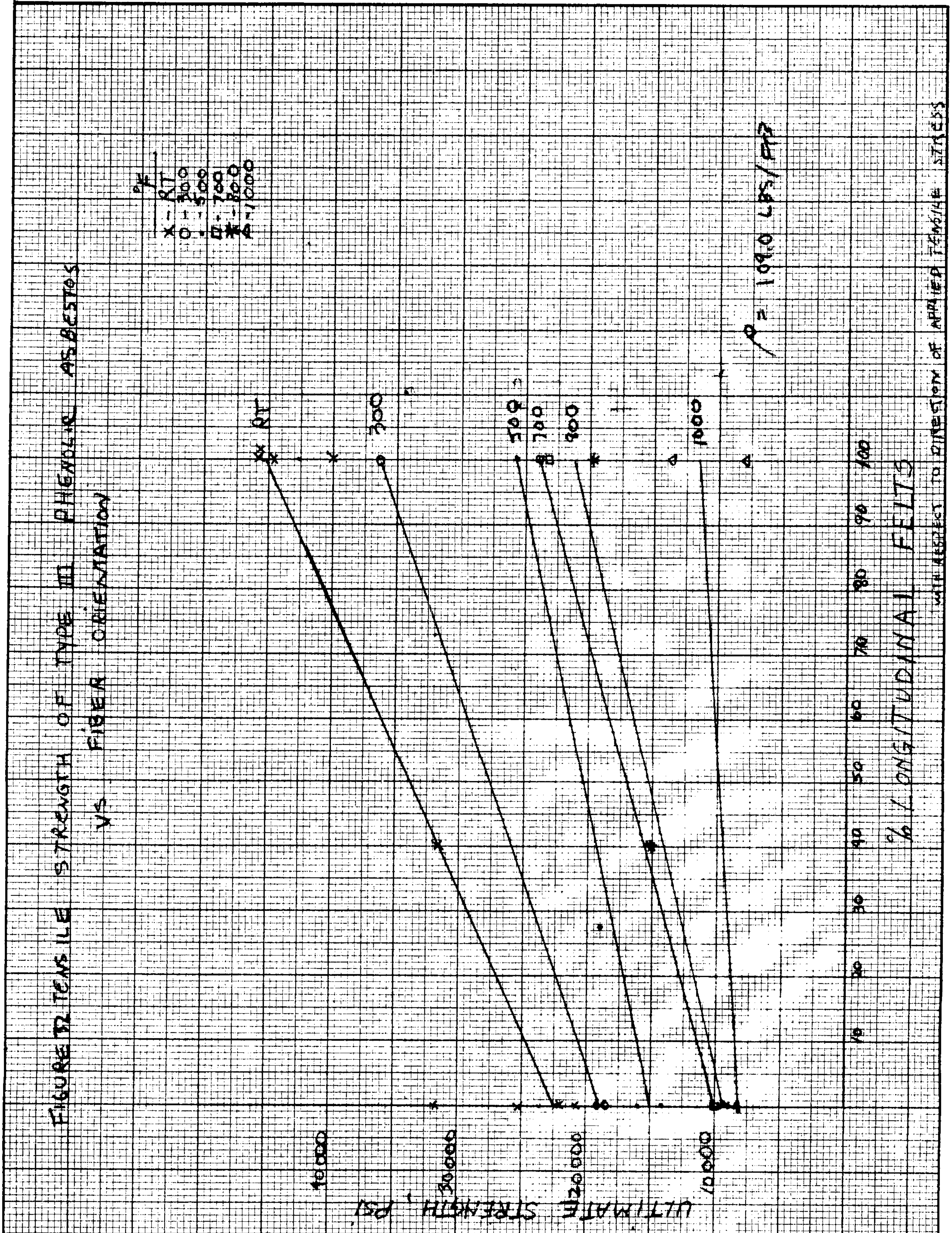


E-1-10A
REV. 2/49

PREPARED ____________ ______

CHECKED ____________ ______

REVISED ____________ ______

REPUBLIC AVIATION

PAGE ____________

REPORT NO. ____________

MODEL ____________

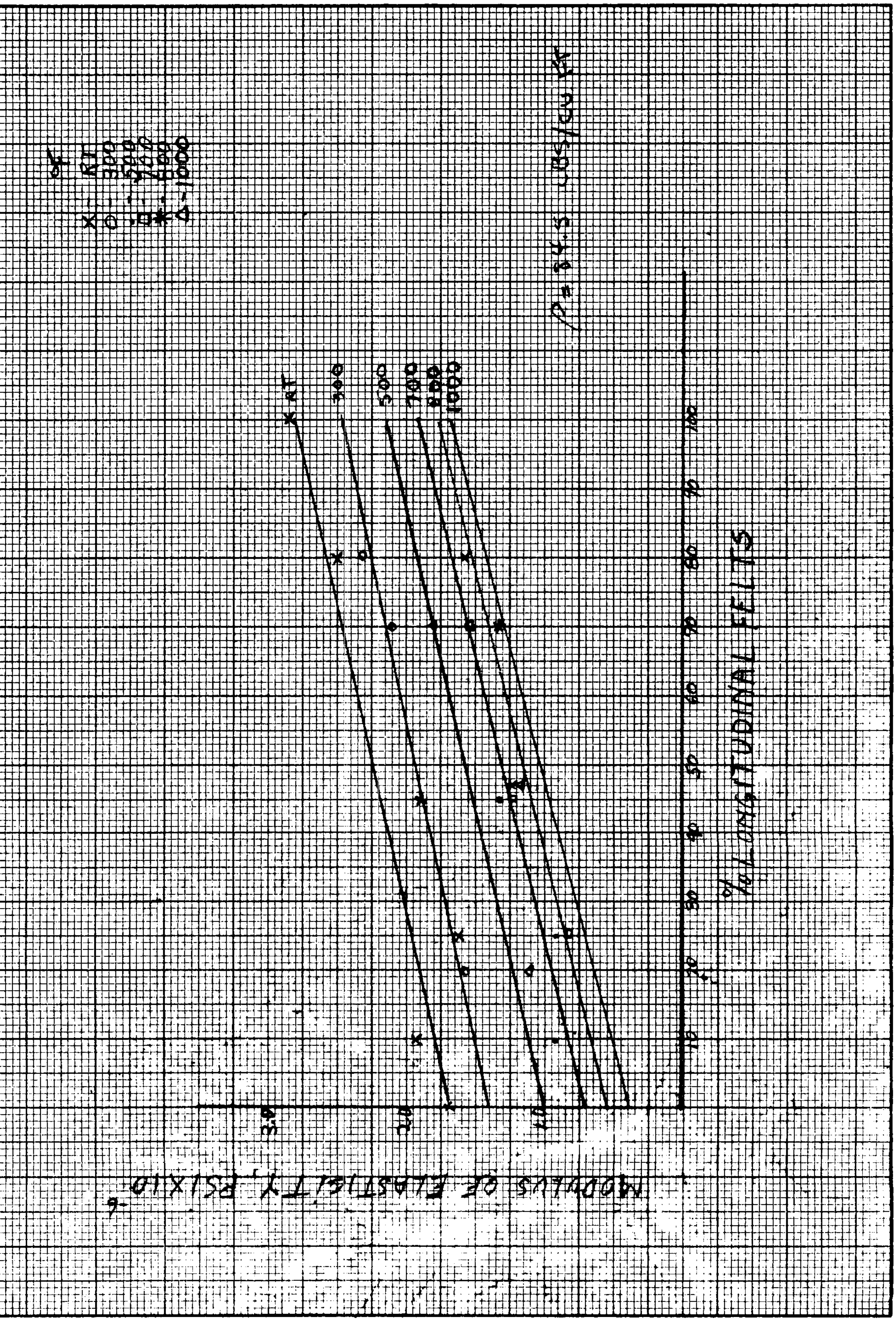


FIGURE 33 MODULUS OF ELASTICITY IN TENSION FOR TYPE I A PHENOLIC ASBESTOS LAMINATE VS FIBER ORIENTATION

E-1-10A
REV. 2/49

PREPARED ______ CHECKED ______ REVISED ______

PAGE ______ REPORT NO. ______ MODEL ______

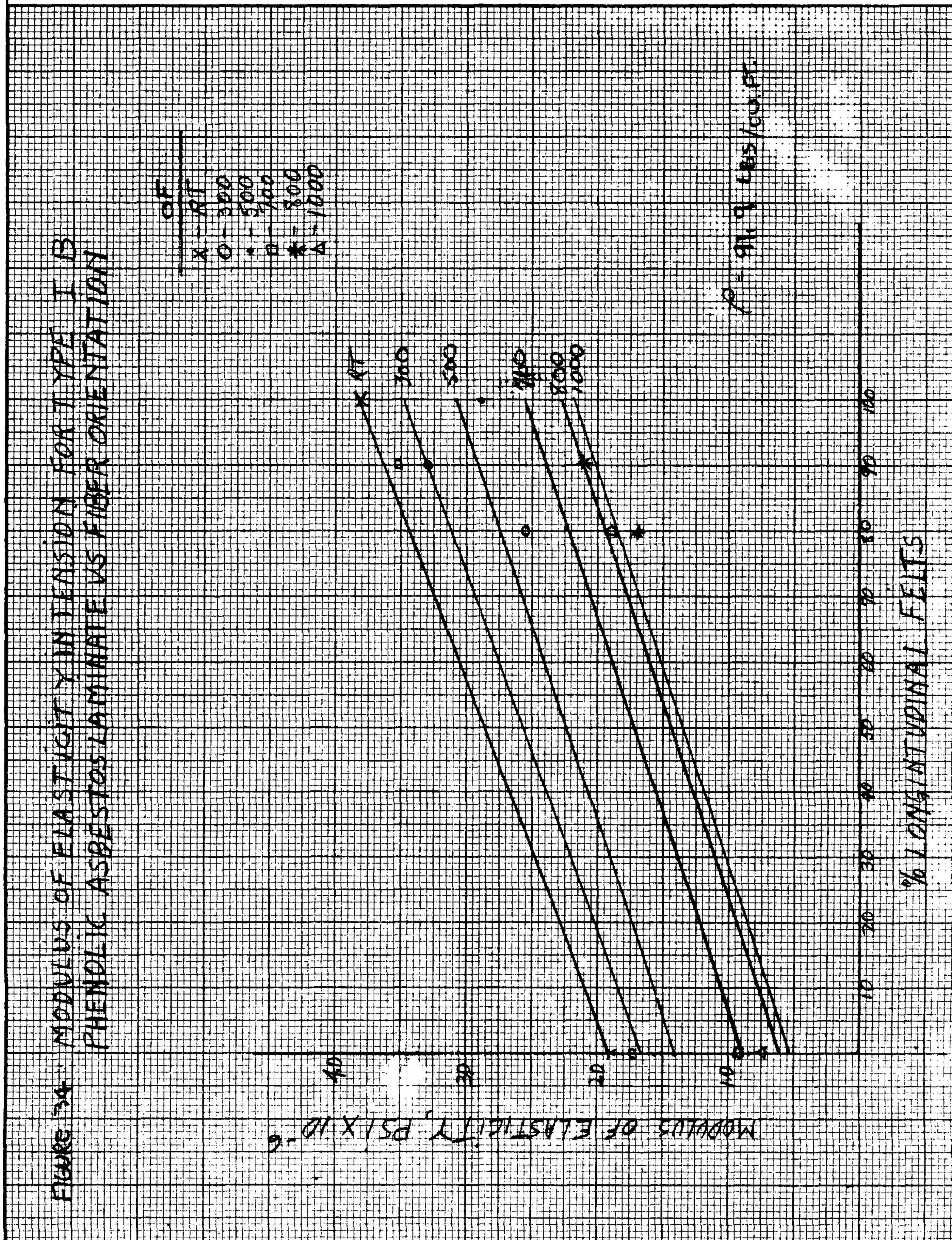


FIGURE 34 MODULUS OF ELASTICITY IN TENSION FOR TYPE I B PHENOLIC ASBESTOS LAMINATE VS FIBER ORIENTATION

E-1-10A
REV. 2/49

FIGURE 35 MODULUS OF ELASTICITY IN TENSION FOR TYPE II PHENOLIC ASBESTOS VS FIBER ORIENTATION

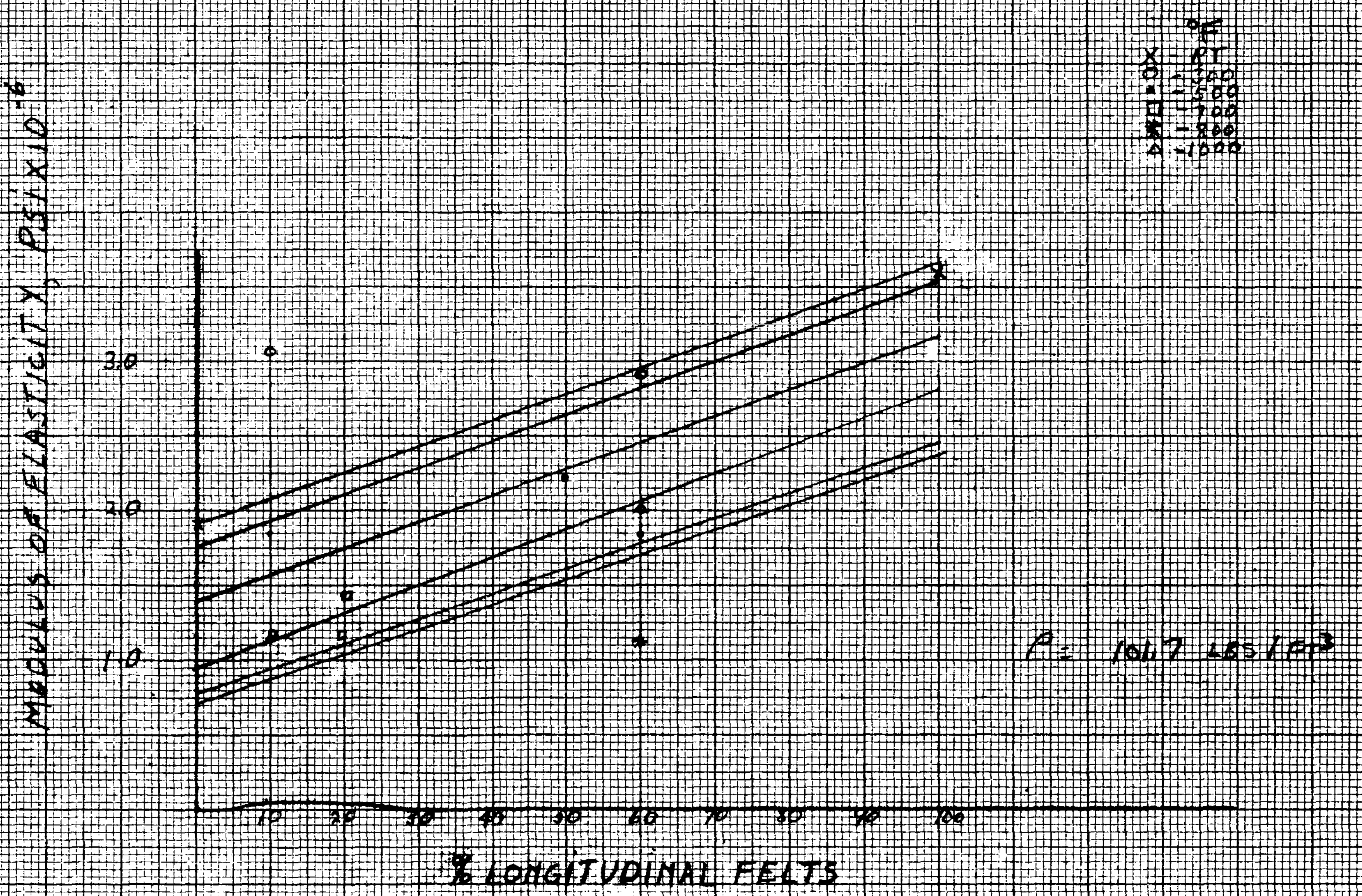

FIG. 36 MODULUS OF ELASTICITY IN TENSION FOR TYPE III PHENOLIC ASBESTOS LAMINATE VS FIBER ORIENTATION

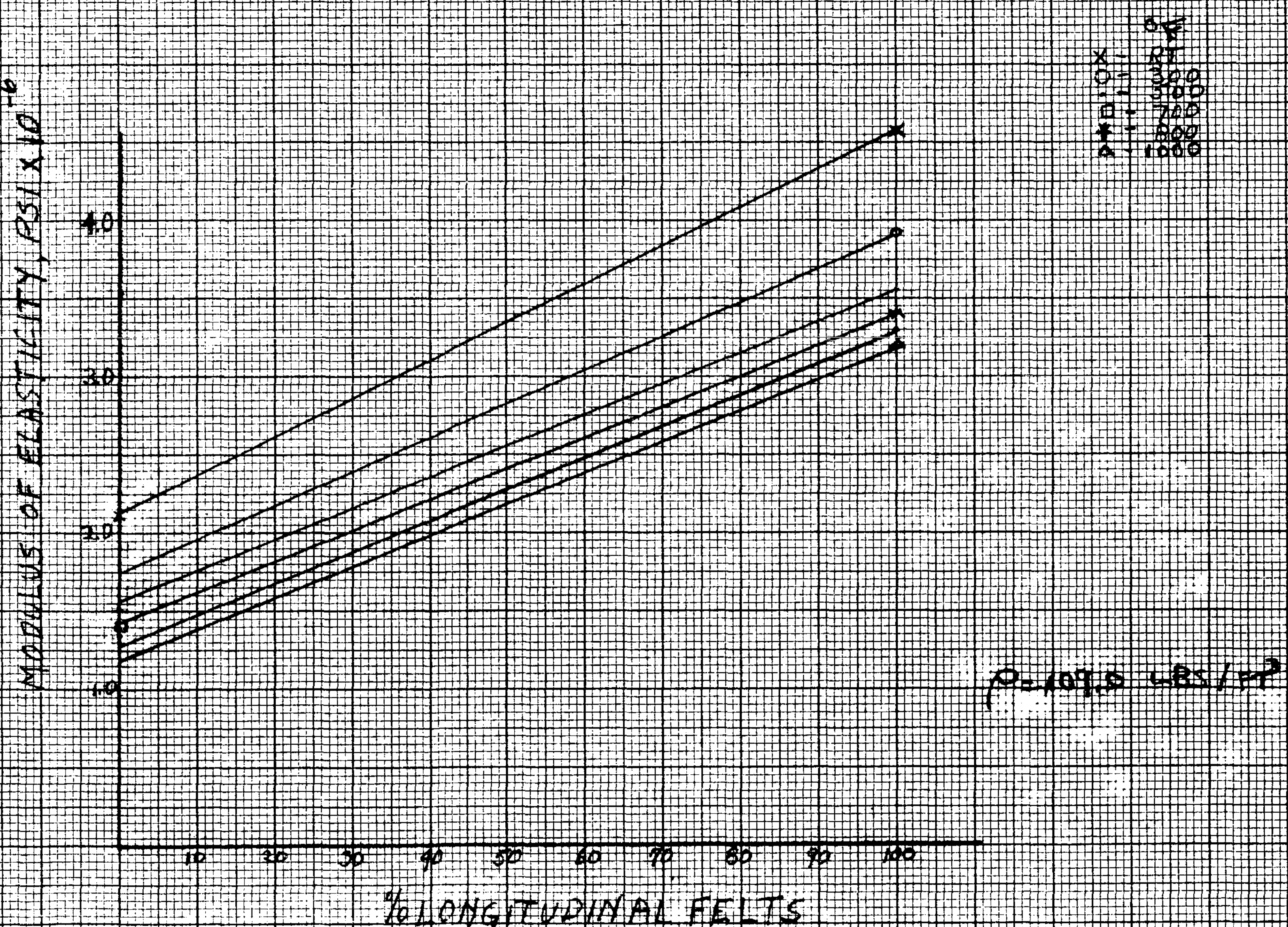


E-1-10A
REV. 2/49

PREPARED
CHECKED
REVISED

REPUBLIC AVIATION

PAGE
REPORT NO.
MODEL

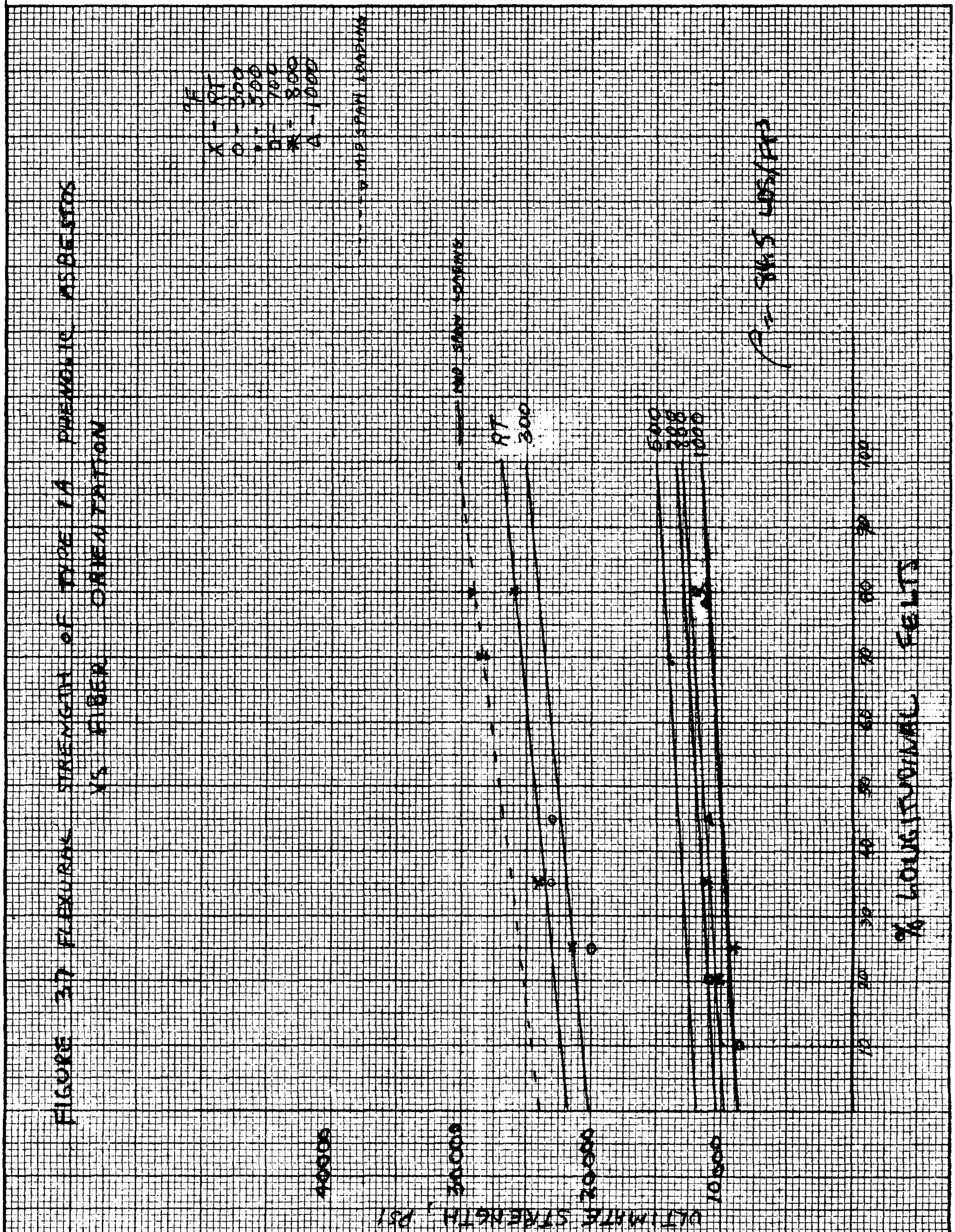


FIGURE 37 FLEXURAL STRENGTH OF TYPE 1A PHENOLIC ASBESTOS VS FIBER ORIENTATION

E-1-10A
REV. 2/49

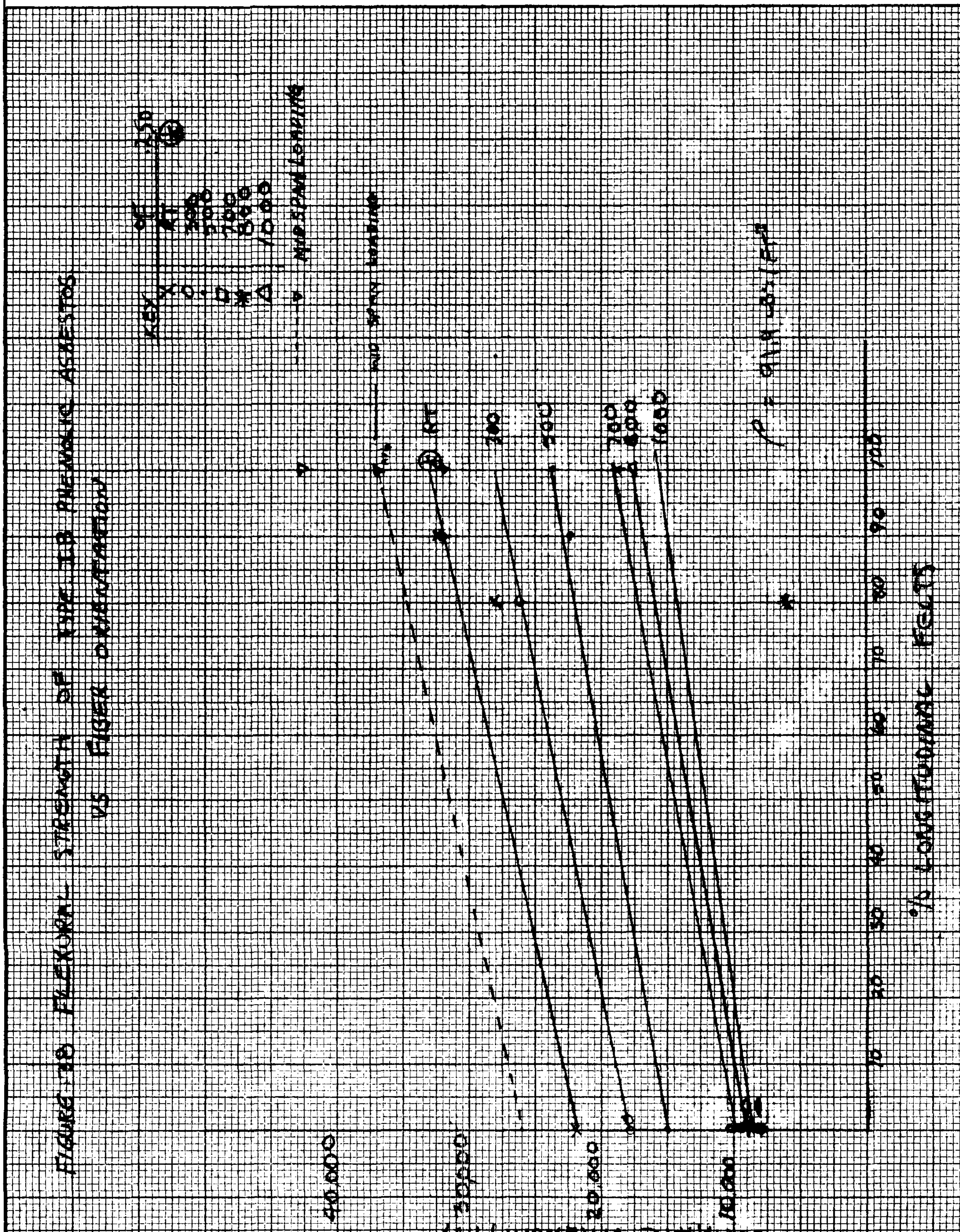


E-1-10A
REV. 2/49

PREPARED ________ ________ PAGE ________

CHECKED ________ ________ REPORT NO. ________

REVISED ________ ________ MODEL ________

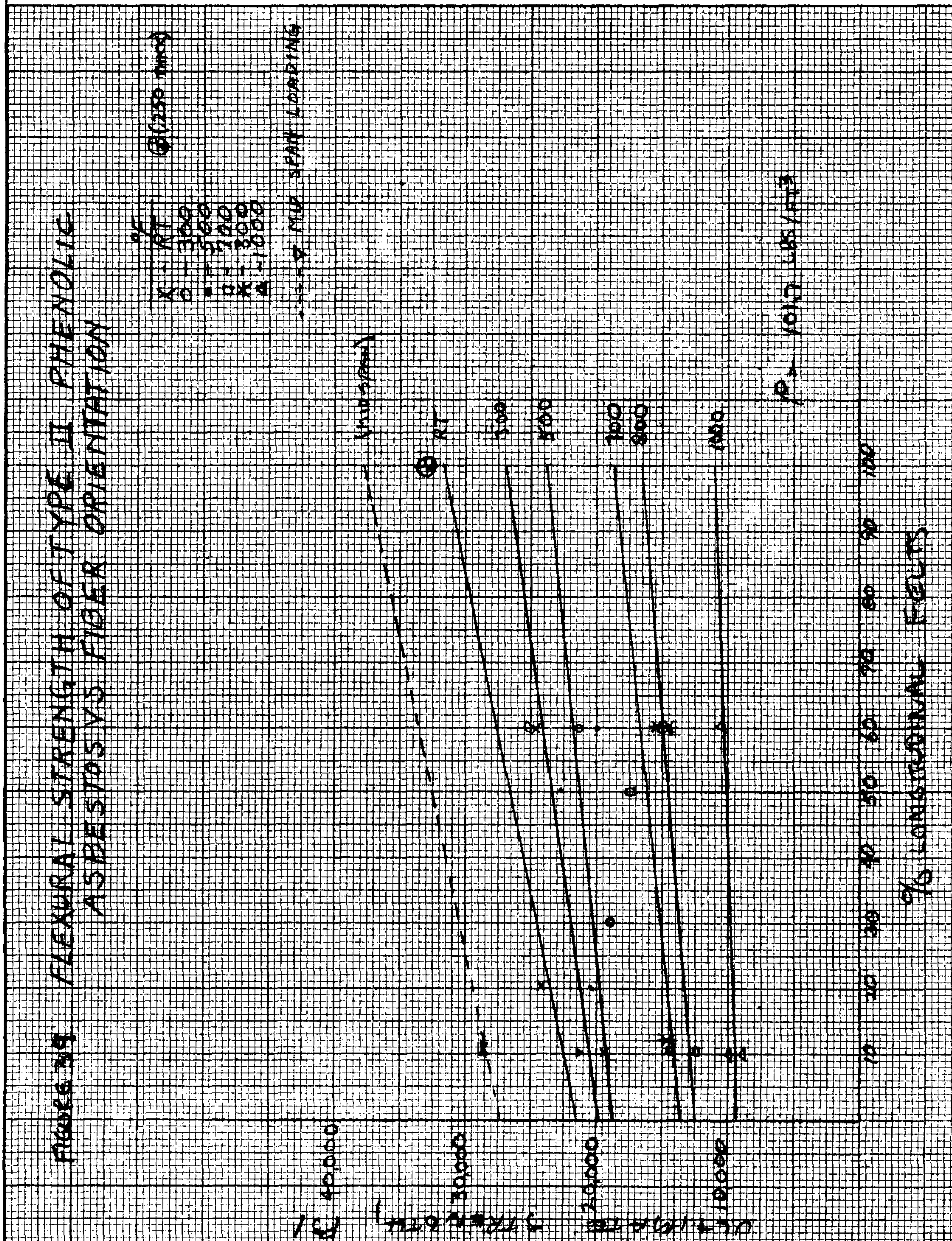


E-1-10A
REV. 2/49

PREPARED
CHECKED
REVISED

PAGE
REPORT NO.
MODEL

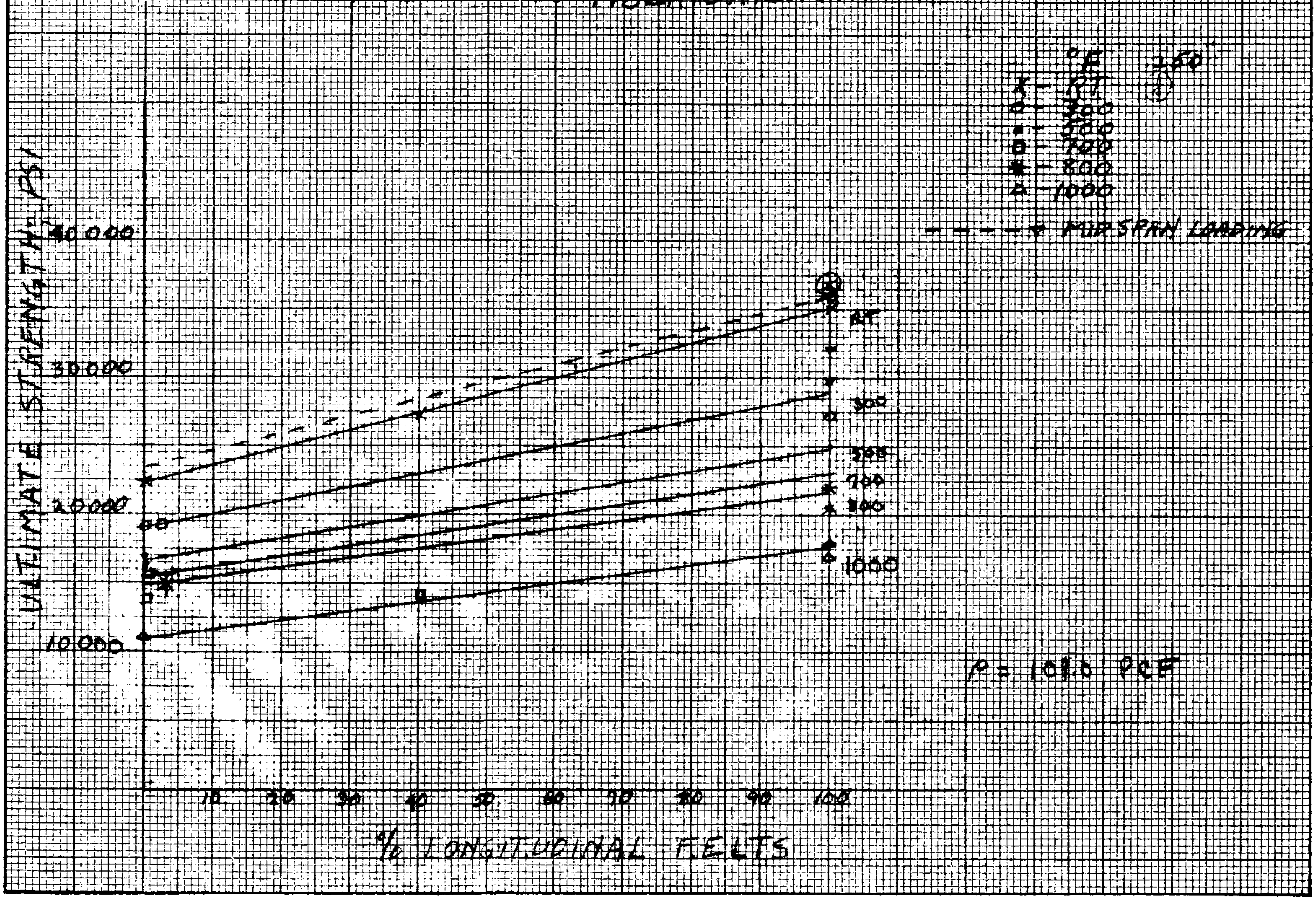


FIGURE 40 FLEXURAL STRENGTH OF TYPE III PHENOLIC ASBESTOS VS FIBER ORIENTATION

E-1-10A
REV. 2/49

PREPARED ____________ ____________

CHECKED ____________ ____________

REVISED ____________ ____________

REPUBLIC AVIATION

PAGE ____________

REPORT NO. ____________

MODEL ____________

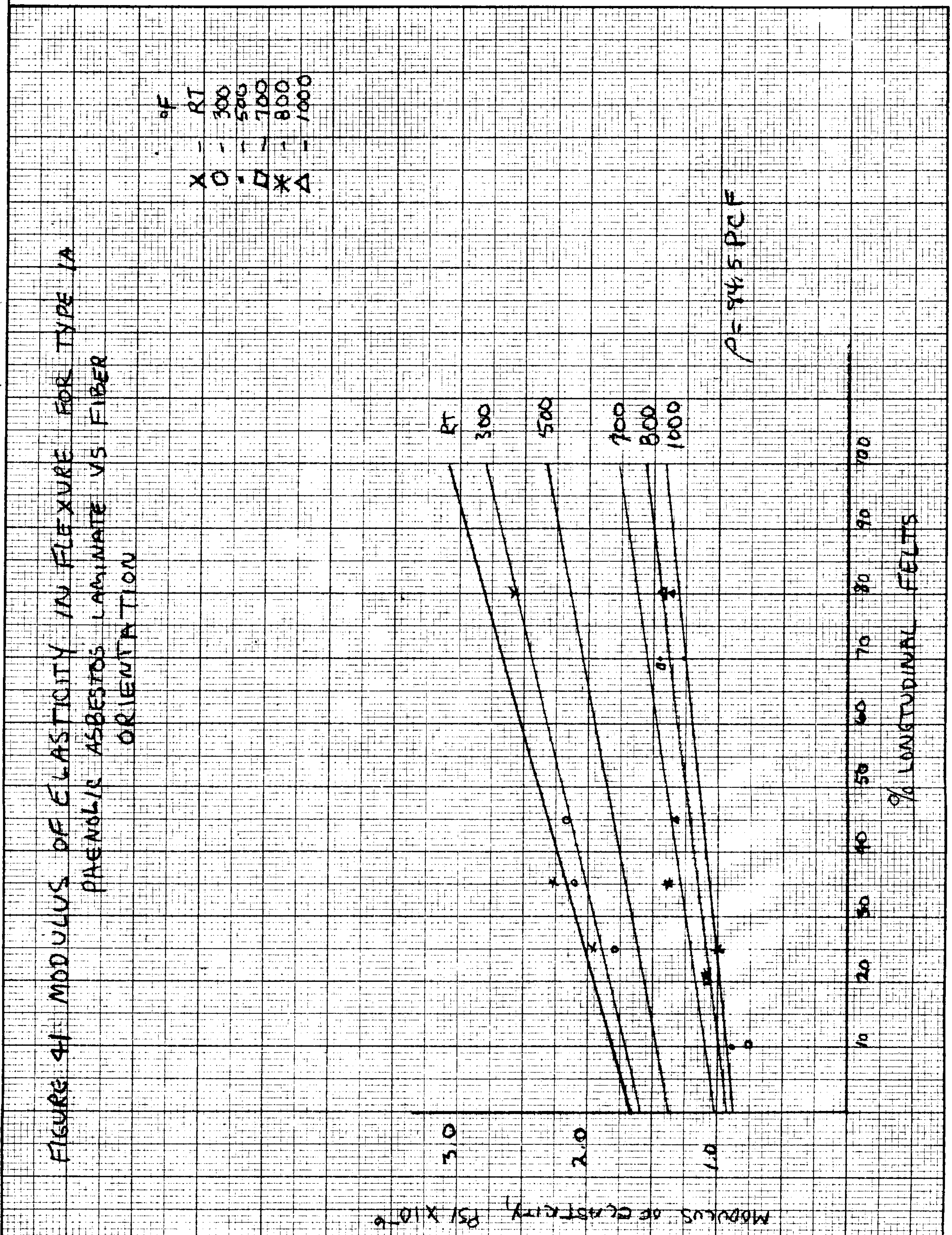


E-1-10A
REV. 2749

PREPARED ____ ____

CHECKED ____ ____

REVISED ____ ____

PAGE ____

REPORT NO. ____

MODEL ____

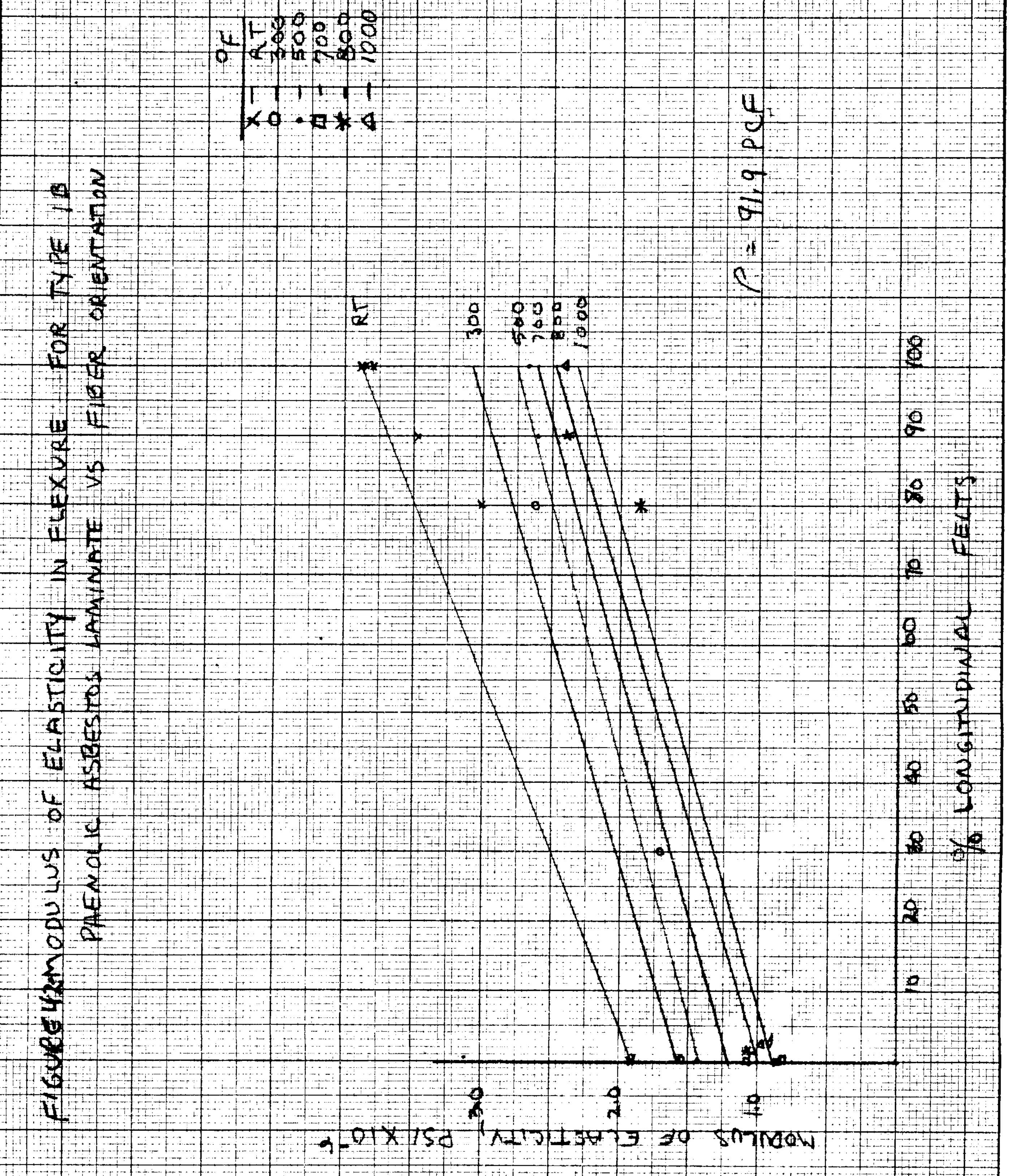


FIGURE 42 MODULUS OF ELASTICITY IN FLEXURE FOR TYPE 1B PHAENOLIC ASBESTOS LAMINATE VS FIBER ORIENTATION

E-1-10A
REV. 2/49

PREPARED ____________ ________

CHECKED ____________ ________

REVISED ____________ ________

PAGE ____________

REPORT NO. ____________

MODEL ____________

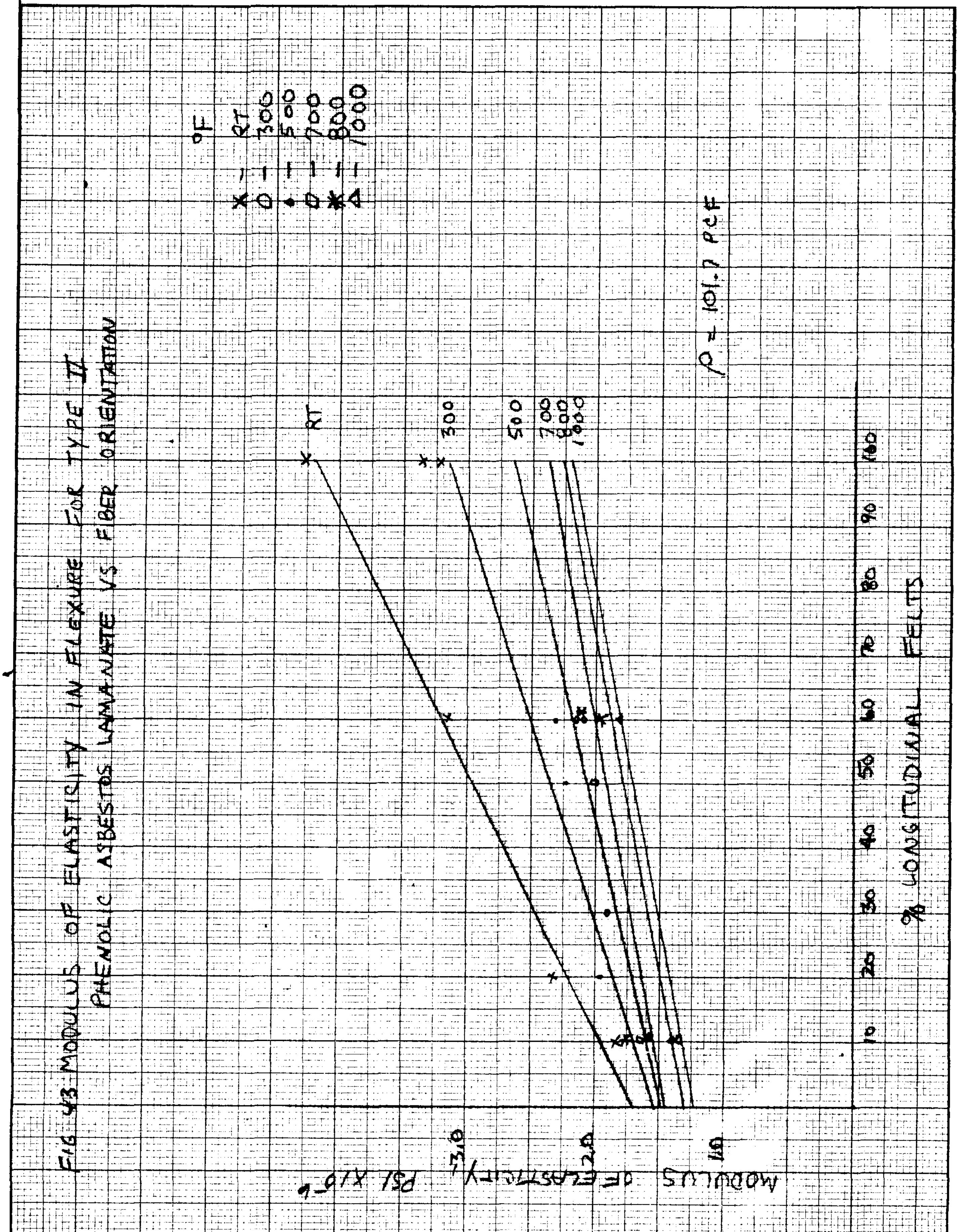


FIG 43 MODULUS OF ELASTICITY IN FLEXURE FOR TYPE II PHENOLIC ASBESTOS LAMINATE VS FIBER ORIENTATION

E-1-10A
REV. 2/49

PREPARED ____ ____
CHECKED ____ ____
REVISED ____ ____

PAGE ____
REPORT NO. ____
MODEL ____

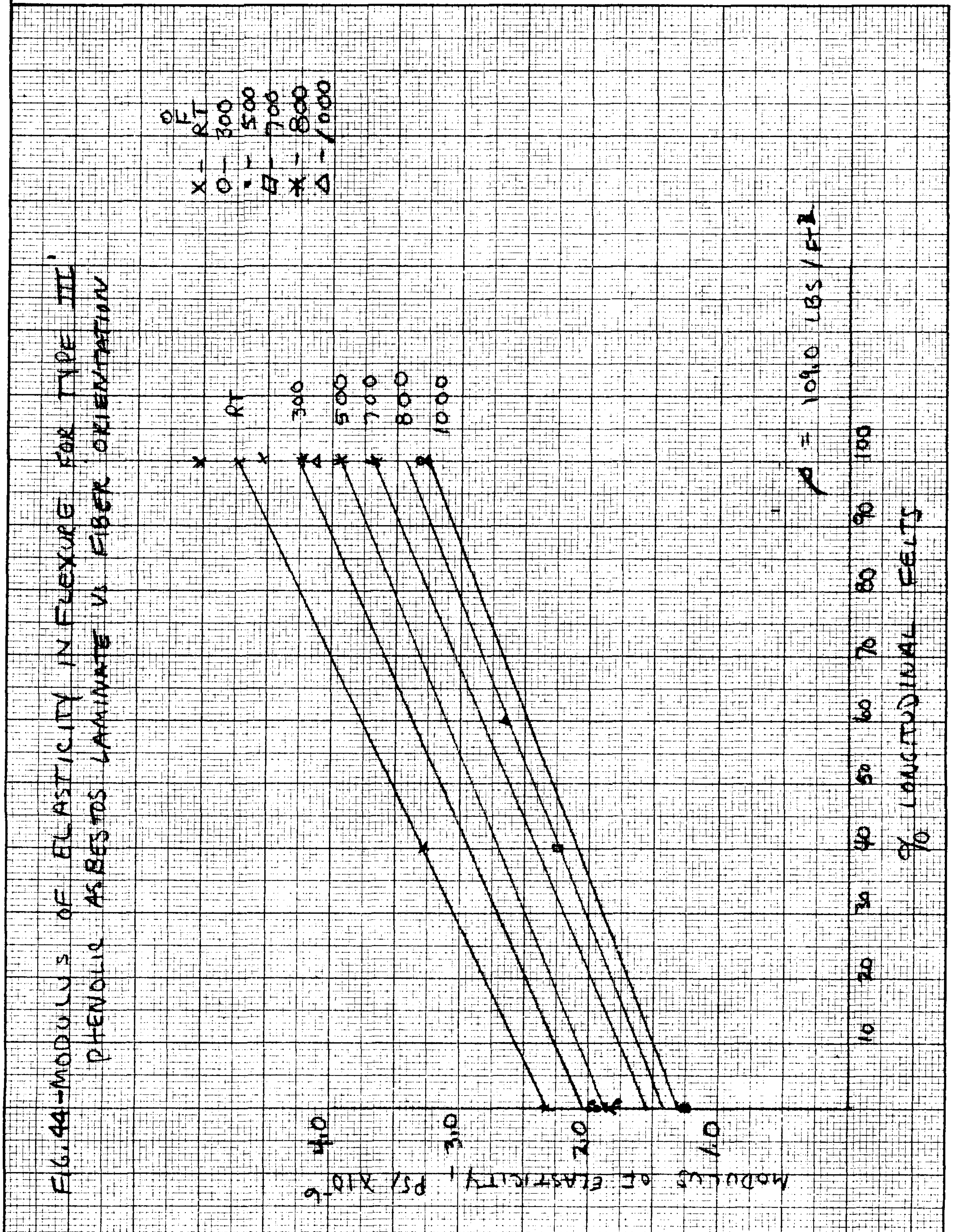


E-1-10A
REV. 2/49

PREPARED
CHECKED
REVISED

REPUBLIC AVIATION

PAGE
REPORT NO.
MODEL

FIG. 45 COMPRESSIVE PROPERTIES OF FOUR STYLES OF PHENOLIC ASBESTOS LAMINATES VS FIBER ORIENTATION

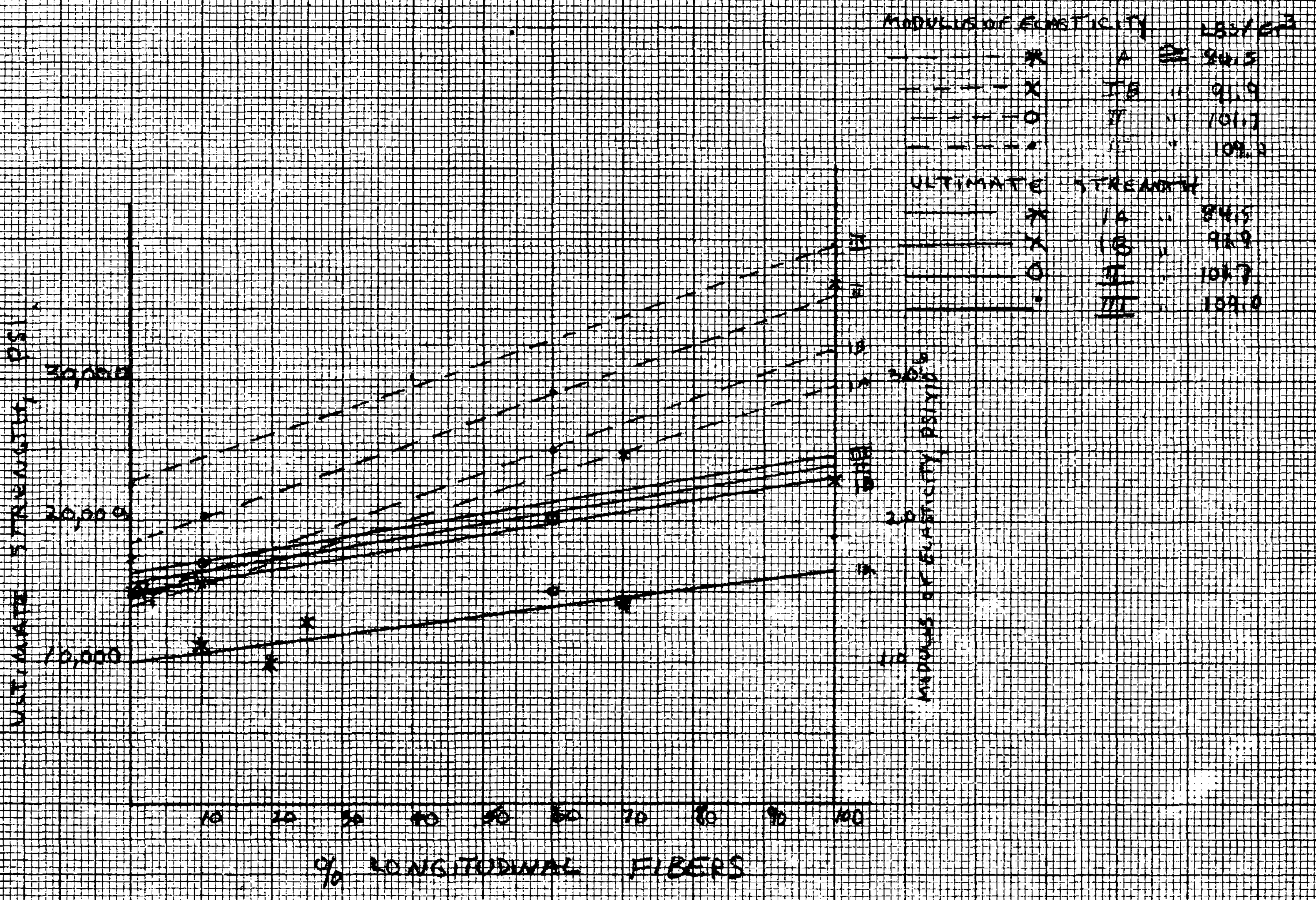




1-10A
REV. 2/49

FIG 46 BEARING STRENGTH OF TYPE IB PHENOLIC ASBESTOS VS FIBER ORIENTATION

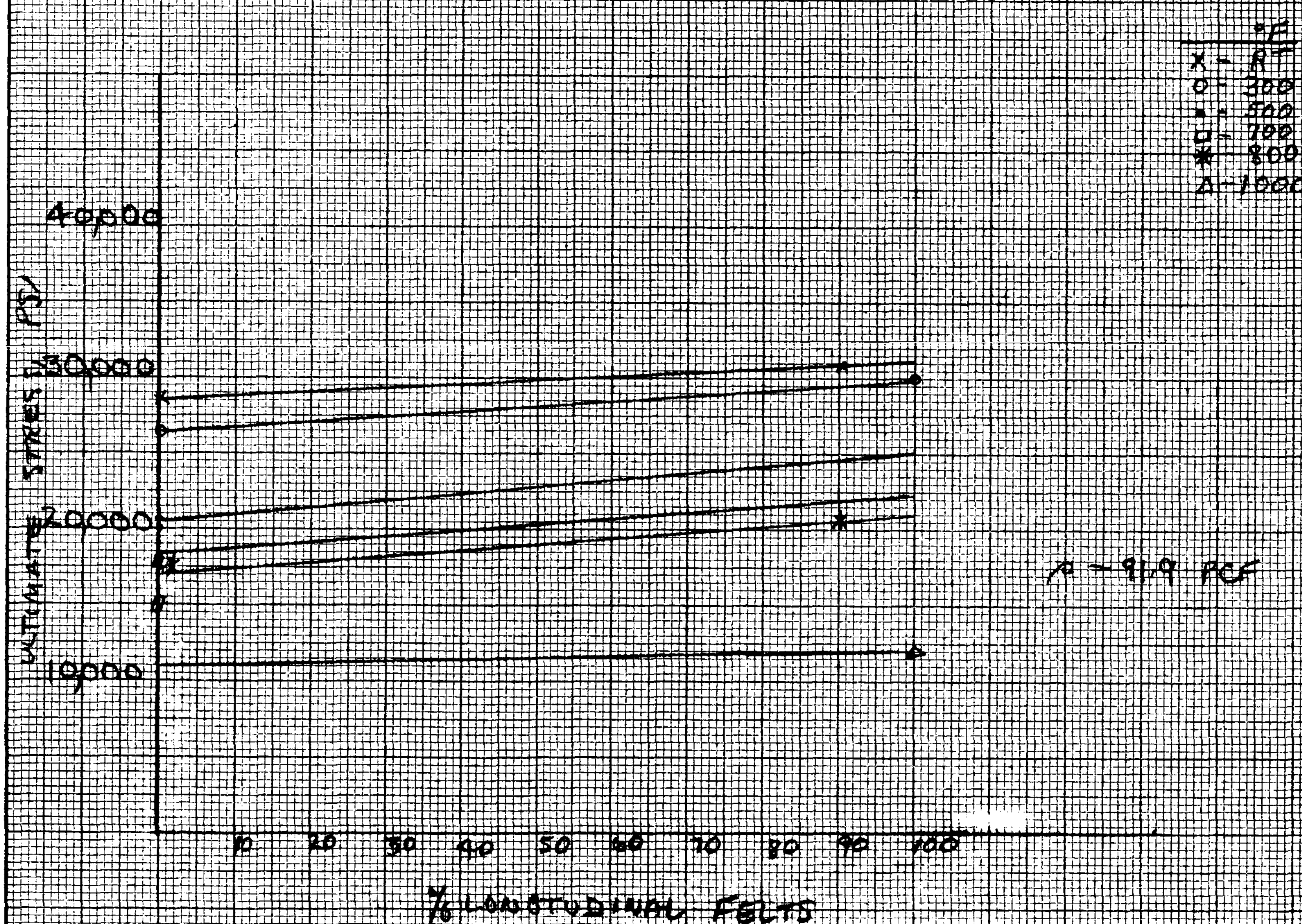

PREPARED ____________ ________

CHECKED ____________ ________

REVISED ____________ ________

REPUBLIC AVIATION

PAGE ____________

REPORT NO. ____________

MODEL ____________

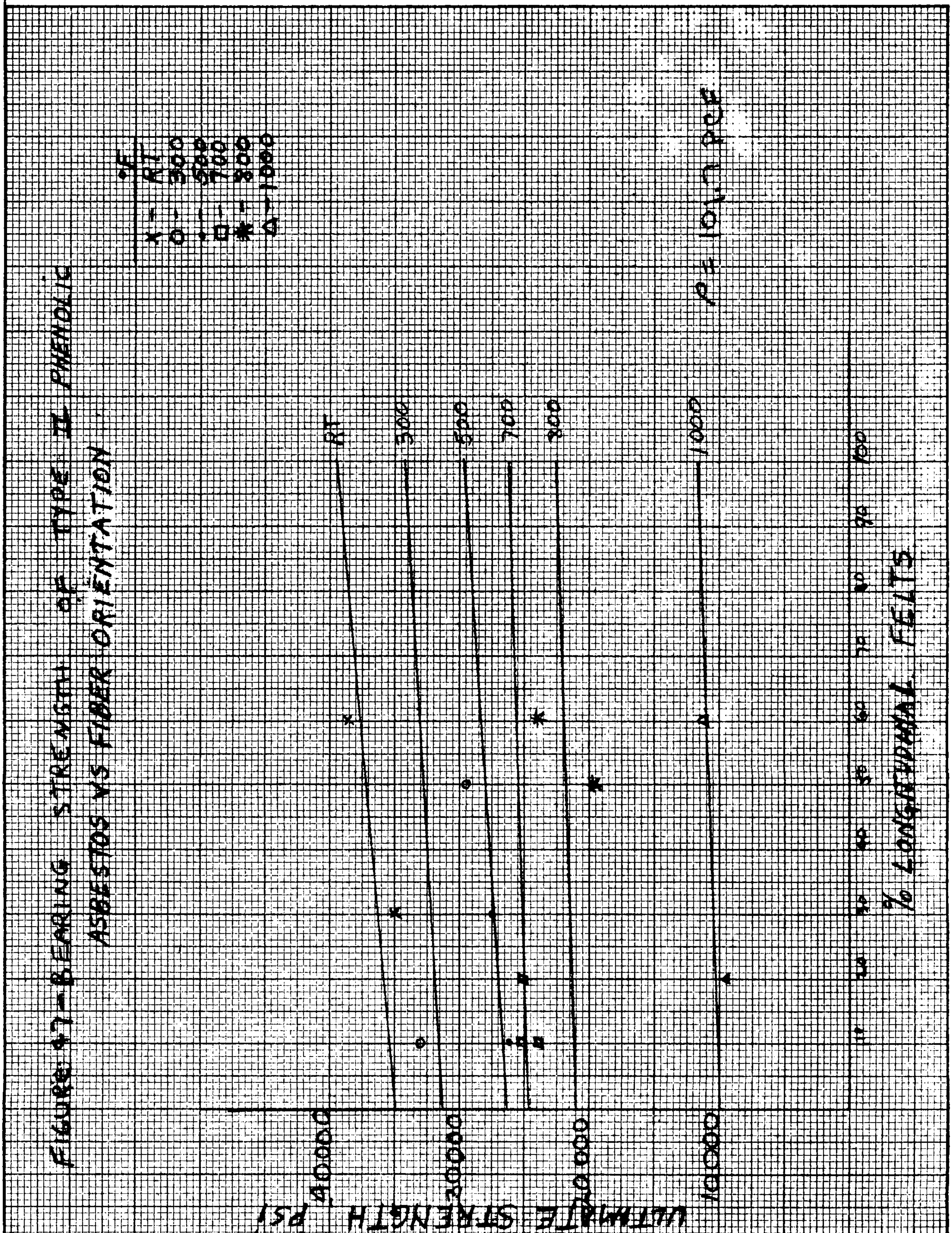


E-1-10A
REV. 2/49

PREPARED ____ ____
CHECKED ____ ____
REVISED ____ ____

REPUBLIC AVIATION

PAGE ____
REPORT NO. ____
MODEL ____

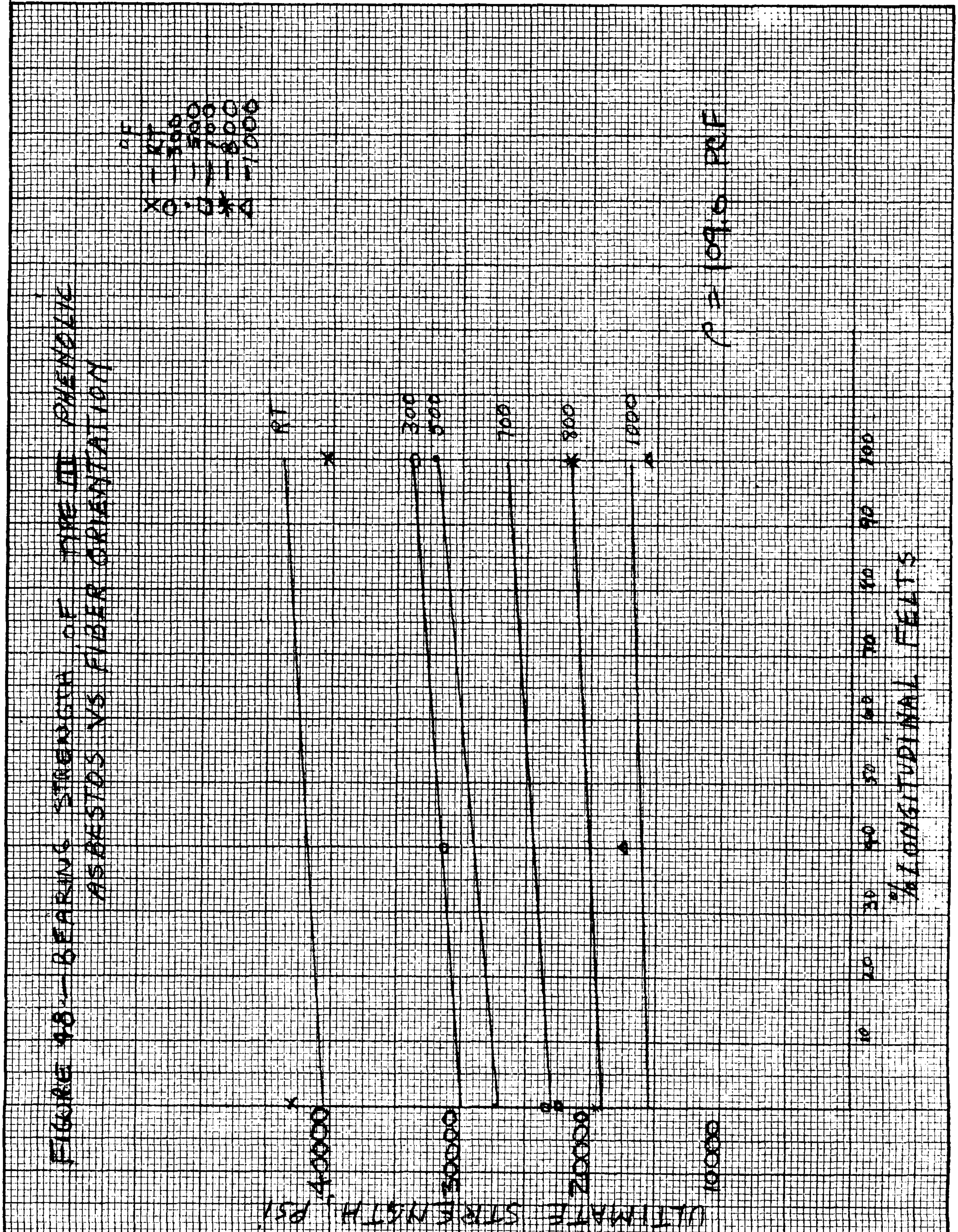


FIGURE 48 - BEARING STRENGTH OF TYPE III PHENOLIC ASBESTOS VS FIBER ORIENTATION

E-1-10A
REV. 2/49

PREPARED ______ ______ REPUBLIC AVIATION PAGE ______

CHECKED ______ ______ REPORT NO. ______

REVISED ______ ______ MODEL ______

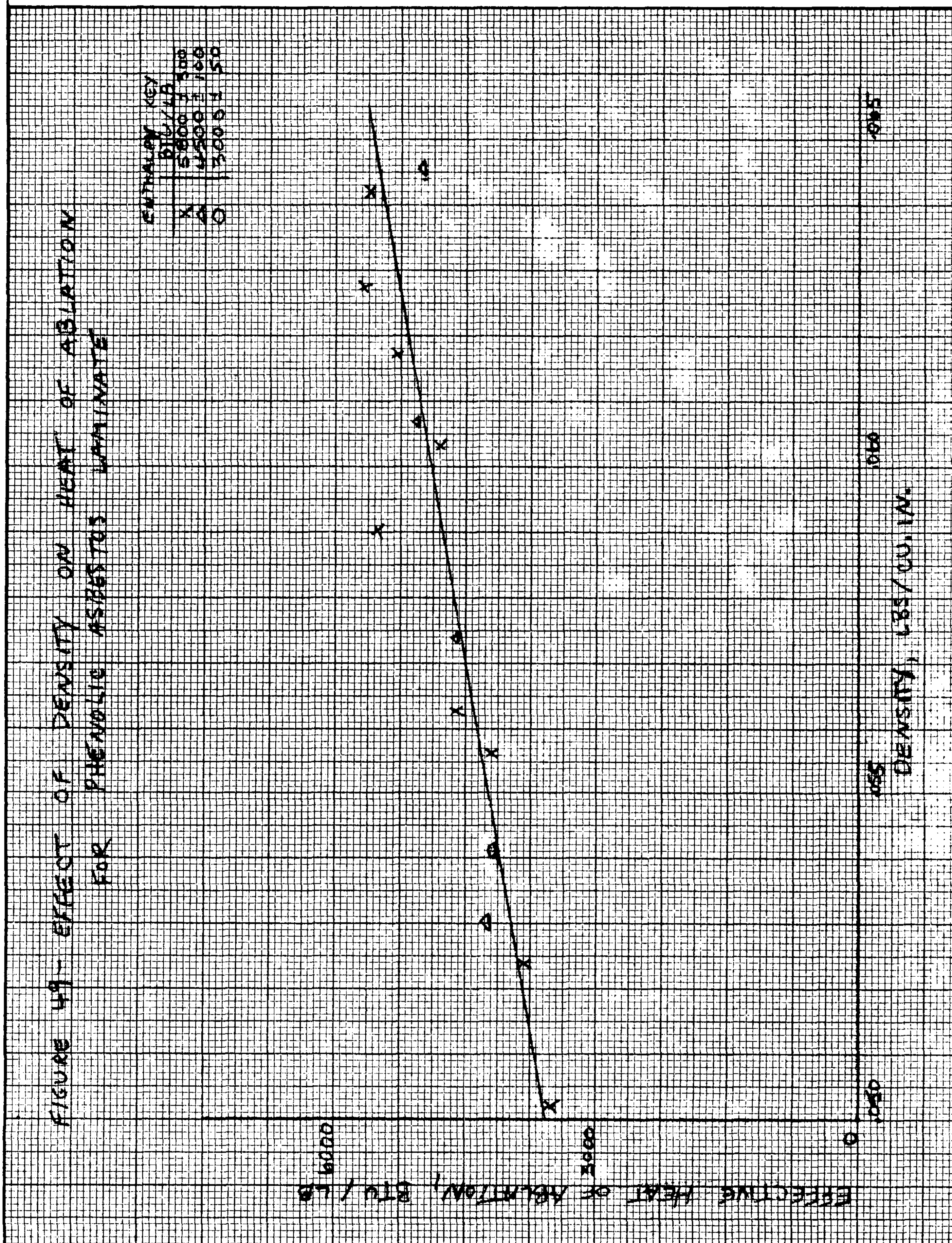


E-1-10A
REV. 2/49

PREPARED ________ ________

CHECKED ________ ________

REVISED ________ ________

REPUBLIC AVIATION

PAGE ________

REPORT NO. ________

MODEL ________

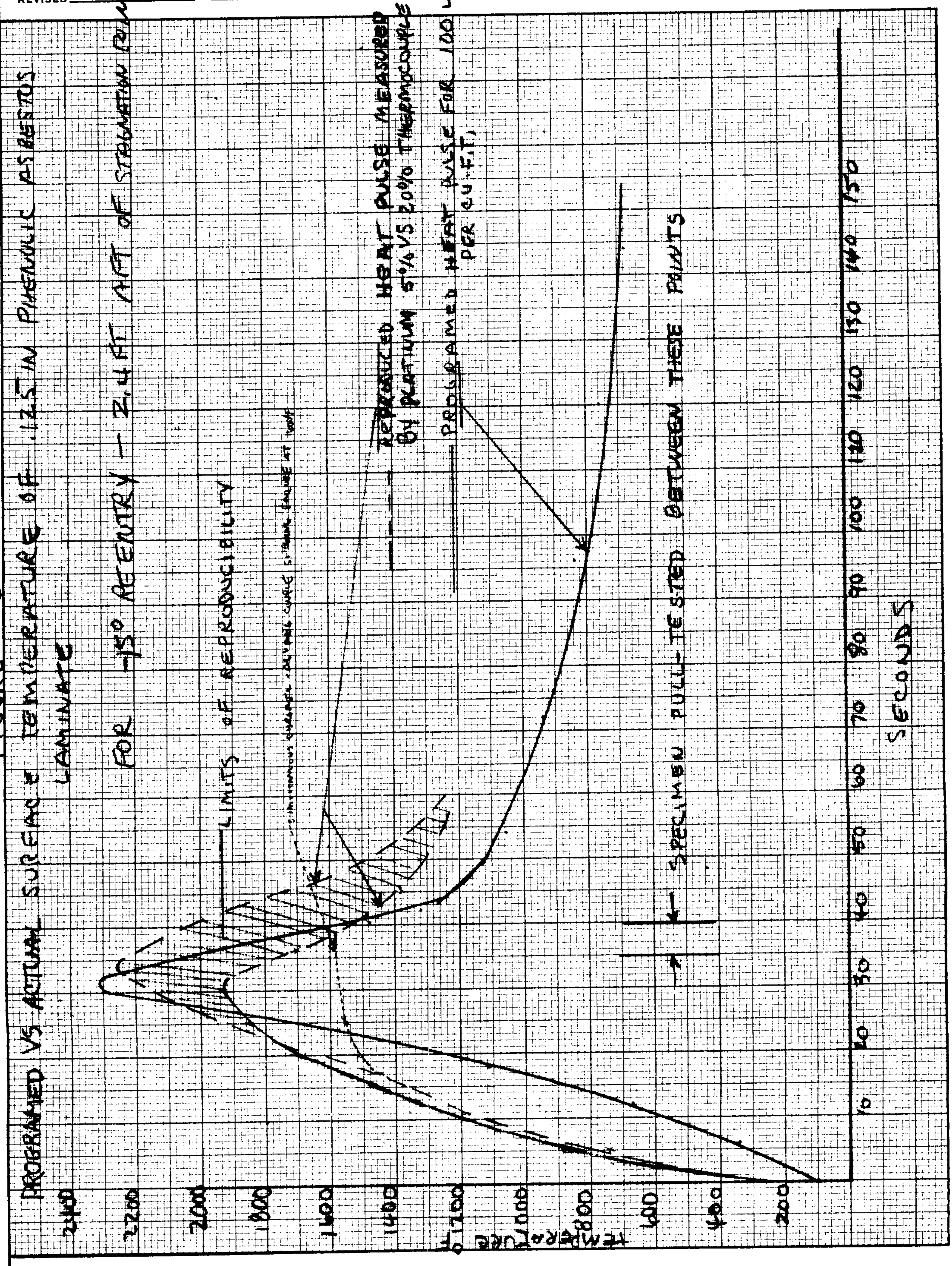


E-1-10A
REV. 2/49

PREPARED ____________ ______

CHECKED ____________ ______

REVISED ____________ ______

PAGE ____________

REPORT NO. ____________

MODEL ____________

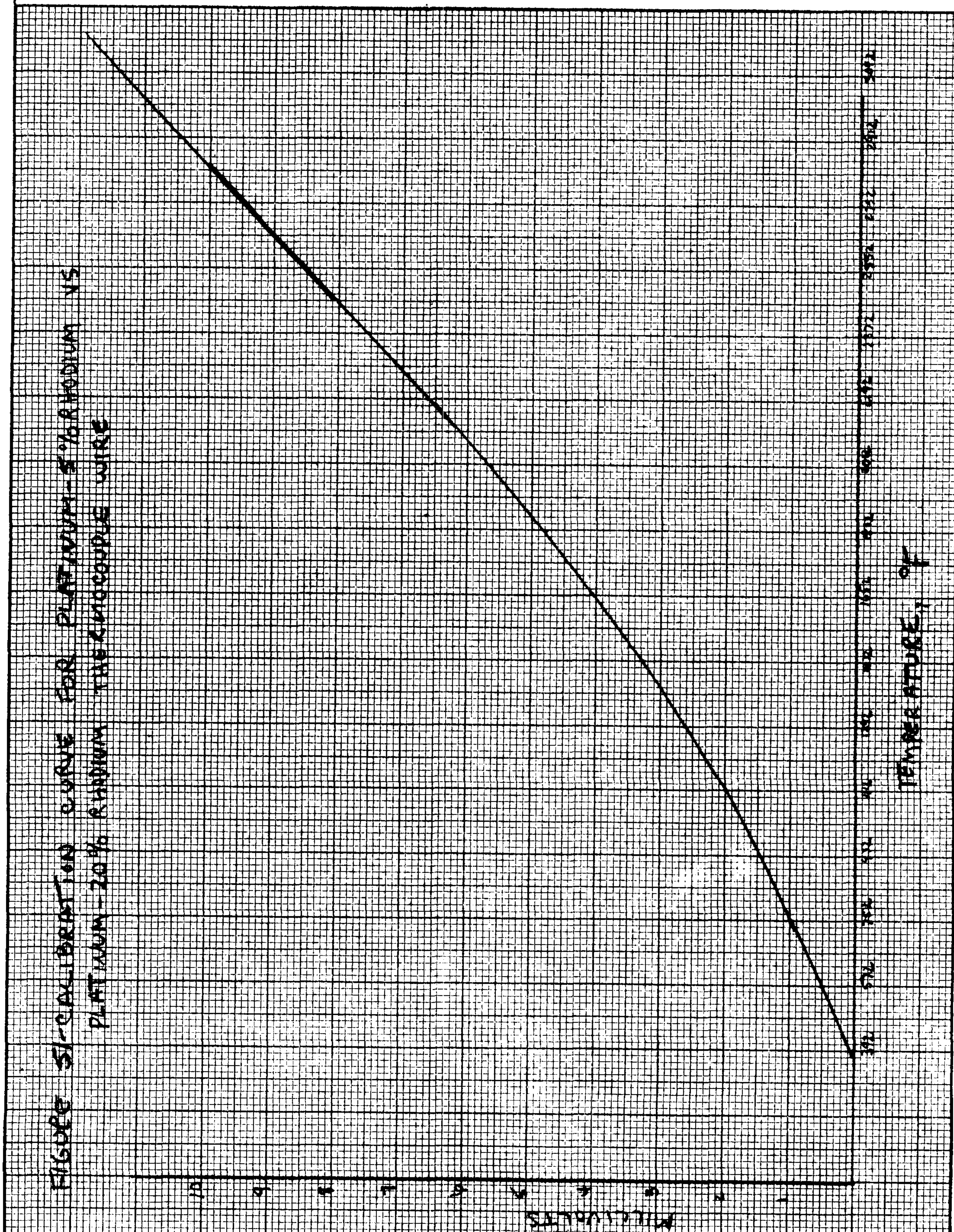


E-1-10A
REV. 2/49

PREPARED

CHECKED

REVISED

PAGE

REPORT NO.

MODEL

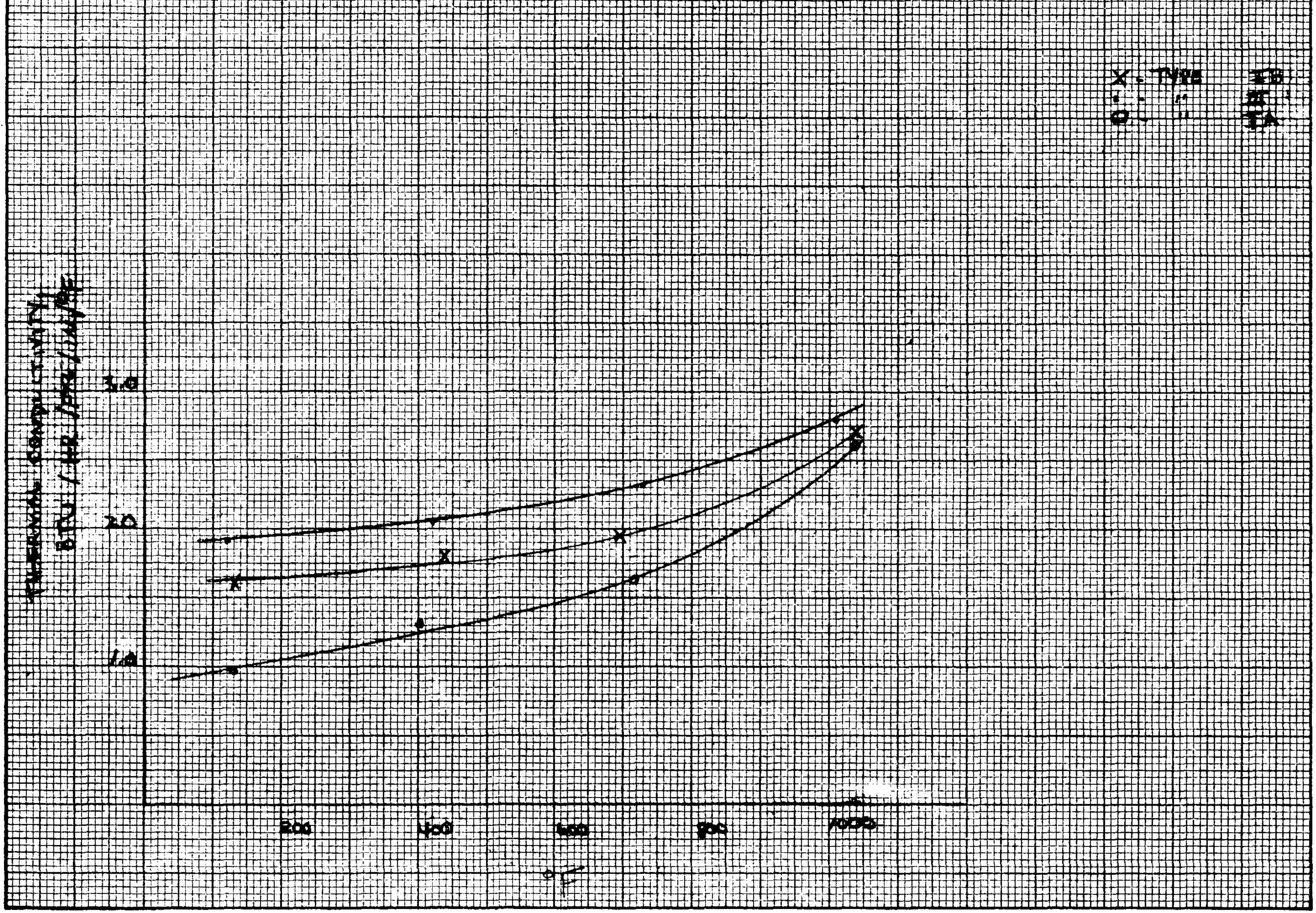


FIGURE 52—THERMAL CONDUCTIVITY VS TEMPERATURE FOR THREE GRADES OF PHENOLIC ASBESTOS LAMINATES

E-1-10A
REV. 2/49

FIGURE 53 THERMAL CONDUCTIVITY VS DENSITY AT FOUR TEMPERATURES FOR PHENOLIC ASBESTOS LAMINATES

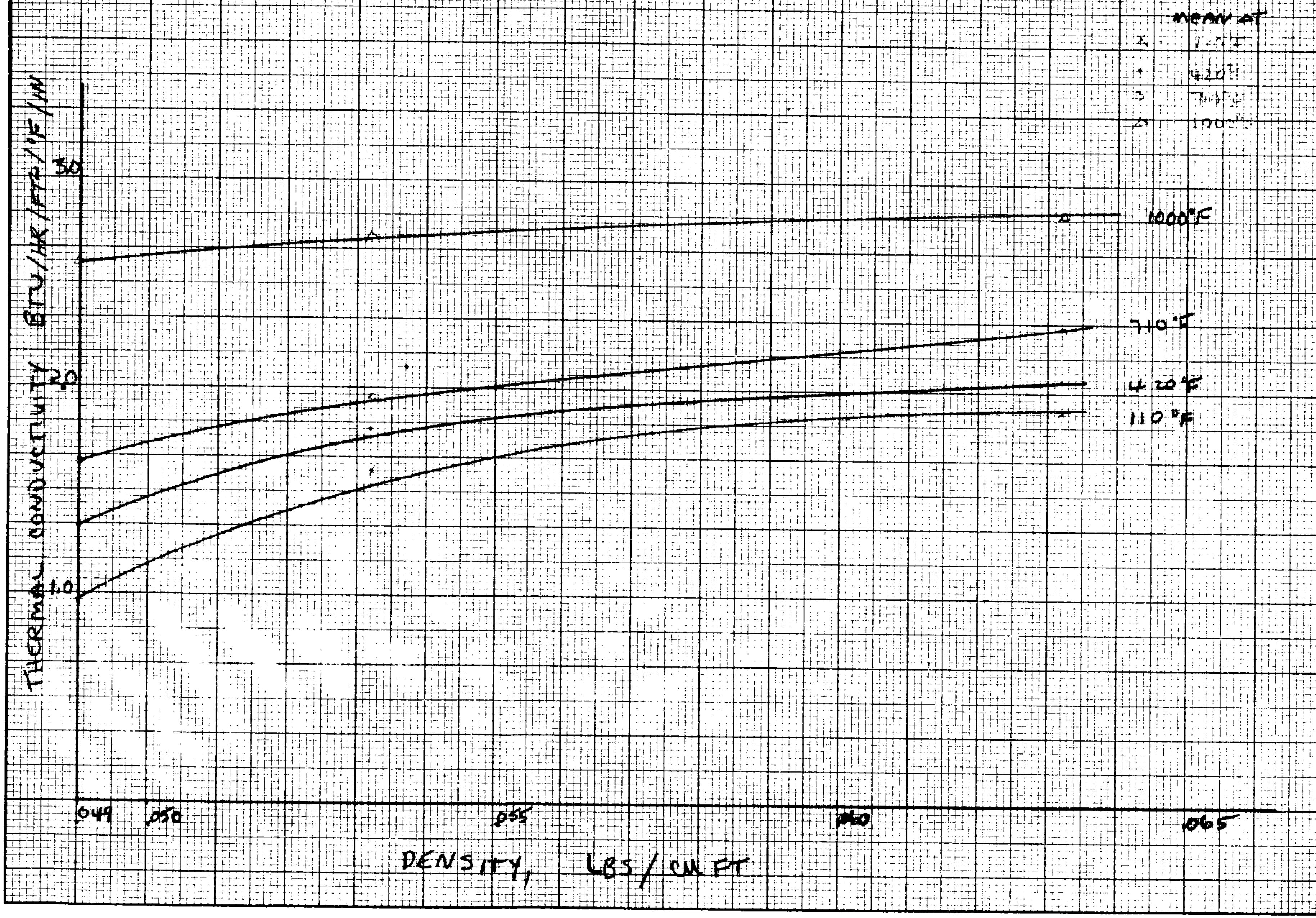

PREPARED

CHECKED

REVISED

REPUBLIC AVIATION

PAGE

REPORT NO.

MODEL

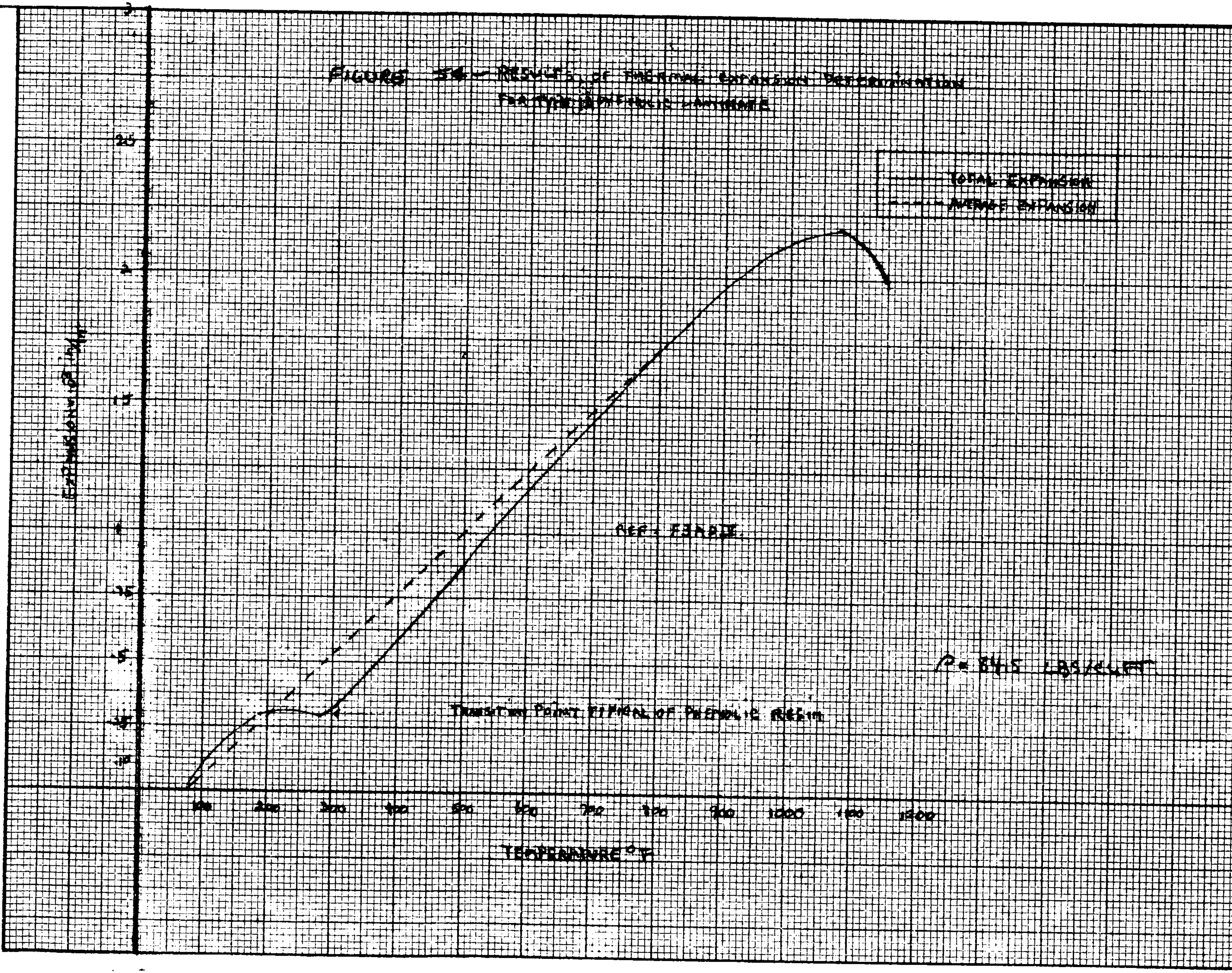


E-1-10A
REV. 2/49

PREPARED
CHECKED
REVISED

PAGE
REPORT NO.
MODEL

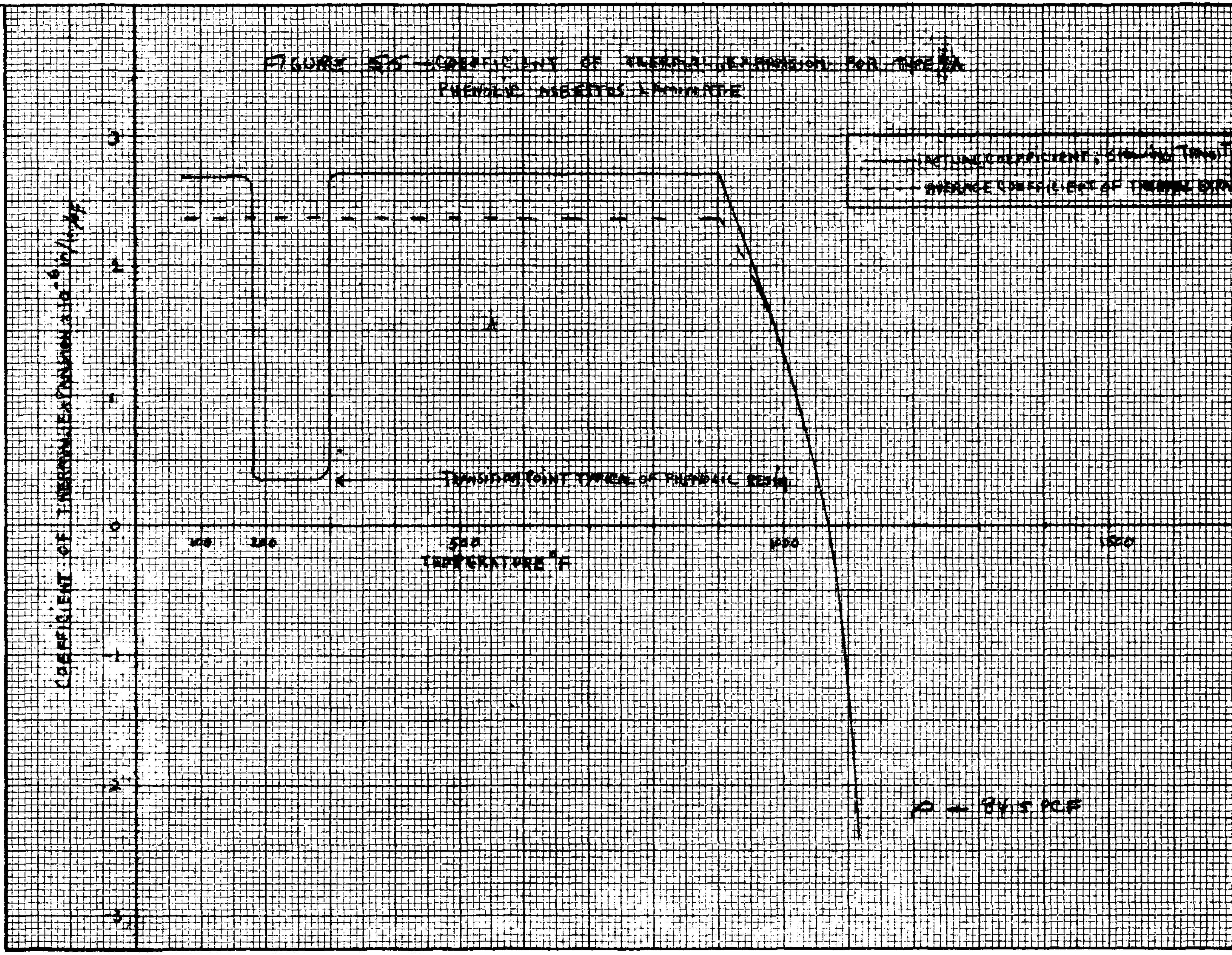


E-1-10A
REV. 2/49

PREPARED ______ ______

CHECKED ______ ______

REVISED ______ ______

PAGE ______

REPORT NO. ______

MODEL ______

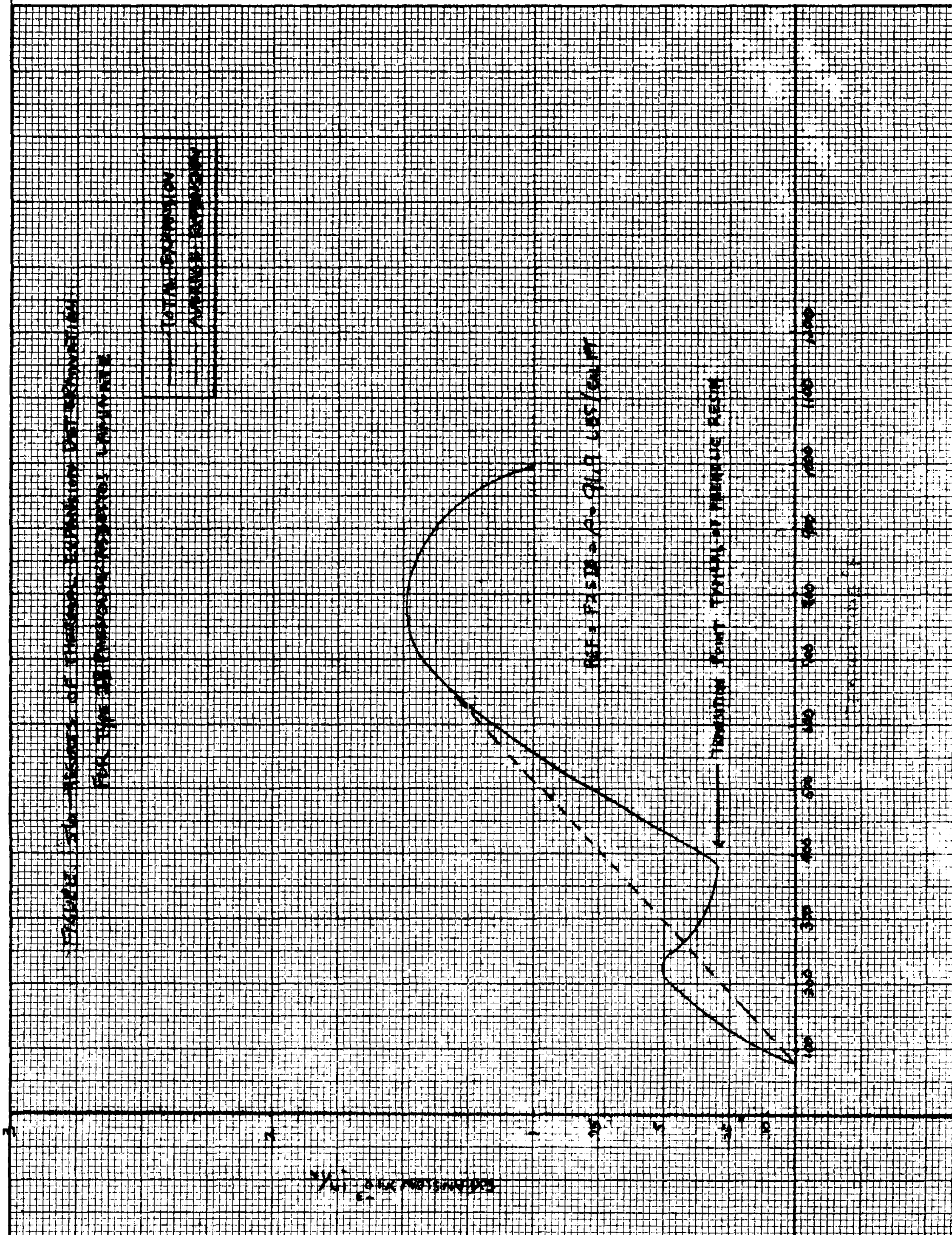


E-1-10A
REV. 2/49

PREPARED ____ CHECKED ____ REVISED ____

REPUBLIC AVIATION

PAGE ____ REPORT NO. ____ MODEL ____

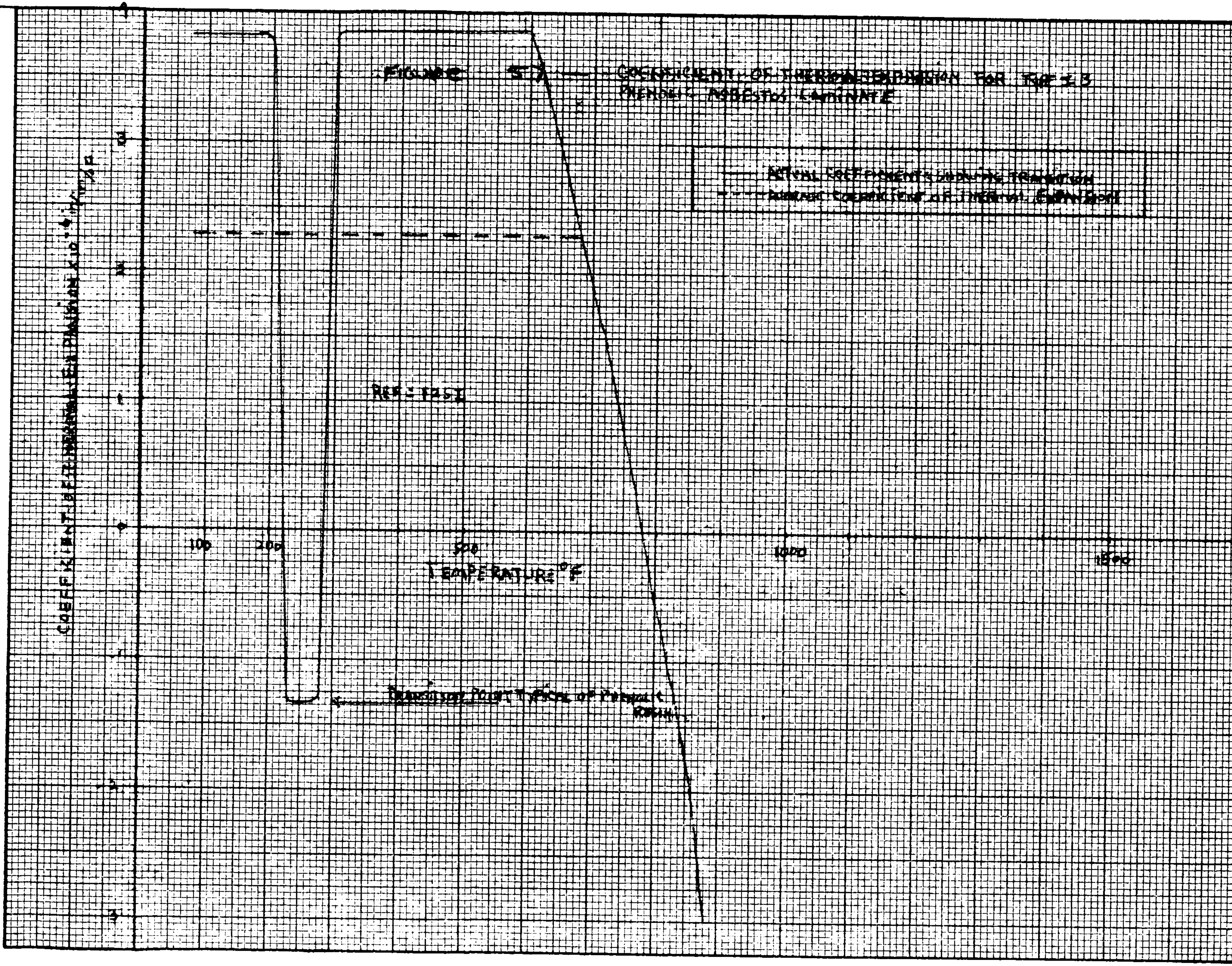


E-1-10A
REV. 2/49

PREPARED ______ ______

CHECKED ______ ______

REVISED ______ ______

PAGE ______

REPORT NO. ______

MODEL ______

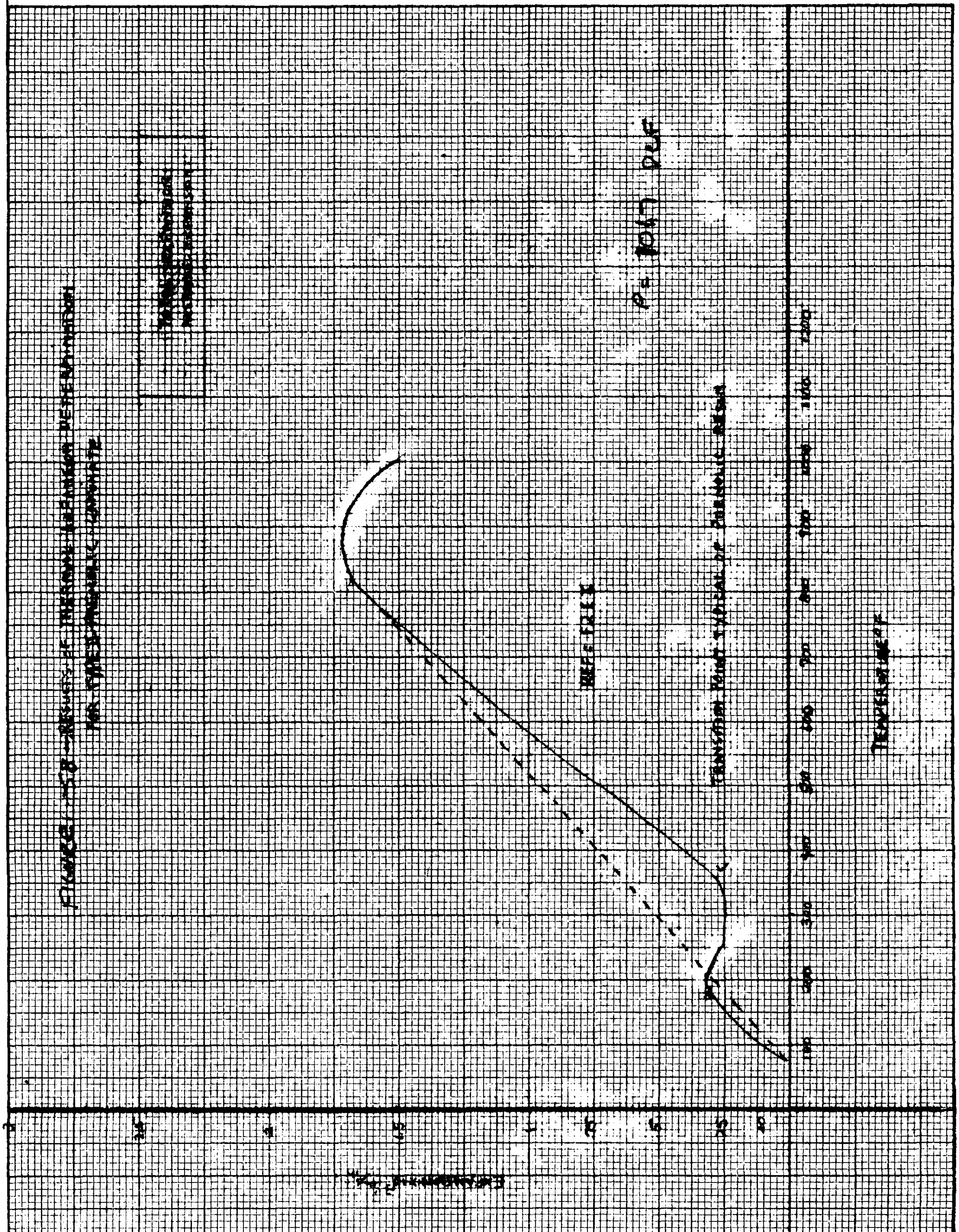


E-1-10A
REV. 2/49

PREPARED ________ ________

CHECKED ________ ________

REVISED ________ ________

PAGE ________

REPORT NO. ________

MODEL ________

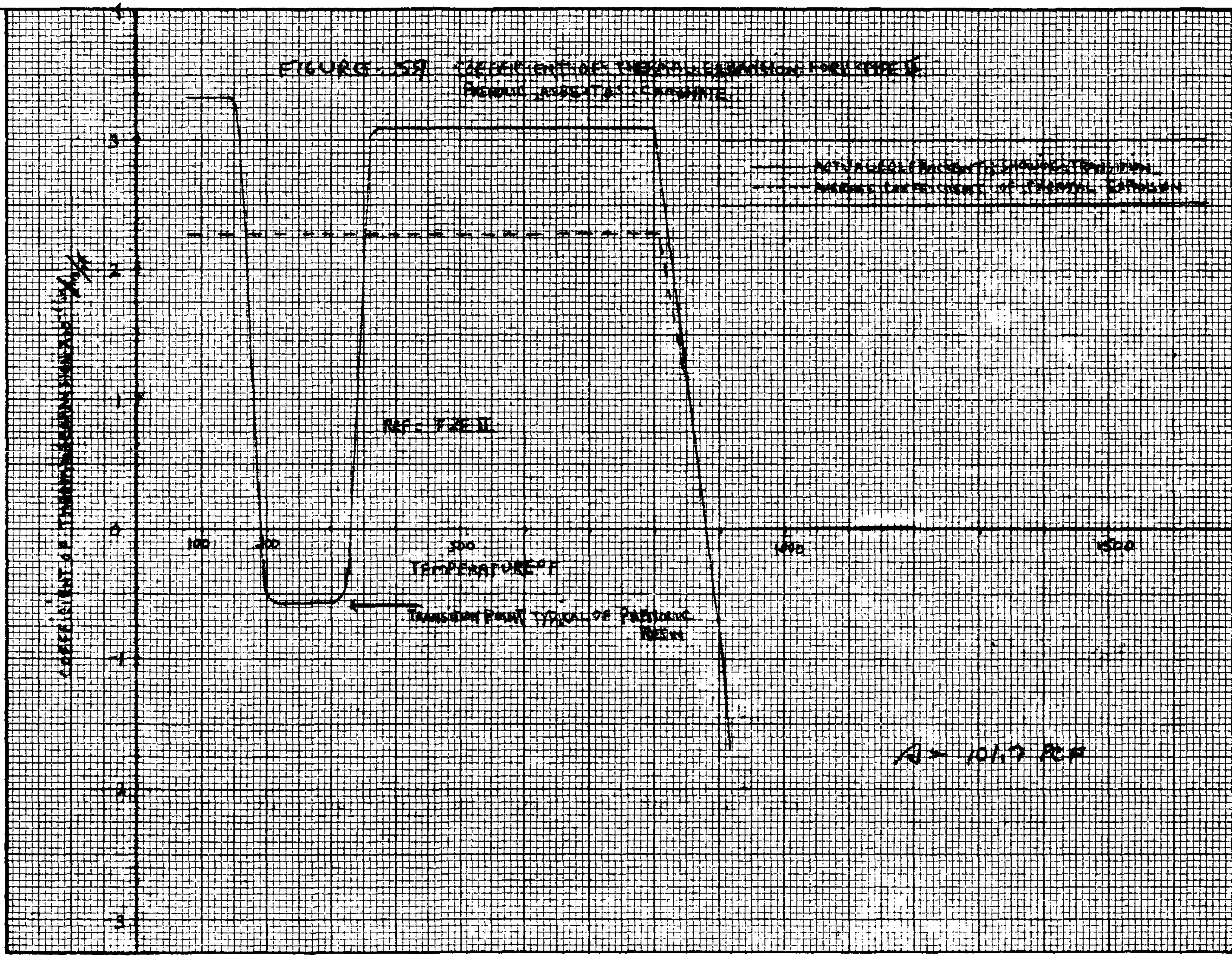


E-1-10A
REV. 2/49

PREPARED
CHECKED
REVISED

PAGE
REPORT NO.
MODEL

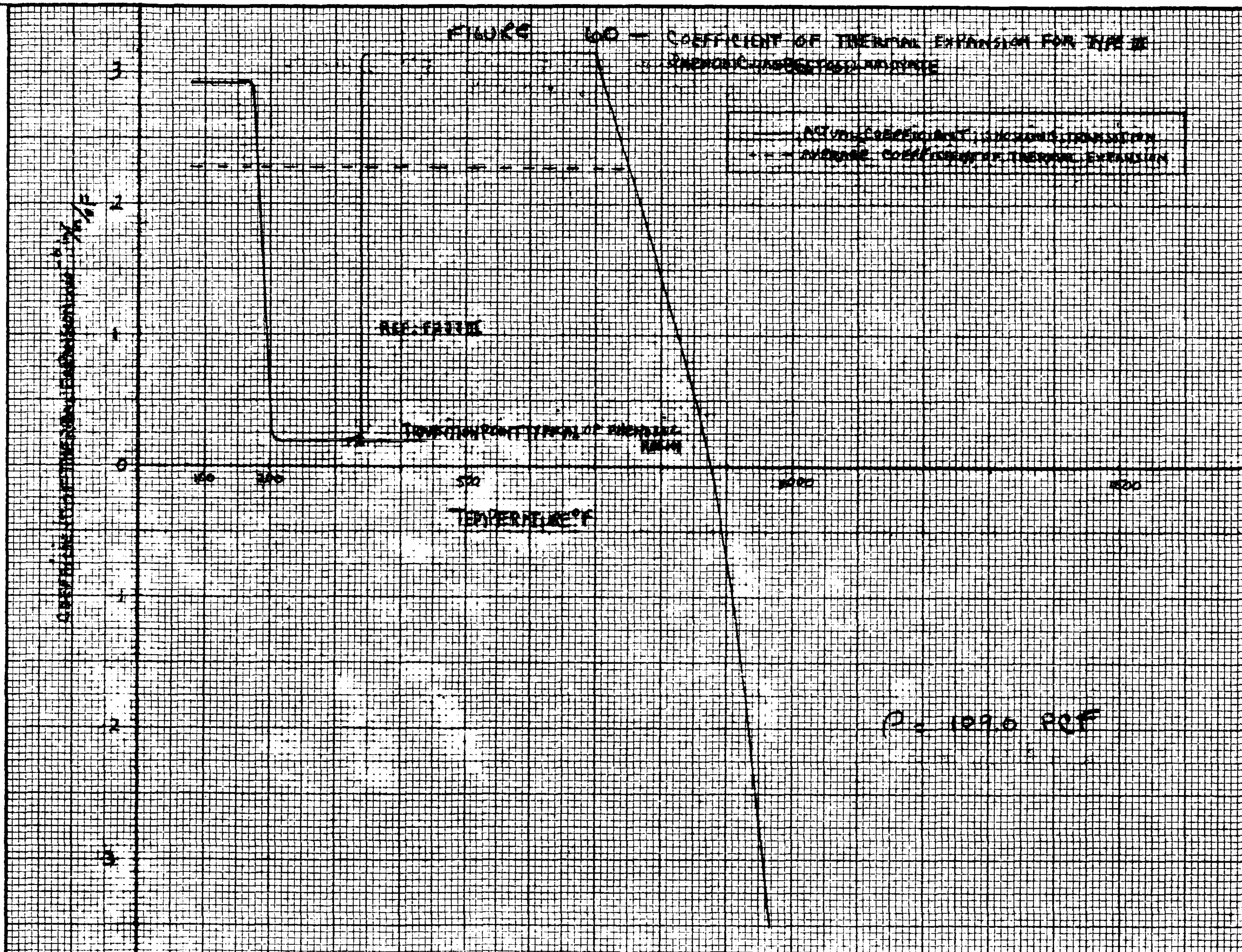


FIGURE 60 — COEFFICIENT OF THERMAL EXPANSION FOR TYPE II

E-1-10A
REV. 2/49

PREPARED
CHECKED
REVISED

PAGE
REPORT NO.
MODEL

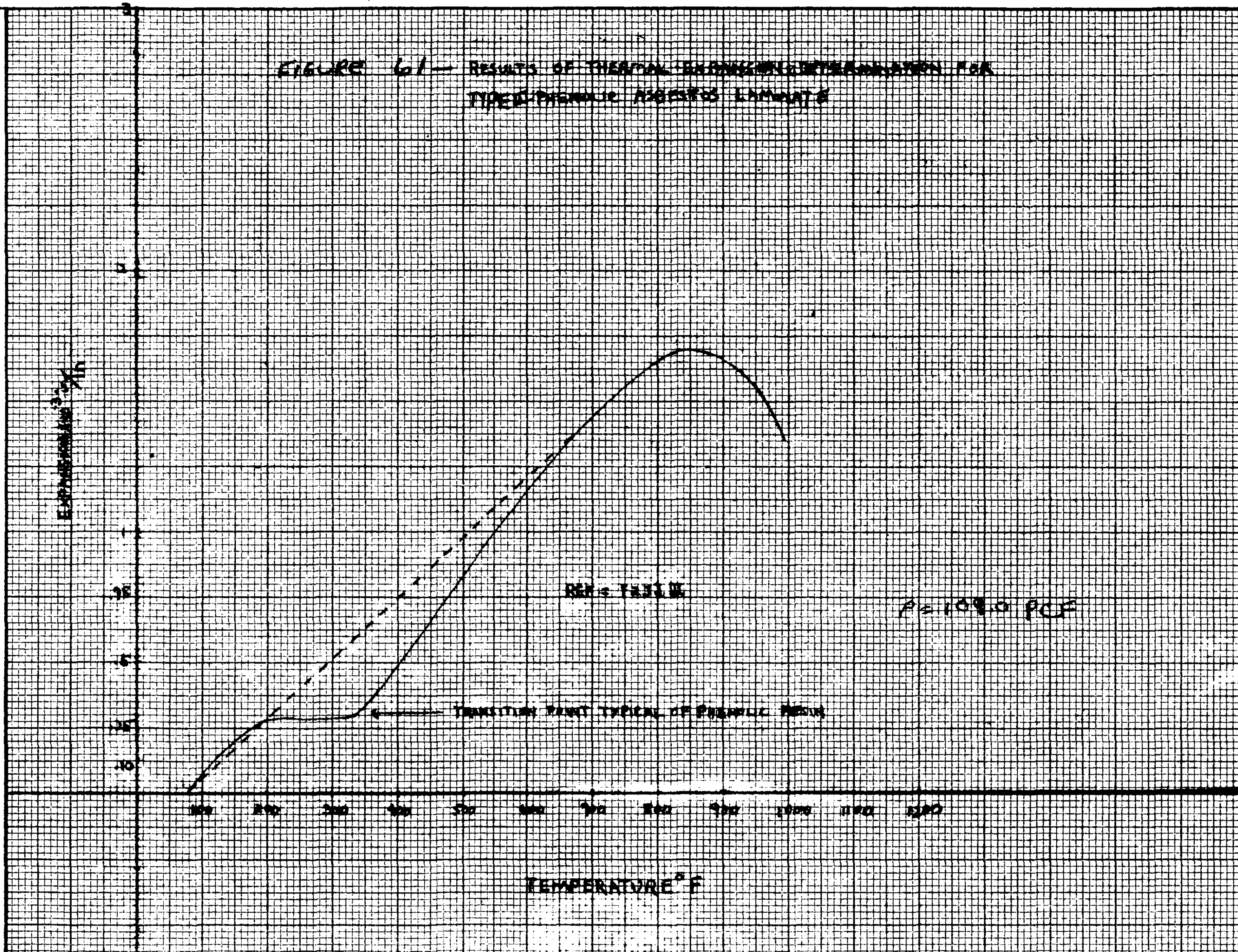


E-1-10A
REV. 2/49

PREPARED ____ ____

CHECKED ____ ____

REVISED ____ ____

PAGE ____

REPORT NO. ____

MODEL ____

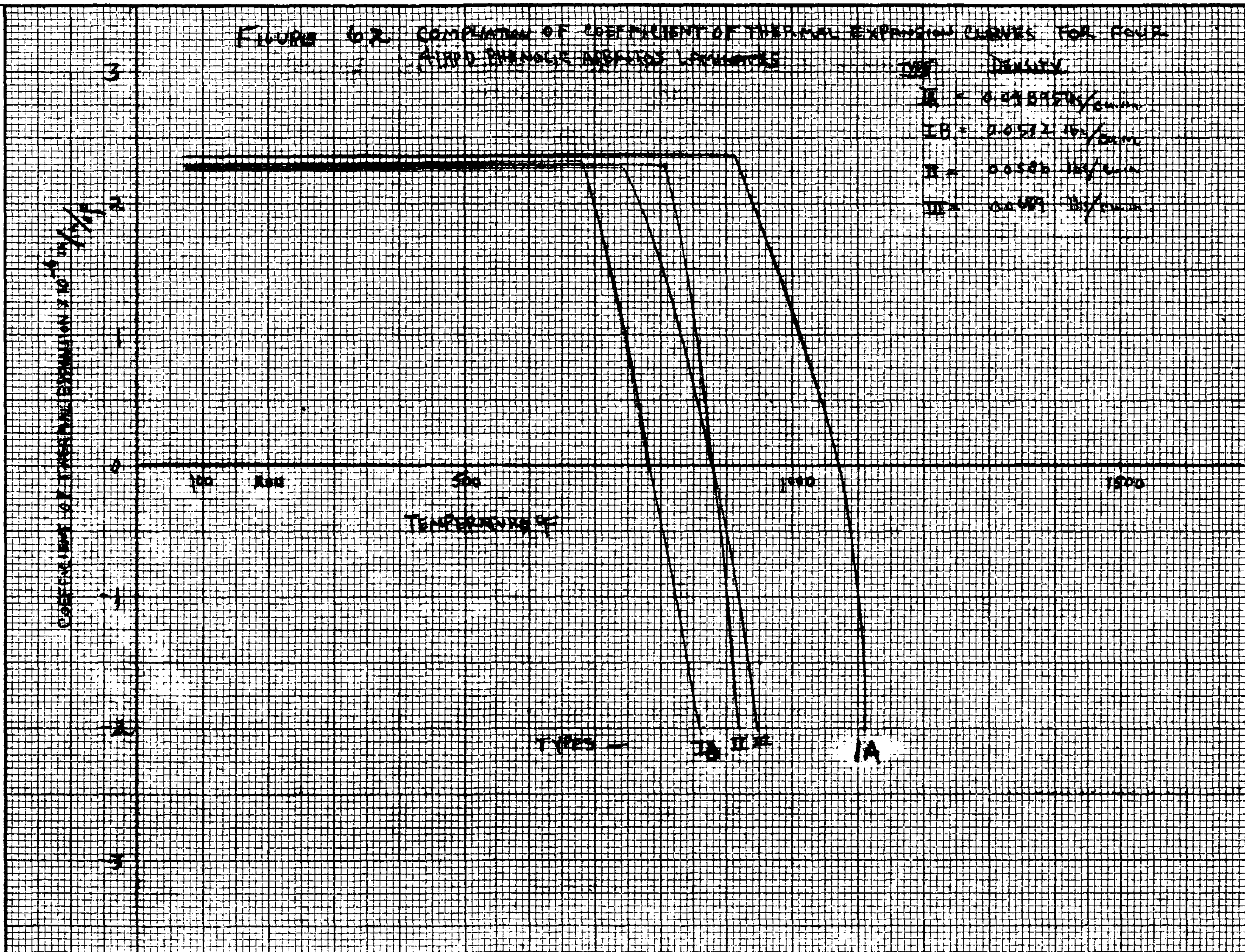


FIGURE 62 COMPILATION OF COEFFICIENT OF THERMAL EXPANSION CURVES FOR FOUR ALKYD PHENOLIC ASBESTOS LAMINATES

E-1-10A
REV. 2/49

PREPARED ______ ______

CHECKED ______ ______

REVISED ______ ______

REPUBLIC AVIATION

PAGE ______

REPORT NO. ______

MODEL ______

FIGURE 63 - TYPICAL TENSILE STRESS-STRAIN CURVE FOR TYPE IA PHENOLIC ASBESTOS LAMINATE AT R.T.

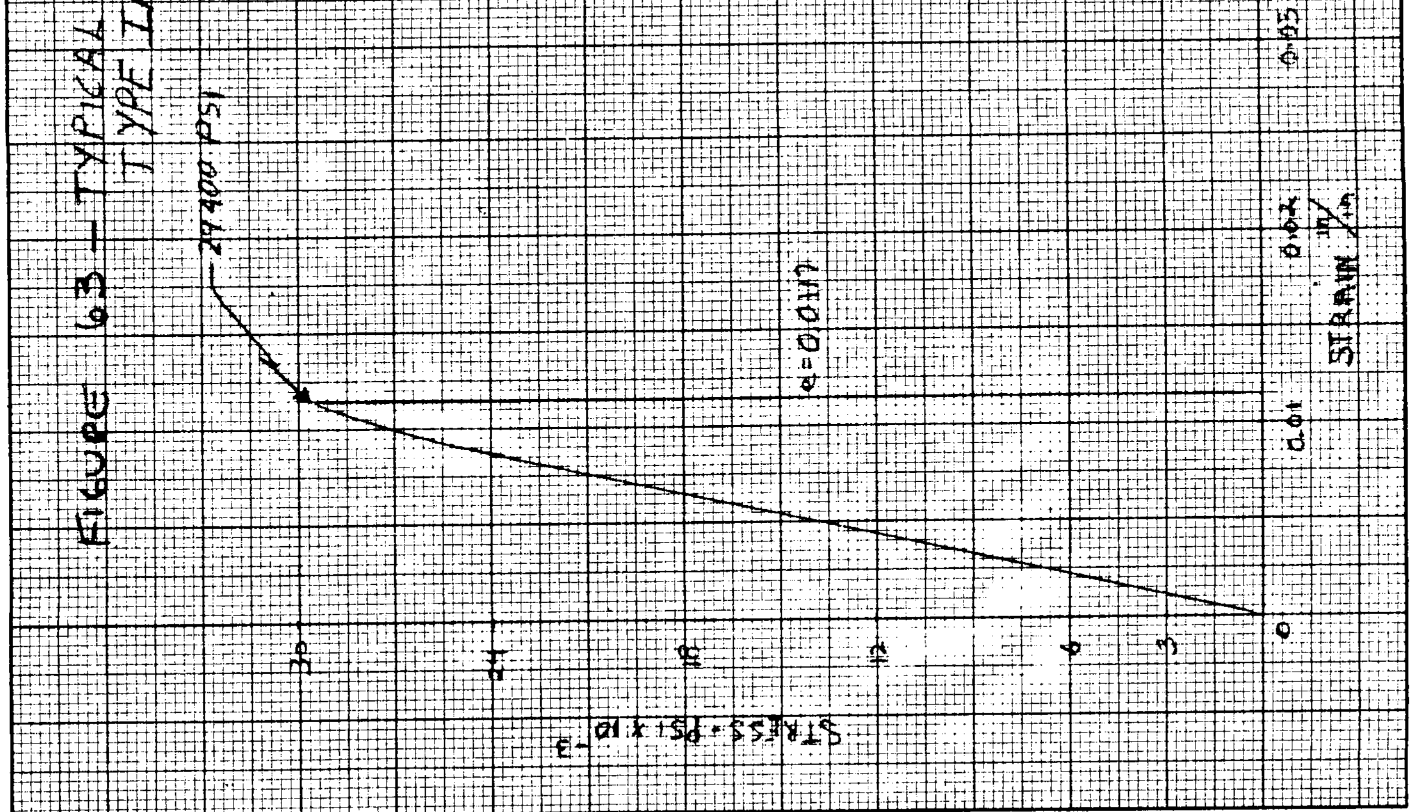


E-1-10A
REV. 2/49

PREPARED
CHECKED
REVISED

PAGE
REPORT NO.
MODEL

FIGURE 64 - TYPICAL TENSILE STRESS - STRAIN CURVE FOR TYPE II PHENOLIC ASBESTOS LAMINATE AT R.T.

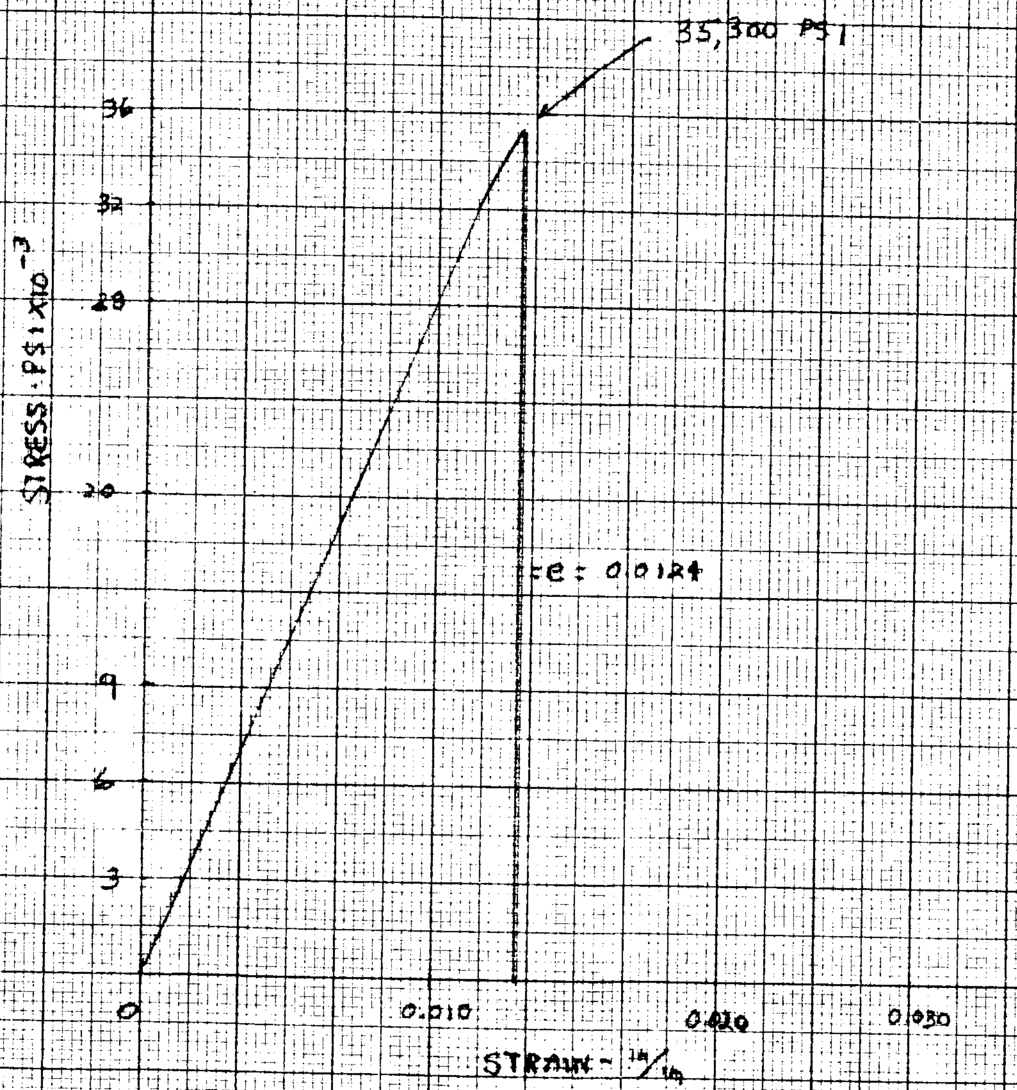


E-1-10A
REV. 2/49

PREPARED ____________ ______

CHECKED ____________ ______

REVISED ____________ ______

REPUBLIC AVIATION

PAGE ____________

REPORT NO. ____________

MODEL ____________

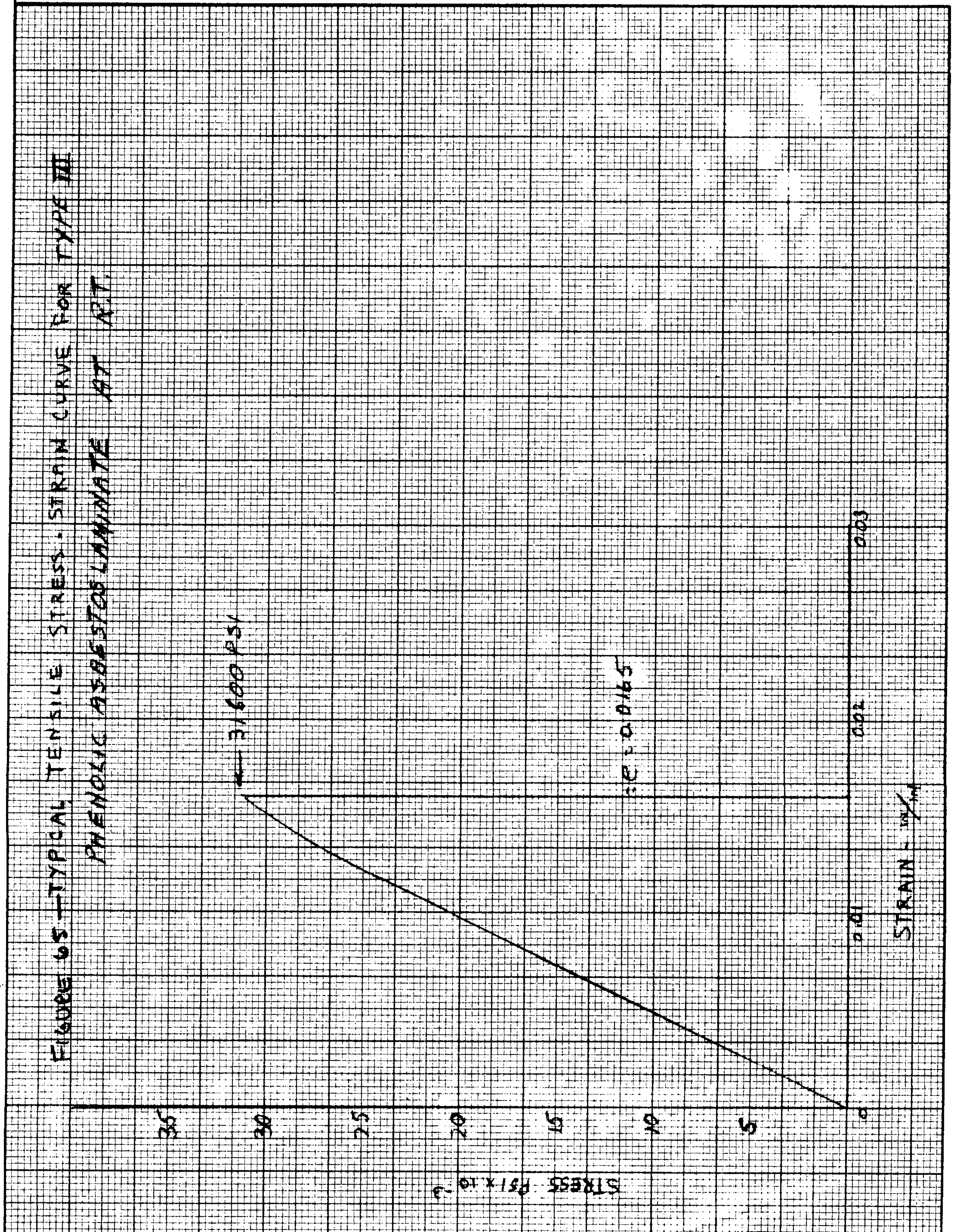


E-1-10A
REV. 2/49

PREPARED ______ ______

CHECKED ______ ______

REVISED ______ ______

PAGE ______

REPORT NO. ______

MODEL ______

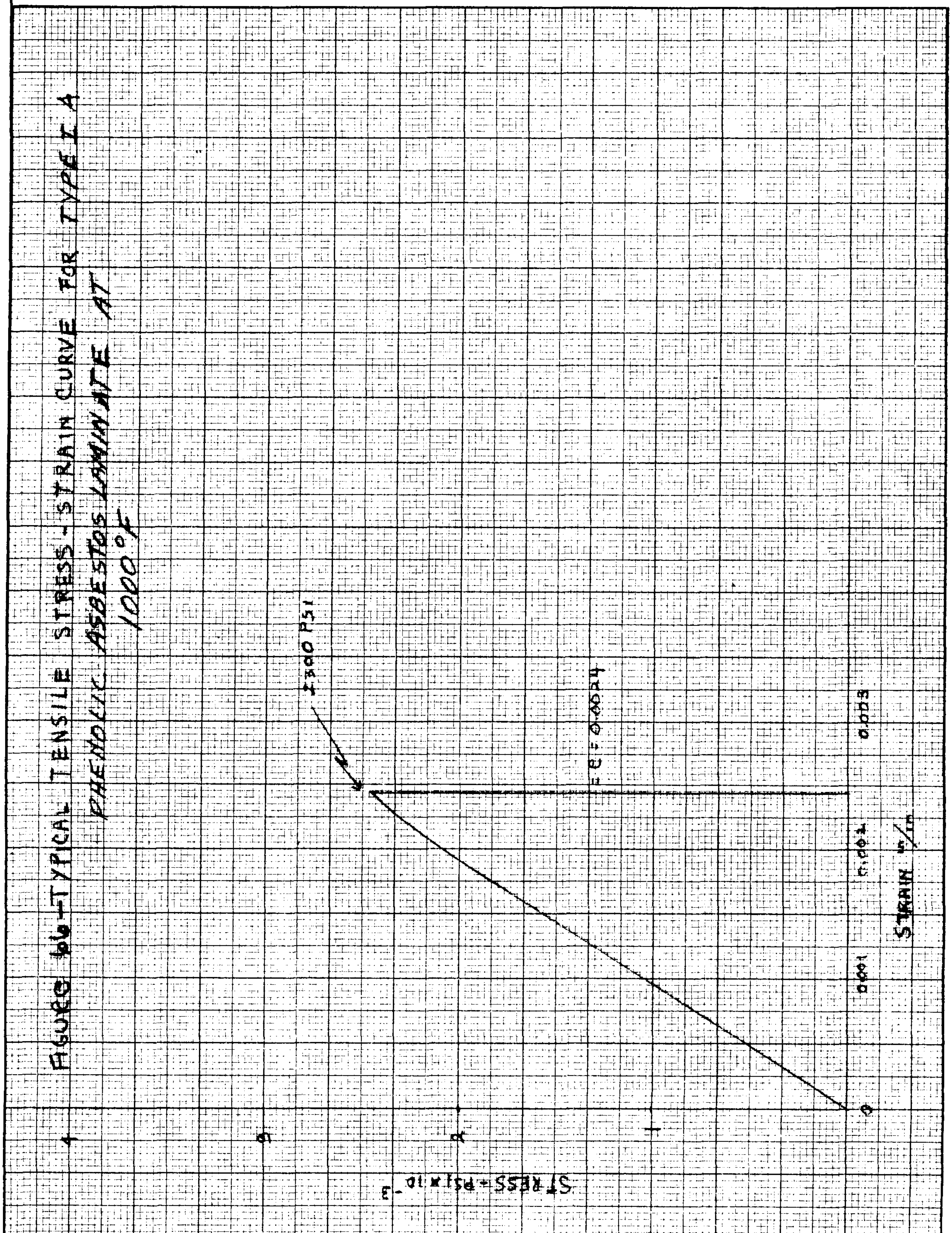


FIGURE 66 — TYPICAL TENSILE STRESS-STRAIN CURVE FOR TYPE I A PHENOLIC ASBESTOS LAMINATE AT 1000°F

E-1-10A
REV. 2/49

PREPARED ______ ______

CHECKED ______ ______

REVISED ______ ______

REPUBLIC AVIATION

PAGE ______

REPORT NO. ______

MODEL ______

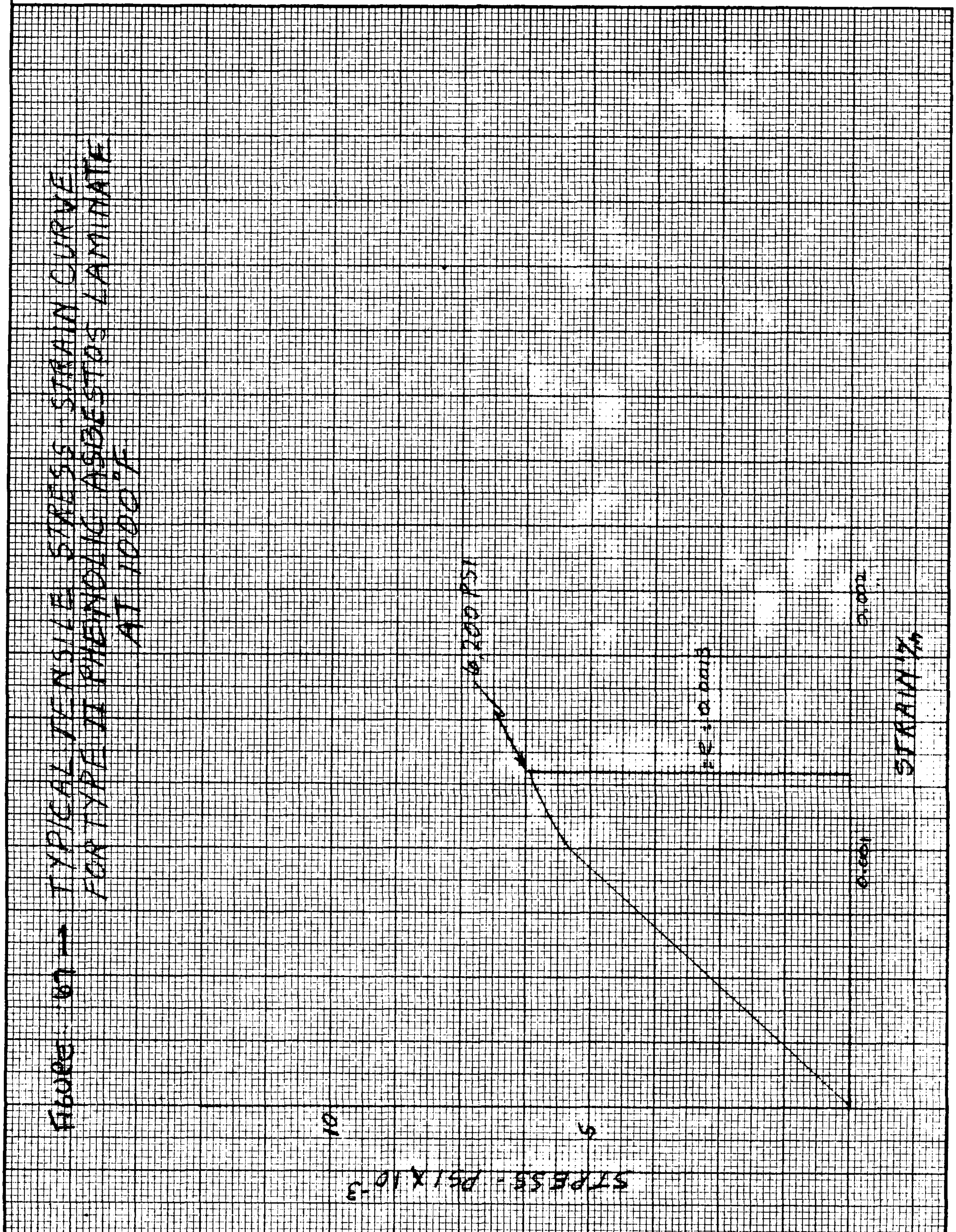


E-1-10A
REV. 2/49

PREPARED ____ ____ PAGE ____

CHECKED ____ ____ REPORT NO. ____

REVISED ____ ____ MODEL ____

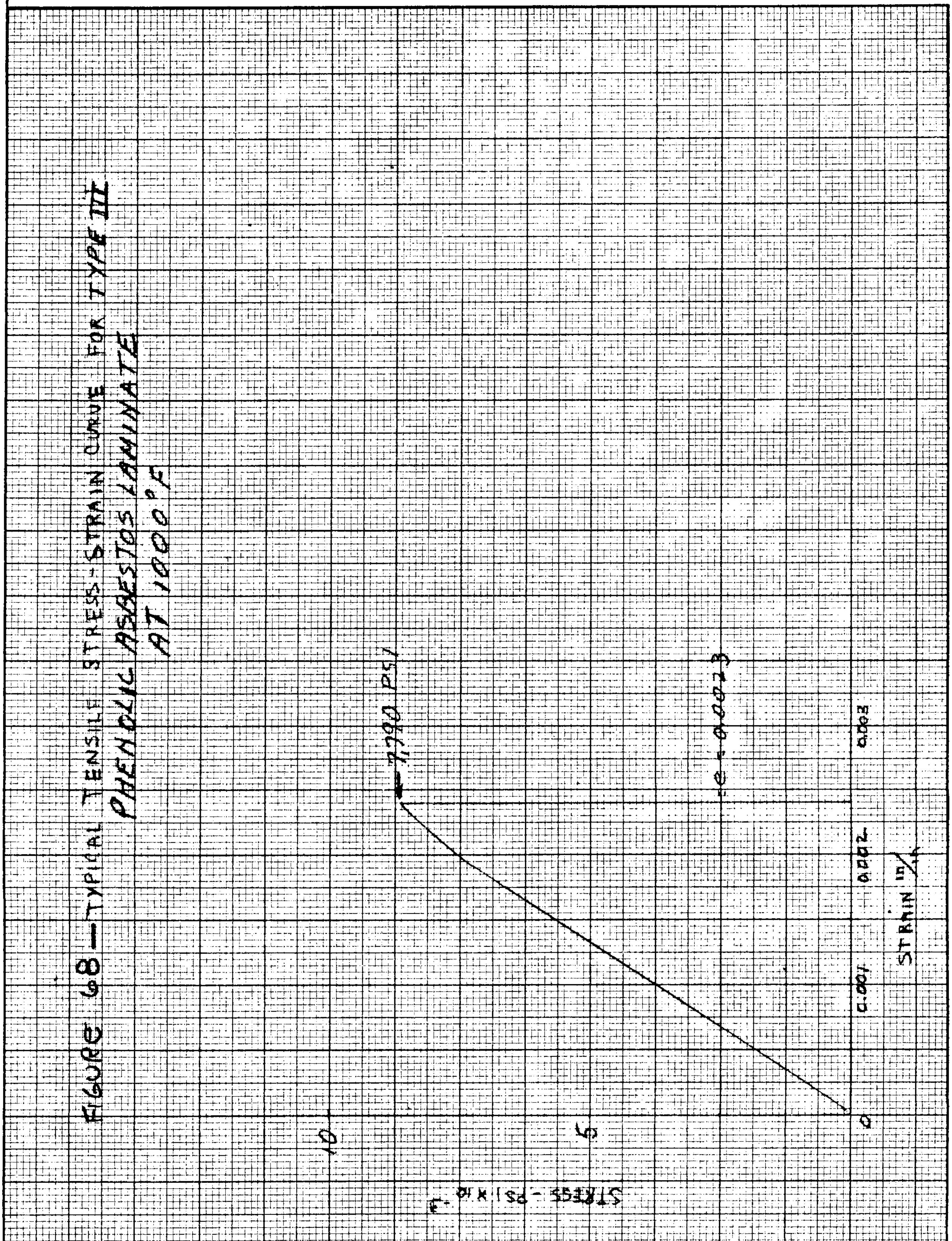


FIGURE 68 — TYPICAL TENSILE STRESS-STRAIN CURVE FOR TYPE III PHENOLIC ASBESTOS LAMINATE AT 1000°F

E-1-10A
REV. 2/49

PREPARED ________ ________ REPUBLIC AVIATION PAGE ________

CHECKED ________ ________ REPORT NO. ________

REVISED ________ ________ MODEL ________

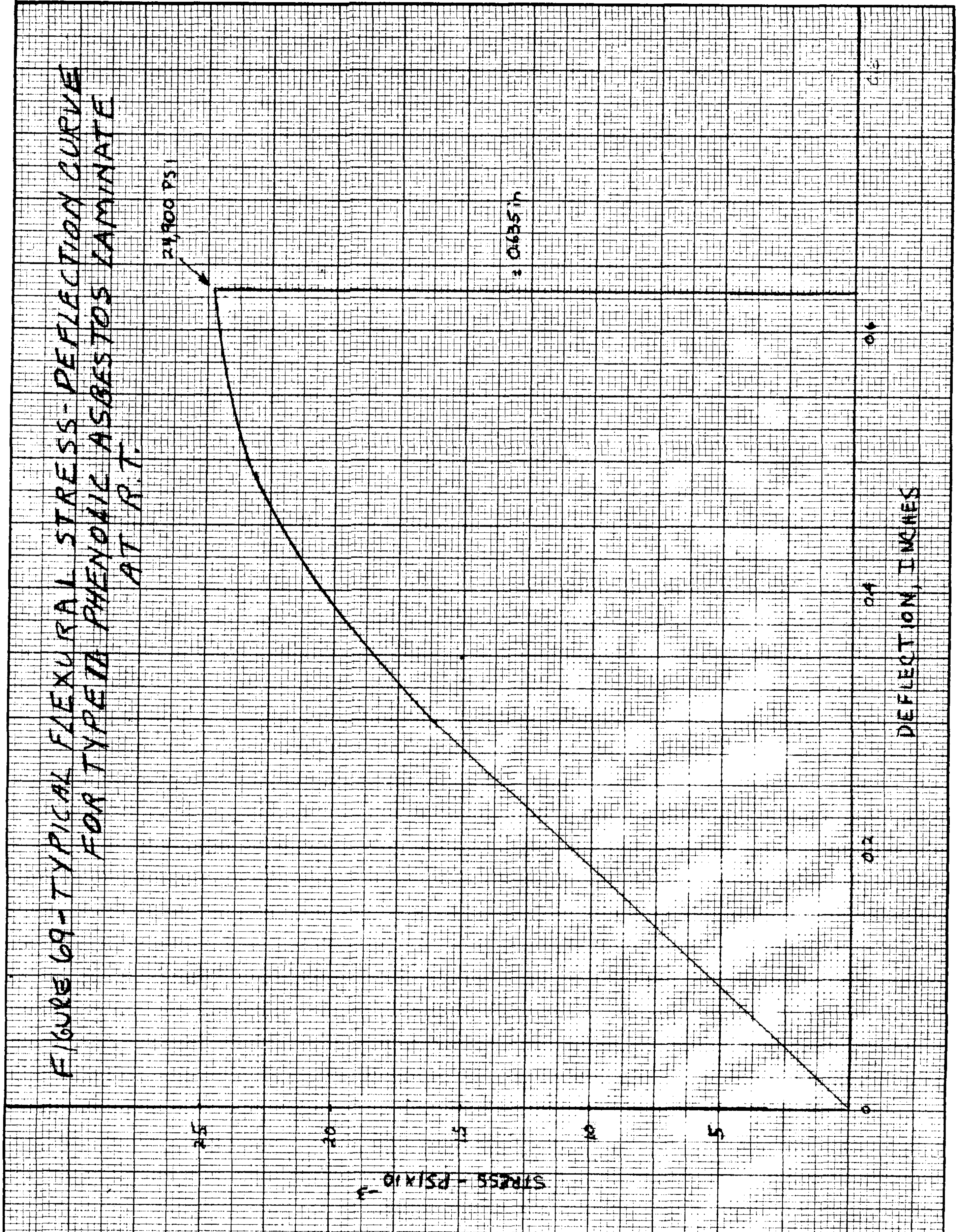


FIGURE 69 - TYPICAL FLEXURAL STRESS-DEFLECTION CURVE FOR TYPE II PHENOLIC ASBESTOS LAMINATE AT R.T.

E-1-10A
REV. 2/49

PREPARED ____ ____
CHECKED ____ ____
REVISED ____ ____

REPUBLIC AVIATION

PAGE ____
REPORT NO. ____
MODEL ____

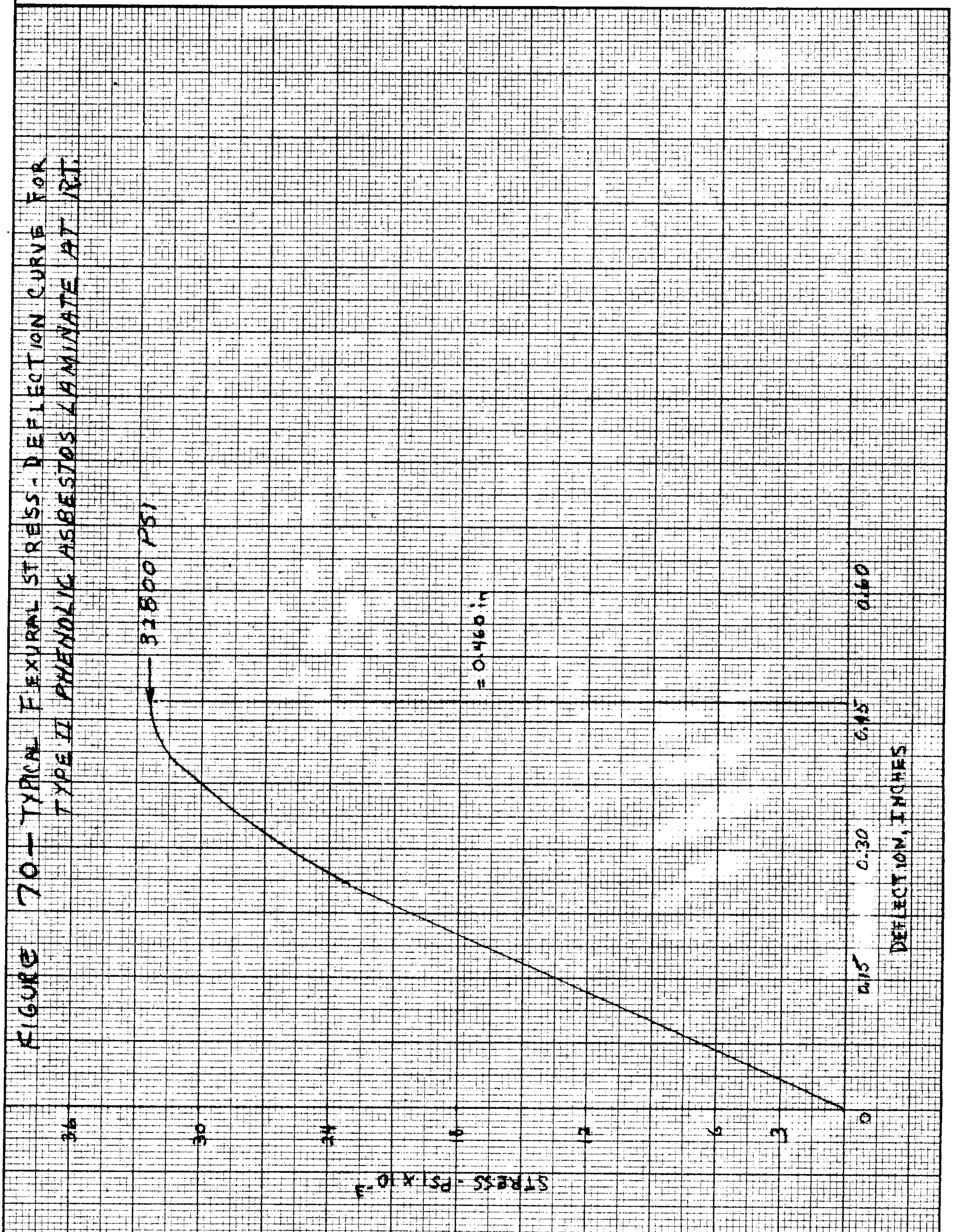


FIGURE 70 — TYPICAL FLEXURAL STRESS - DEFLECTION CURVE FOR TYPE II PHENOLIC ASBESTOS LAMINATE AT R.T.

E-1-10A
REV. 2/49

FIGURE 71 - TYPICAL FLEXURAL STRESS DEFLECTION CURVE
FOR TYPE III PHENOLIC ASBESTOS LAMINATE
AT RT.

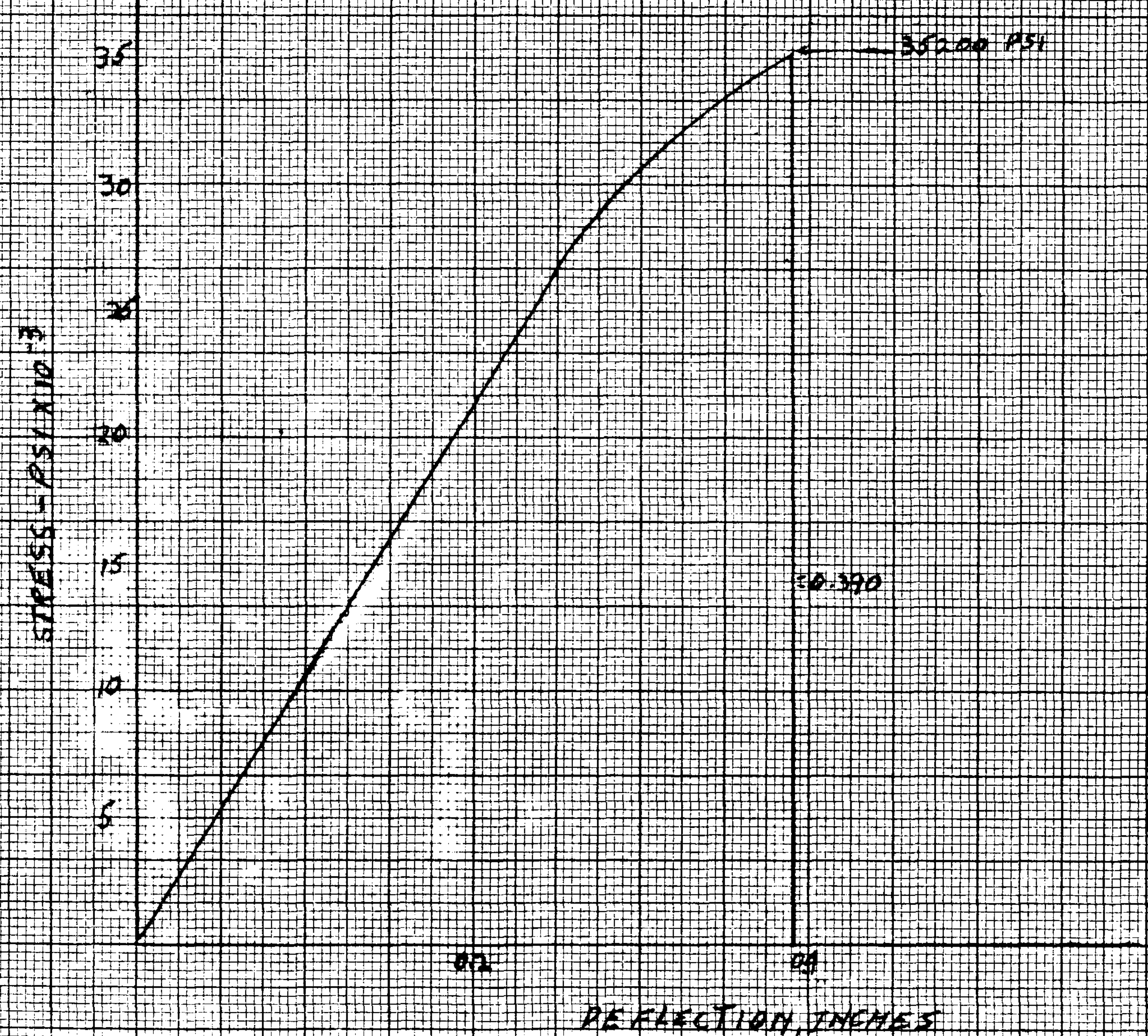


PREPARED ______ ______ REPUBLIC AVIATION PAGE ______

CHECKED ______ ______ REPORT NO. ______

REVISED ______ ______ MODEL ______

E-1-10A
REV. 2/49

PREPARED ______ ______
CHECKED ______ ______
REVISED ______ ______

REPUBLIC AVIATION

PAGE ______
REPORT NO. ______
MODEL ______

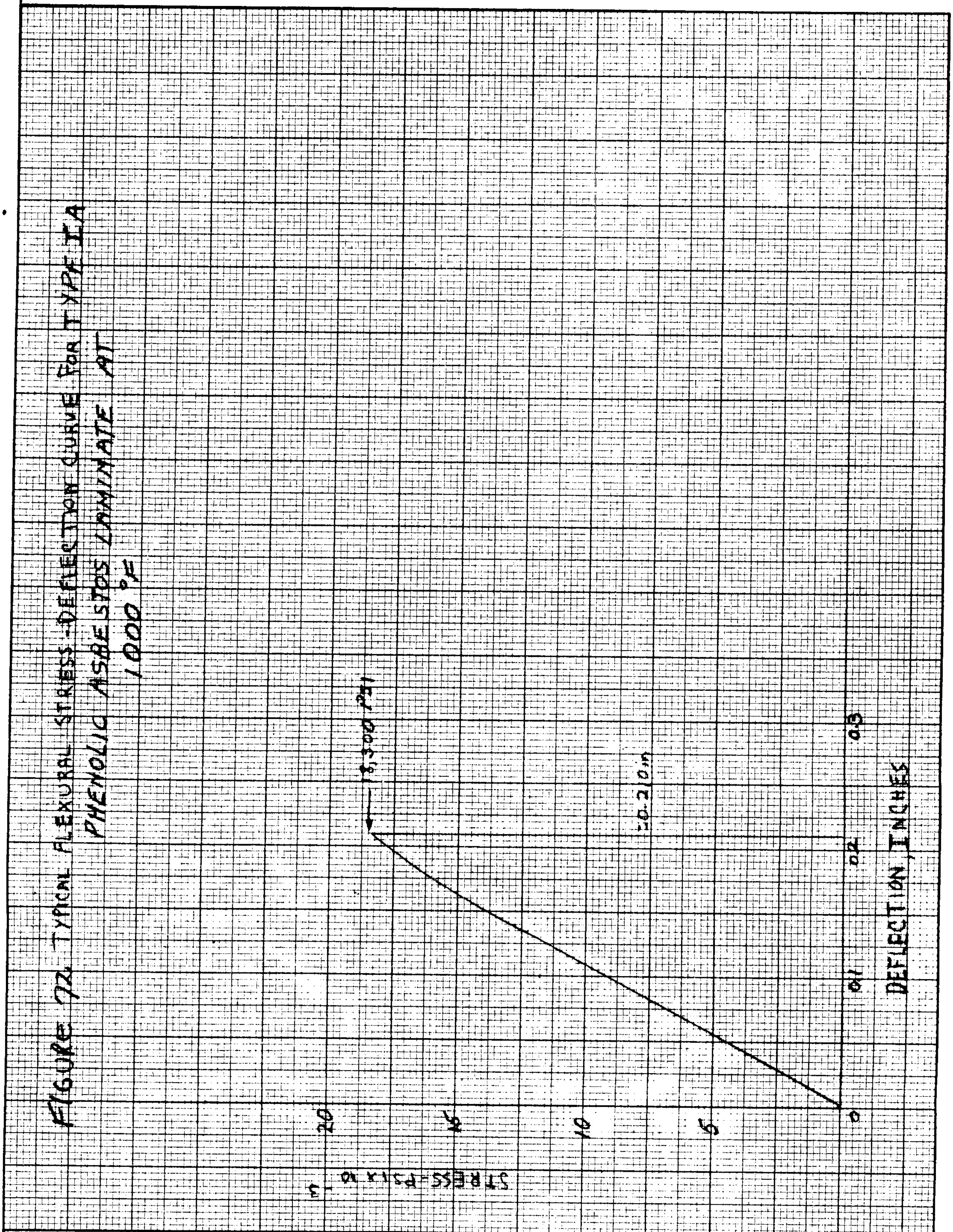


FIGURE 72 TYPICAL FLEXURAL STRESS-DEFLECTION CURVE FOR TYPE IA PHENOLIC ASBESTOS LAMINATE AT 1000 °F

E-1-10A
REV. 2/49

PREPARED

CHECKED

REVISED

PAGE

REPORT NO.

MODEL

FIGURE 73 — TYPICAL FLEXURAL STRESS-DEFLECTION CURVE FOR TYPE II PHENOLIC ASBESTOS LAMINATE AT 1000°F


E-1-10A
REV. 2/49

FIGURE 74 – TYPICAL FLEXURAL STRESS-DEFLECTION CURVE FOR TYPE III PHENOLIC ASBESTOS LAMINATE AT 1000°F

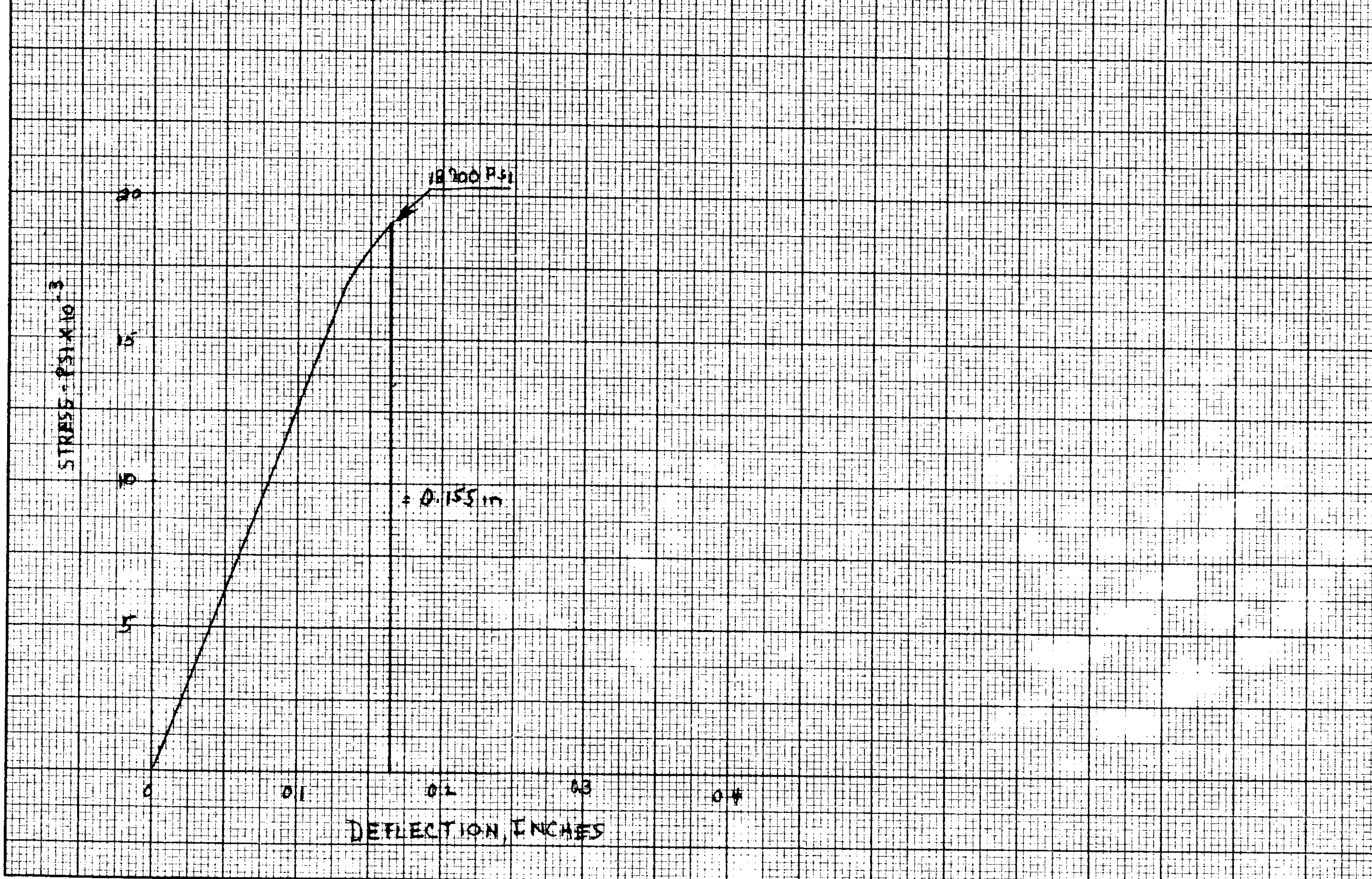

## APPENDIX

### THERMAL CONDUCTIVITY TO 1000°F

Thermal conductivity runs are made with a guarded hot plate, which is a slight modification of the standard ASTM C 177-45 design.

The apparatus consists of a central heater plate surrounded by a guard heater, each separately controlled. The guard ring is maintained at the same temperature as the central heater so that all of the heat flow is normal to the specimen surfaces. The temperature difference between the guard and central sections is measured by means of eight differential-thermocouple junctions connected in series. The plate containing the two heaters is sandwiched between layers of sheet insulation, the hot-face thermocouples, the specimen, cold-face thermocouples, sheet insulation, a copper plate, and finally a cold source to dissipate the heat. The cold source consists of a copper coil enclosed in an aluminum box. In addition to the thermocouples in contact with the specimen, thermocouples are located in the central heater and the outer copper plates.

The thermocouples on the hot side and the cold side are sandwiched between sheets of thin asbestos paper. The ends of the thermocouple leads protrude through one sheet of the paper and are soldered to 1" x 1" squares of brass shim stock. This arrangement insures that there is no air film between the specimen and the thermocouples as well as between the specimen and the hot and the cold plate. The use of the paper and thermocouple getters increases the flexibility of the apparatus for use with materials of varying surface finished; however, for materials with unusual surface finishes, neoprene sheets are inserted on both sides of the specimens. The neoprene deforms to the surface of the specimen thus eliminating the air film. The apparent limitation of this arrangement is the destruction temperature of the neoprene.

Single thermocouples in the center of the heater plate monitor the heater temperature. In addition, five thermocouples are in the cold copper plates. Four of the thermocouples protrude through the plate in contact with asbestos sheets. The fifth thermocouple is soldered to the cold plate to monitor its temperature. These couples, in the heater and the cold plates, are used to monitor the over-all temperature drop through the assembly.

To maintain good contact pressure, a screw loading device holds the entire sandwich assembly pressed firmly together with a total load application up to about 600 pounds.

The assembly is arranged to operate with the specimen placed in the apparatus horizontally as shown in Figure 1. The assembly is insulated around the edges by glass batting, which can be seen on the far sides of the apparatus in Figure 1.

A constant voltage transformer is used in conjunction with the variable control transformers to assure a constant power supply at each setting. The central heater and guard heater are controlled individually by the variable control transformers. The voltage and current to the central heater are monitored by means of a voltmeter and an ammeter, which are switched out of the circuit except when actually being read. The voltage to the guard heater is monitored constantly by a voltmeter.

All of the thermocouple readings are taken on a Leeds and Northrup K-2 potentiometer in conjunction with a galvanometer of 0.43 microvolts per mm deflection sensitivity.

To obtain mean sample temperatures above room temperature, water is circulated through the copper tubing of the cold plates. For mean sample temperatures below room temperature, cold trichloroethylene is pumped through the copper tubing. This coolant is chilled by circulating it through copper coils in a trichloroethylene dry-ice bath. Equilibrium conditions are certified before readings are taken.

Coefficients of thermal conductivity are calculated from the expression:

$$K = \frac{QX}{A\Delta t}$$

where $Q$ = total heat flow - Btu/hr
$X$ = average thickness of specimens - inches
$A$ = area of central heater section - square feet
$\Delta t$ = sum of temperature drops across each sample - °F

Theoretically, Q, the heat input, should split, with exactly half of the input flowing through each sample. The temperature drops indicate that this condition rarely exists. Instead, there is a slight unbalance in the heat flow. The above formula then permits a calculation of the arithmetic average for the two panels.

As a check, the thermal conductivity can be calculated for the specimen with a series expression, knowing the over-all temperature drop from the heater to the cold sink and the conductivity of the asbestos and/or the neoprene.

The original calibration curve from early work on the conductivity apparatus is shown in Figure 2. Several data points also are included that were obtained on some reference specimens at the start of one job to check out the use of smaller specimens, a modified periphery insulation and an improved temperature measuring technique. From this curve, it can be seen that the data had considerable scatter. In spite of this scatter, sufficient information was obtained to establish operation procedure and techniques and to confirm the validity of using smaller specimens.

A more accurate calibration curve was established and is shown in Figure 3. From this data it was determined that the best operating procedure was to measure the face temperature with five thermocouples mounted on small brass "getters" and held against the specimen by a thin sheet of asbestos paper. Also, the copper plates on the hot side were eliminated. These procedures produced data which practically duplicated the previous calibrations on 14" specimens with 6" vermiculite insulation around the apparatus. With copper plates on the hot side, the conductivity obtained was higher, indicating a radial heat loss out through the copper plates on the heater side of the specimens.

Recent calibration of the apparatus had been with plexiglas as a reference specimen. The results of the calibration runs are shown in Figure 4, including reference data by other investigators. The excellent agreement further established the reliability of the equipment.

The present procedure, which includes thermocouples soldered to brass "getters" on both sides of the specimen, was also calibrated with the plexiglas specimen. The results, also shown in Figure 4, established the latter procedure to be as good or possibly better than the previous procedures.

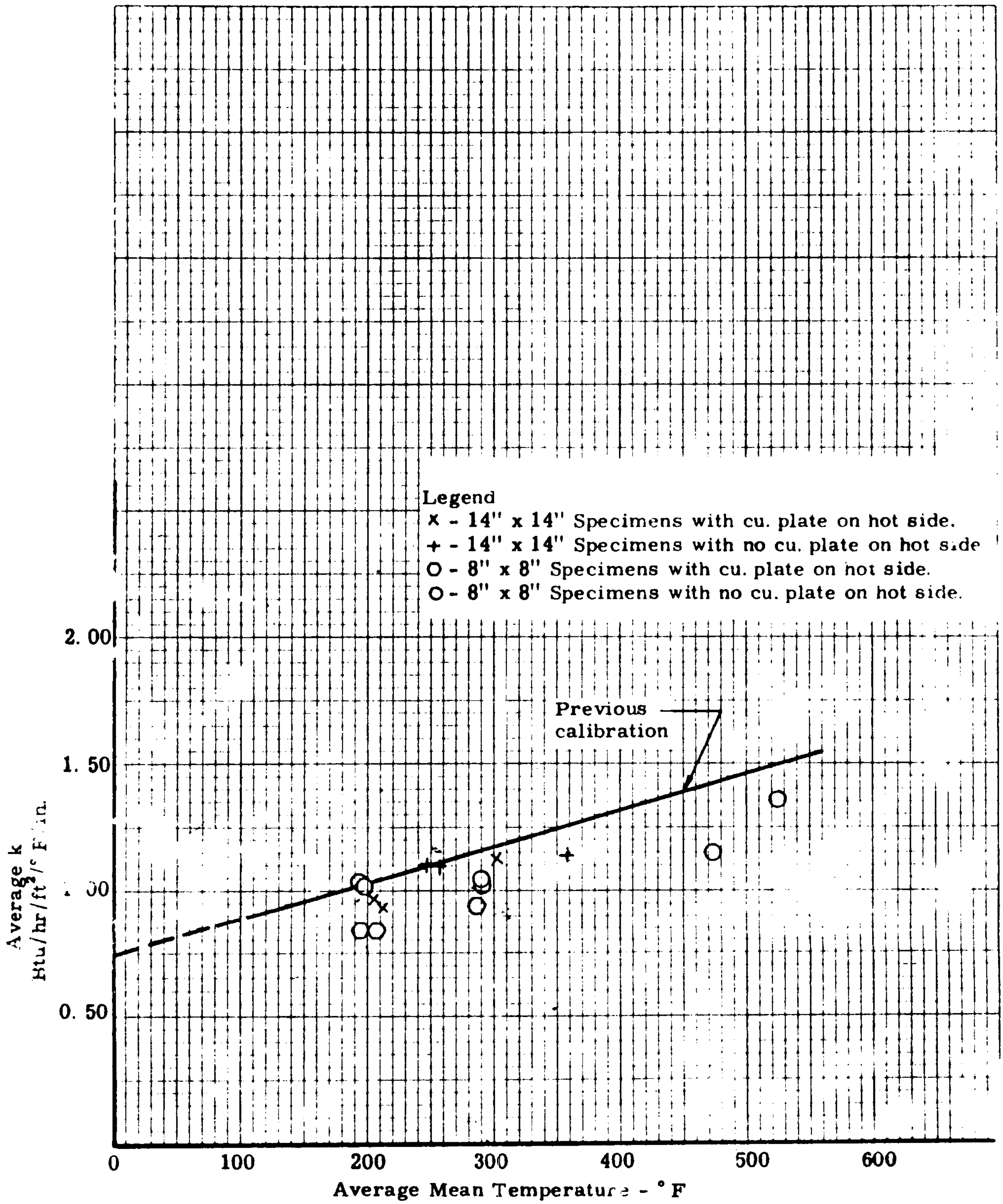


**Figure 2. Original Calibration Curve Using Various Size Specimens and Various Measuring Devices.**

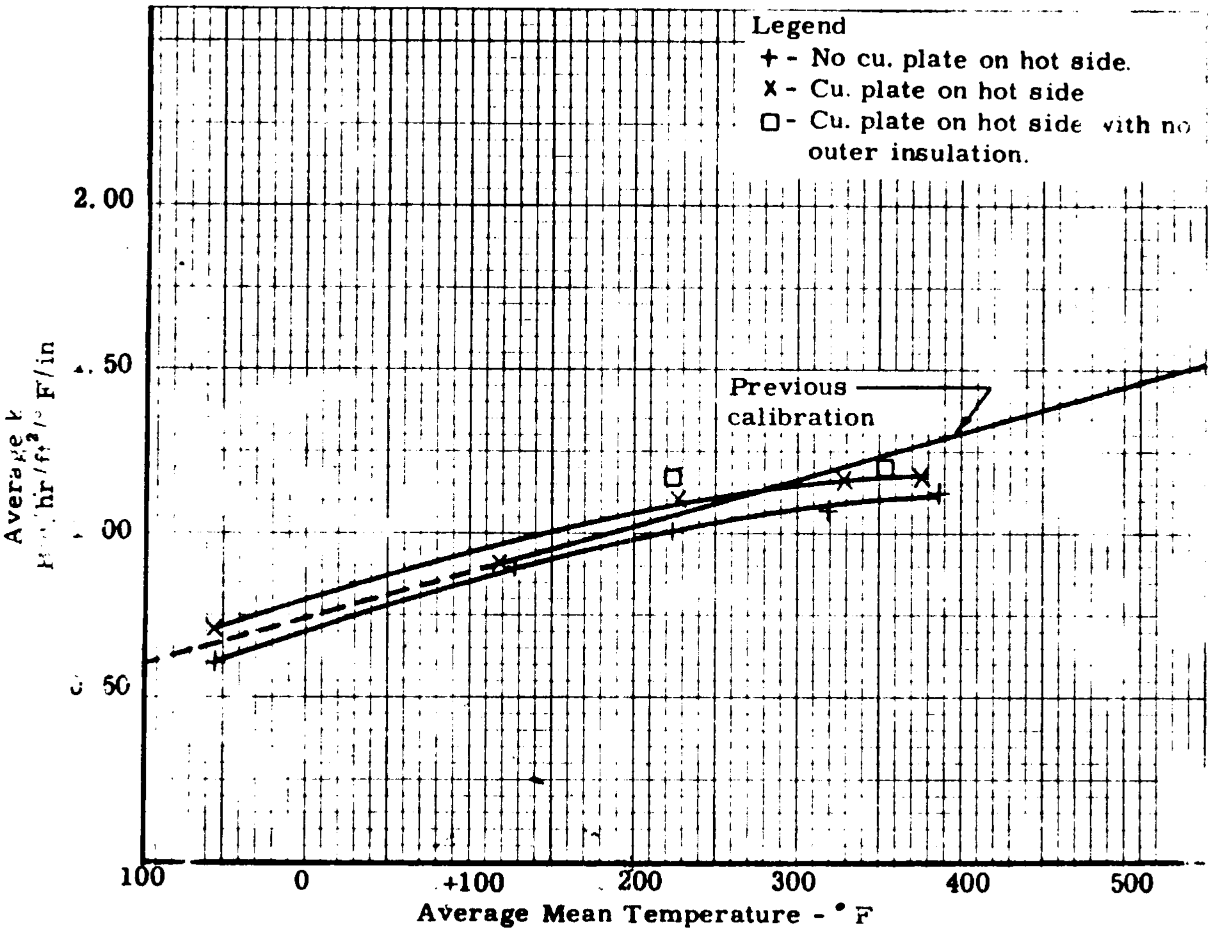


Figure 3. Final Calibration Curve.

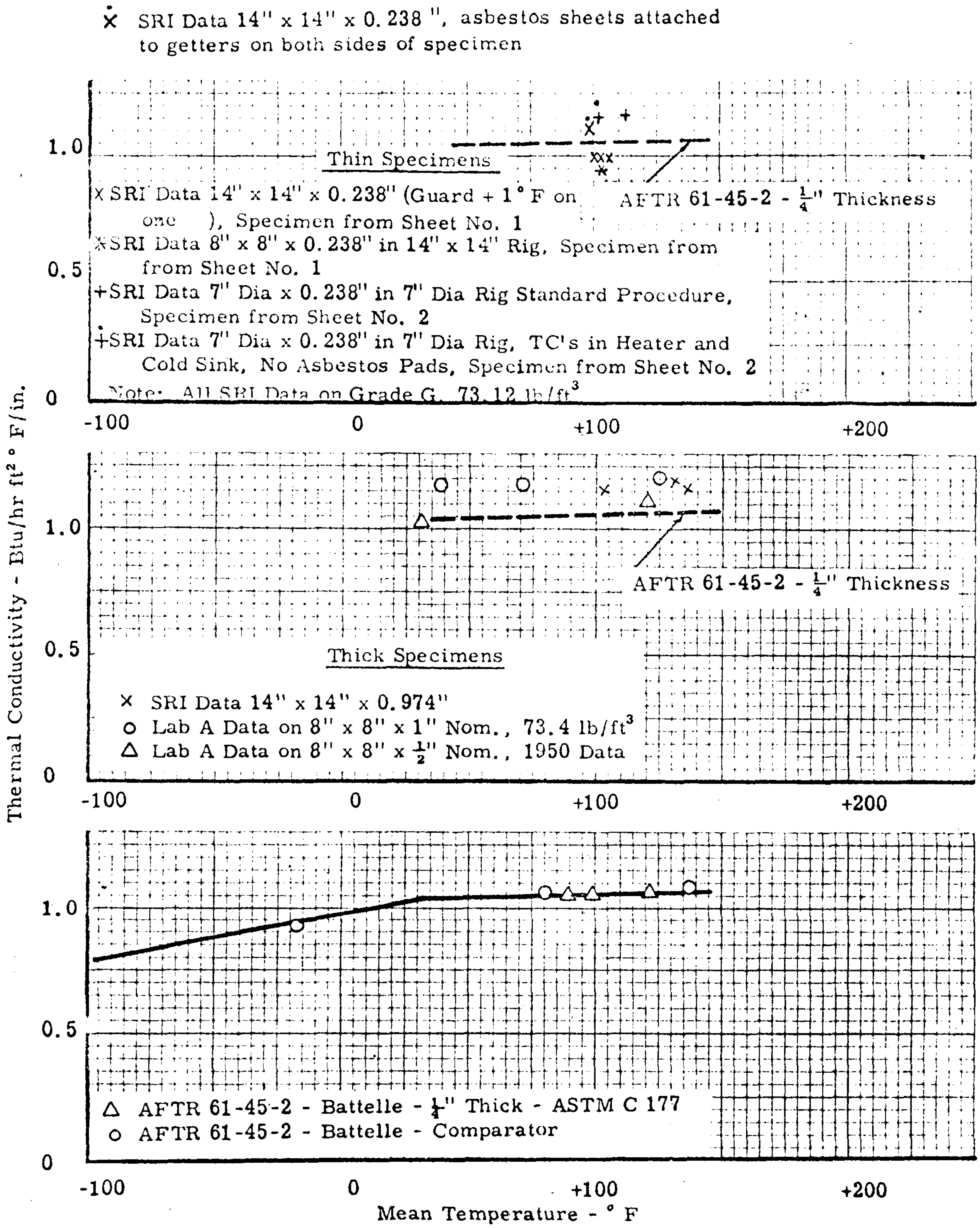


Figure 4. Comparison of Thermal Conductivity of Plexiglas by Different Investigators.